10-7-2020 7:00 AM

Biomechanical analysis of Total Knee Arthroplasty performed on a 6 degree of freedom joint motion simulator linked to a virtual ligament model in mechanical and kinematic alignments

Jance McGale, *The University of Western Ontario*

Supervisor: Lanting, Brent, *The University of Western Ontario*
Co-Supervisor: Willing, Ryan, *The University of Western Ontario*
A thesis submitted in partial fulfillment of the requirements for the Master of Science degree in Surgery

Abstract

Total knee arthroplasty (TKA) is a very successful surgery providing many patients with increased quality of life. Despite this, some patients are dissatisfied. There are also complications with total knee arthroplasty that lead to the need for revision surgery. Improvements in stability, soft tissue balance, joint kinematics and overall patient satisfaction may lead to a decrease in TKA revisions. It is still unclear what the optimal soft tissue tension, balance or alignment is to provide superior patient outcomes. Computational models provide a means to effectively parameterize ligaments and simulate multiple scenarios of TKA. This work implemented a sophisticated 6-degree of freedom joint motion simulator merged with a virtual soft tissue model, eliciting the soft-tissues properties used to balance TKAs. Through testing joint kinematics and soft tissue laxity through 90° of neutral flexion and extension and simulated Activities of Daily Living (ADLs) we were able to reproduce a model that elicited joint kinematics in a balanced TKA similar to what has been shown in the literature. We also compared mechanically aligned (MA) and kinematically aligned (KA) TKAs. This work offers a baseline computational model that reproduces appropriate TKA joint kinematics and laxities, which can then be used for future studies providing better understanding of total knee arthroplasty.

Keywords

Total knee arthroplasty, Total knee replacement, Mechanical alignment, Kinematic alignment, Computational model, Virtual Ligament model, Joint motion simulation, Kinematics, Laxity

Summary for Lay Audience

Total knee arthroplasty (TKA) is a very successful surgery providing many patients with increased quality of life. Despite this, some patients are dissatisfied. There are also complications with total knee arthroplasty that lead to the need for revision surgery. Improvements in stability, soft tissue balance, joint kinematics and overall patient satisfaction may lead to a decrease in TKA revisions. It is still unclear what the optimal soft tissue tension, balance or alignment is to provide superior patient outcomes. Computational models provide a means to effectively parameterize ligaments and simulate multiple scenarios of TKA. This work implemented a sophisticated 6-degree of freedom joint motion simulator merged with a virtual soft tissue model, eliciting the soft-tissues properties used to balance TKAs. Through testing joint kinematics and soft tissue laxity through 90° of neutral flexion and extension and simulated Activities of Daily Living (ADLs) we were able to reproduce a model that elicited joint kinematics in a balanced TKA similar to what has been shown in the literature. We also compared mechanically aligned (MA) and kinematically aligned (KA) TKAs. This work offers a baseline computational model that reproduces appropriate TKA joint kinematics and laxities, which can then be used for future studies providing better understanding of total knee arthroplasty.

Co-Authorship Statement

This study was performed in collaboration with both members from the department of orthopedic surgery as well as department of biomechanical engineering. Dr. Brent Lanting MD, MSc, FRCSC assumed the role as primary supervisor, while Dr. Ryan Willing PhD, B.Sc.E assumed the role as co-supervisor. Liam Montgomery also provided significant support to the development of the computational model and methodologies. My responsibilities for this work included consultation on developing the computational model, operation of the joint motion simulator, data collection and final analysis. I authored this original thesis with the guidance of Dr. Brent Lanting and Dr. Ryan Willing.

Acknowledgments

I would like to thank my masters supervisor Dr. Brent Lanting for inspiring me to go forward with this project. Also for all the Orthopedic surgery career advice in both the academic and surgical realms. I would like to thank him for the added instruction and teaching to help me understand in more detail the intricacies of total joint arthroplasty, especially in the knee.

I would also like to thank Dr. Ryan Willing, who patiently and tirelessly supported me in attempting to understand the complexities of the engineering world. I would not have been able to understand or carryout the operations of the VIVO or the ligament model without his significant contributions. Also all the assistance with data collection, smoothing and organizing. Thank you for allowing me to be a part of your lab and work with you.

Also I would like to thank Liam Montgomery for all the long hours and late nights he went through developing our CAD models and virtual ligament properties. Thank you for devoting a lot of your energy into understanding the anatomy of the knee and the subtleties of TKA with it's different constructs and alignments.

I would like to thank the Masters in Surgery program for the instruction through the year and all the other individuals that contributed to portions of this work and my education over my fellowship year.

Lastly, I thank my family and their sacrifice and support, allowing me to devote time to accomplishing this master goal.

Table of Contents

List of Tables

List of Figures

List of Appendices

List of Abbreviations

AA: Anatomic Alignment

ADL: Activity of Daily Living

ACL: Anterior Cruciate Ligament

aMA: adjusted Mechanical Alignment

AP: Anterior-Posterior

CAD: Computer Aided Design

CR: Cruciate Retaining

CS: Condylar Stabilized

CSxPCL: Condylar Stabilized without PCL

dMCL: deep Medial Collateral Ligament

ER: External Rotation

FE: Flexion-Extension

FEA: Finite element analysis

IE: Internal-External

IR: Internal Rotation

IT: Iliotibial

KA: Kinematic Alignment

KOOS: Knee injury and Osteoarthritis Outcome Score

LCL: Lateral Collateral Ligament

LFC: Lateral Femoral Condyle

MA: Mechanical Alignment

MFC: Medial Femoral Condyle

MPFL: Medial Patellofemoral Ligament

NSAID: Non-Steroidal Anti-Inflammatory Drug

OA: Osteoarthritis

PA: Posterior-Anterior

PCL: Posterior Cruciate Ligament

Poly: Polyethylene Tray

PS: Posterior Stabilized

ROM: Range Of Motion

sMCL: superficial Medial Collateral Ligament

TEA: Trans-epicondylar axis

TFA: Tibiofemoral Angle

TKA: Total Knee Arthroplasty

VV: Varus-Valgus

WOMAC: Western Ontario and McMaster Universities Arthritis index

Chapter 1

1 Background and Literature Review for biomechanical analysis of soft tissue balancing in total knee arthroplasty (TKA) in both mechanically and kinematically aligned implants

1.1 Introduction

Total knee arthroplasty has revolutionized the quality of life for individuals suffering from end stage knee arthritis. Since it's advent there have been many design changes and improvements to better replicate the native knee biomechanics[1]. Despite these improvements, 15-20% of patients are still unhappy with the outcome of their total knee [2,3]; often this is due to residual pain or functional impairments. Poorly balanced knees, or unequal tension across the soft tissues, may be a reason for this residual pain or overall dissatisfaction. Dissatisfied TKA patients have lower quality of life and higher healthcare resource burdens[4]. Occasionally, these patients will require a revision operation to alleviate their symptoms and improve their quality of life and function. TKA revision causes enormous burden on patients, hospitals, surgeons and the healthcare system. With the number of joint replacement surgeries increasing, it is likely the number of revision surgeries will subsequently be increasing. In 2010, in the United States alone, over 55,000 TKA revision surgeries were carried out to accrue $2.7 billion in hospital charges; this number is projected to be $13 billion annually by 2030[5]. With the total number of TKA surgeries projected to be 3.48 million per year by 2030[1], the economic burden caused by TKA revision will be astronomical. Research efforts have been ongoing to eliminate or decrease the main reasons for revision to effect patient outcomes and quality of life as well as substantially decrease the economic burden of TKA revision surgery.

One of the top three most common reasons for TKA revision is instability[6,7]. Approximately 63% of TKA failures occur in the first 5 years post op[8]. Of these failures that occur in the first 5 years, 35% of them can be attributed to soft tissue imbalance[9]. Proper ligament balancing and alignment is considered a requirement for achieving good functional outcome and long-term survival of total knee arthroplasty. It is still unclear

what the optimum soft tissue balancing or alignment is for implant survival and superior patient satisfaction, as this may differ with various implant designs. There have been well-defined properties of intact knees, and the ultimate goal of a TKA system is to replicate the functional properties of intact knees.

1.2 Knee Anatomy[10,11]

1.2.1 Osteology

The knee is comprised of an articulation between the two largest long bones and the largest sesamoid bone of the body. The distal femur articulates with the proximal tibia and the posterior surface of the patella. These surfaces are covered with hyaline cartilage to allow for smooth, low friction movement. The femur and tibia articulate as a modified hinge type joint; this is referred to as the tibiofemoral joint. The femur and patella comprise a gliding joint referred to as the patellofemoral joint. These articulations together create the knee joint.

The distal femur articular surface is comprised of the lateral and medial condyles, which are separated anteriorly by the trochlear groove and posteriorly by the intercondylar notch. The posterior aspect of the patella articulates with the trochlear groove. The articular surface of the patella has two facets: the medial facet and the lateral facet. The medial facet is shorter in length and steeper in angulation than the lateral facet, and their geometries match the trochlear groove portion of the medial and lateral femoral condyles respectively. The articular surface of the proximal tibia is comprised of the medial condyle and lateral condyle, which are separated by the tibial eminences. The medial condyle surface area is larger and slightly concave, whereas the lateral condyle is slightly smaller and is convex.

Figure 1-1. Anterior and Posterior view of the boney anatomy of the Patella. Reprinted with permission from TeachMeAnatomy.com

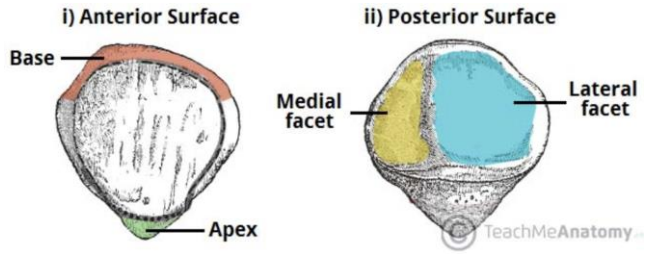

The distal femur is comprised of multiple bony landmarks that allow for soft tissue attachments around the knee joint. Within the intercondylar notch there is attachment for both the anterior cruciate and posterior cruciate ligaments (ACL and PCL). The PCL attaches to the anterolateral surface of the medial condyle, starting anteriorly just behind the hyaline cartilage. The PCL footprint is centered over the bifurcate prominence. This prominence separates the anterolateral bundle and the posteromedial bundles of the PCL. The ACL attaches to the posteromedial surface of the lateral condyle, starting posteriorly just in front of the hyaline cartilage. The ACL is centered over the bifurcate ridge, which separates the anteromedial bundle and the posterolateral bundle of the ACL.

Figure 1-2. Boney anatomy of the anterior distal femur (left) and posterior distal femur (right). Reprinted with permission from TeachMeAnatomy.com

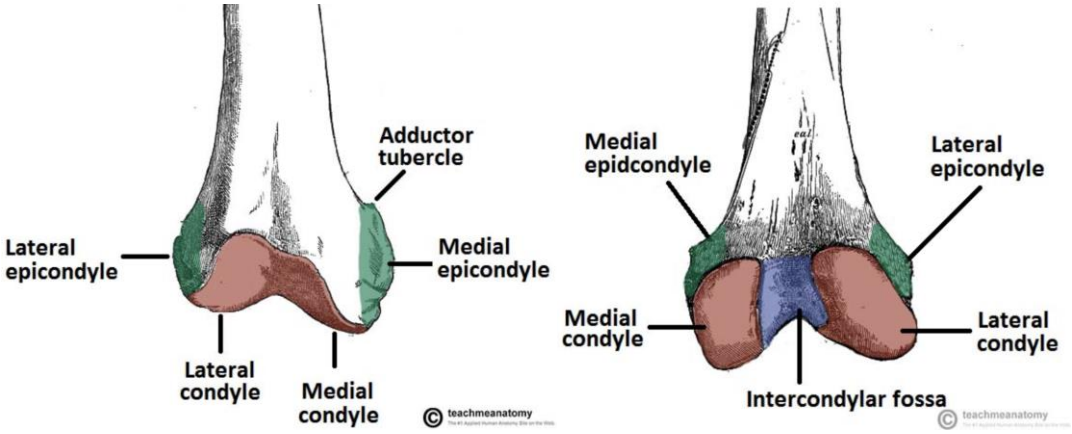

On the lateral condyle, the lateral epicondyle is a small tubercle for the attachment of the lateral collateral ligament (LCL). The lateral epicondyle is on average 23mm proximal to the joint line in the mid-coronal plane[12]. Just distal to the lateral epicondyle runs the popliteal sulcus, allowing the popliteal tendon to pass within the sulcus and deep to the LCL. The popliteus insertion point is anterior and distal to the lateral epicondyle. Thus the popliteus tendon crosses under the LCL and attaches near the edge of the hyaline cartilage. Posteriorly on the lateral condyle, the capsule attaches just proximally to the hyaline cartilage edge. Just proximal to that, there is a pit for the origin of the lateral head of the gastrocnemius muscle. The capsular attachment continues medially just proximal to the posterior intercondylar notch and onto the proximal portion of the medial condyle. Again in a pit just proximal to the capsular attachment on the medial side is the origin of the medial head of the gastrocnemius muscle. On the medial condyle there is the medial epicondyle which allows attachment of the deep and superficial medial collateral ligaments (dMCL and sMCL). The medial epicondyle is on average 28mm proximal to the joint line in the mid-coronal plane[12]. The medial epicondyle has a small horseshoe-shaped sulcus in which the dMCL attaches, and the sMCL attaches on the more proximal ridge of the sulcus. Just anterior and proximal to the medial epicondylar sulcus is the attachment of the medial patellofemoral ligament (MPFL). As the capsule wraps over the posterior edge of the medial condyle, it courses along the curvature of the medial condyle near the hyaline cartilage edge. The capsule then continues its attachment anteriorly and courses more proximally to create the suprapatellar pouch.

The proximal tibia also has multiple boney landmarks that allow for soft tissue attachments around the knee. Separating the two condyles is the tibial eminence or tibial spines. This is made up of medial and lateral intercondylar tubercles. Just anterior to both is found the footprint for the ACL tibial insertion. The anteromedial bundle attaches more anteriorly and slightly medial on the tibial footprint, whereas the posterolateral bundle attaches slightly posterior and lateral within the footprint. The anterior horns of the medial and lateral menisci insert on either side of the ACL footprint, just anterior to the medial and lateral spines respectively. Posterior to the tubercles and sloping slightly

distally along the posterior aspect of the tibia is the insertion of the PCL in the posterior intercondylar area or PCL fovea. The anterolateral bundle attaches closest to the top of the tibial ramp, and the posteromedial bundle attaches in an "L" shape around the posterior and medial footprint of the anterolateral bundle. Directly posterior to the medial and lateral tibial spines are found the insertion points of the posterior horn of the medial and lateral meniscus respectively.

Figure 1-3. Boney anatomy of the proximal tibia. Reprinted with permission from TeachMeAnatomy.com

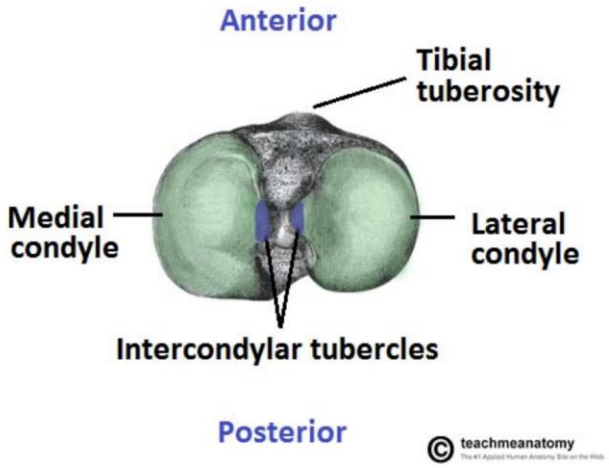

Anteriorly and inferior to the joint line is the large tibial tubercle, which is the insertion point of the patellar tendon. The capsular attachment circumferentially around the tibia is found approximately within 1cm of the joint line. Moving medially from the tibial tubercle and distal to the capsule is the pes anserinus, where the semitendinosus, gracilis, and sartorius muscles insert. Deep to the pes and wrapping more medially the sMCL has a long insertion approximately 4-5cm below the joint line. The dMCL attaches confluently with the capsule close to the joint line in the mid-coronal plane but deep to the sMCL. On the posterior medial corner of the tibia the semimembranosus inserts and distal to that wrapping posterolaterally is the origin of the popliteus muscle. Within the posterior lateral corner there is a capsular hiatus for the popliteal tendon to pass through and become intraarticular. The capsule attachment to the posterior lateral aspect of the tibia is robust; there are multiple ligaments supporting the posterior lateral capsule

namely the oblique posterior ligament, arcuate ligament, popliteal capsular extension, popliteofibular ligament, and fabellofibular ligament. There are also fibular head attachments of the biceps femoris and LCL. On the anterolateral aspect of the tibia just distal to the capsular attachment is Gerdy's tubercle which is an attachment for the insertion of the iliotibial (IT) Band.

1.2.2 Musculature

There are twelve muscles that cross the knee joint and aid in knee function. Anteriorly, the quadriceps is a large group of four muscles. The rectus femoris, vastus intermedius, vastus lateralis and vastus medialis. These four muscles combine to form the quads tendon and insert collectively to the superior portion of the patella. Their mechanism of action combined is extension of the knee joint by transferring their force through the patella and onto the tibial tubercle via the patellar tendon. They are all innervated by the femoral nerve. The sartorius muscle also starts anteriorly in the thigh and inserts distally crossing the knee medially and attaching to the tibia as part of the pes anserinus. It is innervated by the femoral nerve and has a small influence on flexion of the knee.

Figure 1-4. Muscular anatomy of the anterior compartment. Muscles that cross the knee joint: Rectus femoris, Vastus intermedius, Vastus lateralis, Vastus medialis and Sartorius. Reprinted with permission from TeachMeAnatomy.com

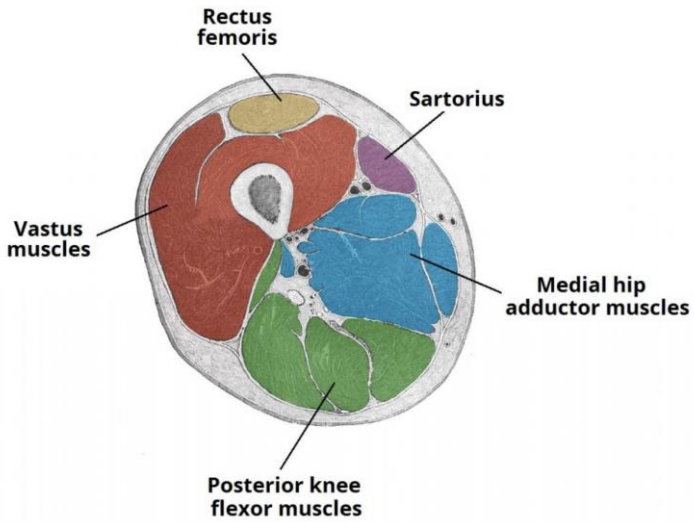

Originating medially there is only one muscle that crosses the knee, the gracilis muscle. Its insertion point distally is also one of the tendons attaching to the proximal medial tibia at the pes anserinus. It is innervated by the obturator nerve and aids in knee flexion.

Figure 1-5. Muscular anatomy of the medial compartment. Muscles that cross the knee joint: Gracilis. Reprinted with permission from TeachMeAnatomy.com

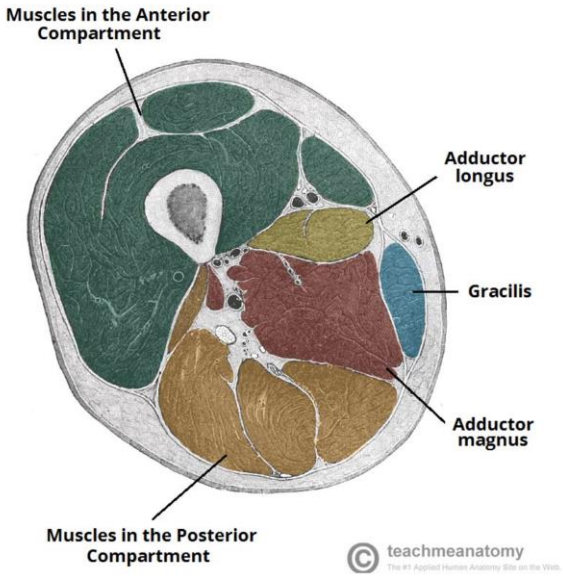

Posteriorly, the hamstring group of muscles is comprised of four muscles as well. The semimembranosus, semitendinosus and biceps femoris (long and short heads). The semimembranosus crosses the knee joint posteriorly and attaches to the posteromedial tibial condyle. The semitendinosus crosses the knee posteromedially and wraps anteriorly as it courses distally. It inserts onto the proximal medial tibia as part of the pes anserinus. The biceps femoris crosses the knee posterolaterally and inserts distally at the posterior aspect of the fibular head with a portion of the short head attaching to the lateral tibia. The primary function of all the hamstring muscles at the knee is flexion. The innervation of all these muscles is through the sciatic nerve, specifically the tibial branch for all except the short head of the biceps femoris which is innervated by the peroneal branch of the sciatic nerve.

Figure 1-6. Muscular anatomy of the posterior compartment. Muscles that cross the knee joint: Biceps femoris (long and short heads), Semitendinosus and Semimembranosus. Reprinted with permission from TeachMeAnatomy.com

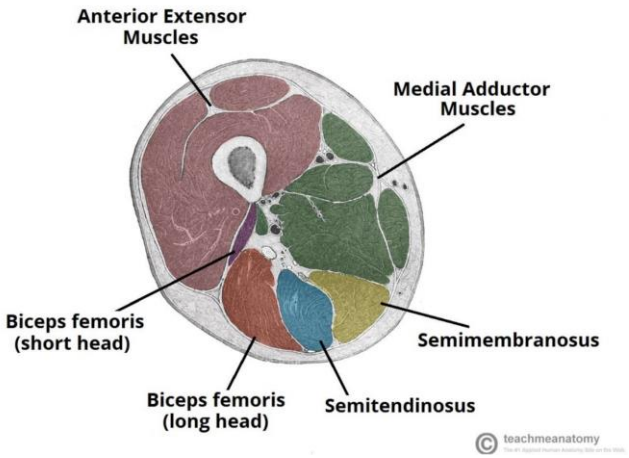

Three more muscles originate posteriorly namely the gastrocnemius, plantaris and popliteus muscles. The gastrocnemius originates at the posterior distal femur with the medial and lateral heads attaching just superior to the capsule in line with the medial and lateral condyles respectively. The gastrocnemius crosses the knee joint posteriorly to combine with the sartorius and attach to the calcaneus via the achilles tendon. Its action across the knee is to aid in flexion. The plantaris muscle originates just superiorly to the lateral head of the gastrocnemius on the posterior lateral condyle of the femur. It passes posterior to the knee and has negligible effects across the knee joint. The popliteus inserts on the proximal posterior medial aspect of the tibia and courses intraarticularly to originate on the lateral femoral condyle just anteriorly and distal to the LCL. Its primary action is to resist external rotation (ER) of the tibia on the femur. It unlocks and internally rotates (IR) the knee joint to initiate flexion and during the swing phase of gait. All three of these muscles are innervated by the tibial nerve.

Figure 1-7. Muscular anatomy from the lower leg that crosses the knee joint: Gastrocnemius (medial and lateral heads), Plantaris and Popliteus. Reprinted with permission from TeachMeAnatomy.com

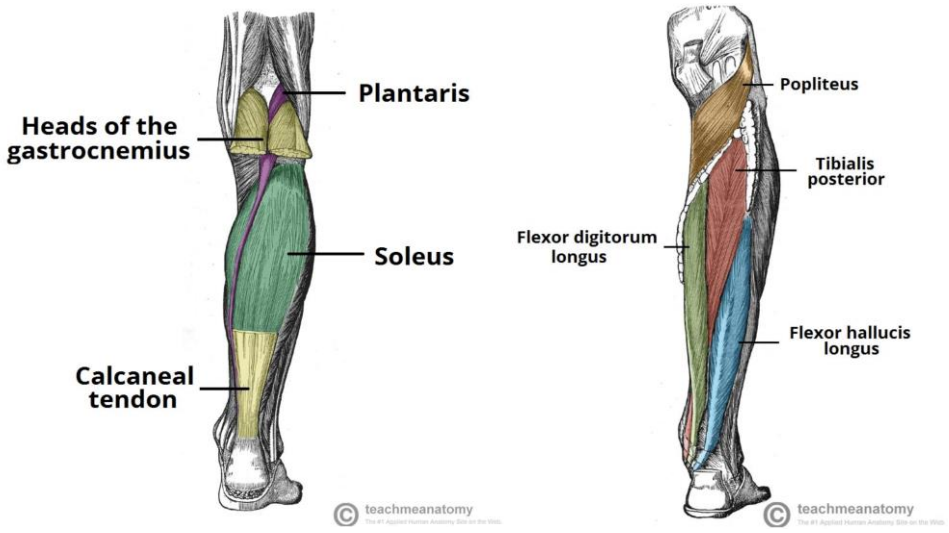

1.2.3 Ligaments

There are a multitude of ligaments and stabilizing structures around the knee joint; however, there are three main ligaments that affect the balancing in total knee arthroplasty. I will focus on these three ligaments: the posterior cruciate ligament (PCL), the lateral collateral ligament (LCL) and the medial collateral ligament (MCL). The anterior cruciate ligament (ACL) is also a very significant ligament that plays a role in the balance and biomechanics of the native knee joint. However, the ACL is sacrificed in the vast majority of total knee component designs today. Also the ACL often becomes deficient in patients with advanced osteoarthritic changes within their knee. The ACL is comprised of two bundles: the anteromedial and posterolateral. The anteromedial bundle is tight in knee flexion and lax in extension, while the posterolateral bundle is tight in extension and lax in flexion. It attaches to the posterior medial aspect of the lateral condyle of the femur and the anterior tibial eminence. It acts as the primary restraint to anterior tibial translation. Secondarily, it resists internal rotation (IR) of the tibia with respect to the femur and varus in extension.

Figure 1-8. Ligamentous anatomy of the primary stabilizing ligaments of the knee and the menisci. Reprinted with permission from TeachMeAnatomy.com

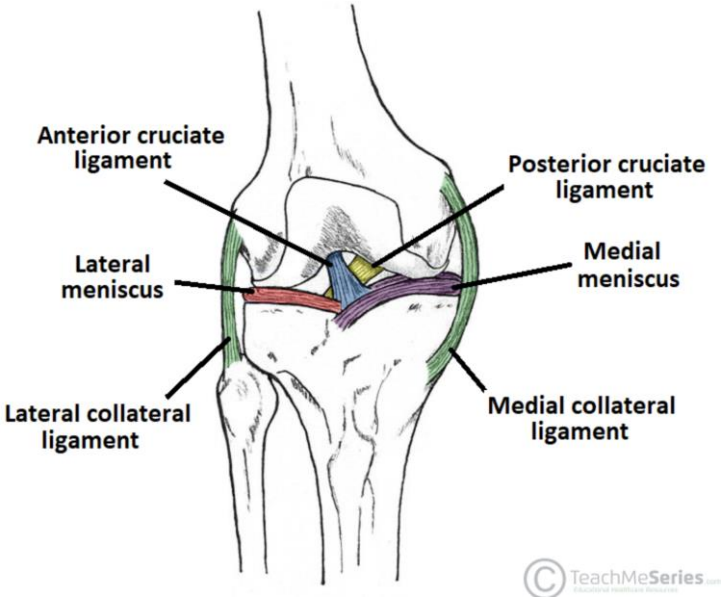

The PCL also plays a vital role in the biomechanics of the native knee and is either preserved or sacrificed in TKA. Occasionally, the PCL can be partially released to help balance a cruciate retaining (CR) knee. Some surgeons will prefer to use a cruciate sacrificing (CS) or anterior lipped poly to help compensate for the PCL release. If accidentally cut or with planned resection of the PCL, some surgeons will use a posterior stabilized (PS) poly which has a cam and post mechanism and substitutes the role of the PCL. This then allows adequate femoral rollback and deeper knee bend. The PCL is comprised of two bundles: the anterolateral and posteromedial bundle. The anterolateral bundle is tight in knee flexion and lax in extension, while the posteromedial bundle is tight in extension and lax in flexion. Traditionally it was thought that these bundles worked separately and distinctly from each other; however, more recent biomechanical studies have shown a more synergistic effect[13]. The primary action of the PCL is a restraint to posterior translation of the tibia on the femur. It secondarily resists internal rotation of the tibia with respect to the femur during normal joint kinematics and particularly between 90° and 120° of flexion. It is also a restraint to both IR and ER of the tibia on the femur when an external torque is applied to the knee[13]. The PCL also plays an important function in femoral roll back during flexion of the knee. The

attachment of the PCL is to the lateral aspect of the medial femoral condyle near the anterior aspect of the femoral notch. It attaches to the posterior proximal tibia within the intercondylar sulcus. The anterolateral bundle attaches anteriorly on the femur and lateral on the tibia in reference to the posteromedial bundle which in turn attaches posteriorly on the femur and medial on the tibia. The bundles have very distinct attachments on the femoral side, but become more confluent on the tibial side[13]. The femoral attachment is a broad, crescent-shaped area on average 30mm long and 5mm wide. The tibial attachment is central in the tibia within the intercondylar sulcus, and the proximal portion of the footprint starts approximately 10-15mm below the articular surface[13–15]. The average dimensions of the PCL are 38mm long and 13mm thick[14].

The MCL is essential for knee stability in the coronal plane. It must be protected at all times during primary total knee arthroplasty as complete release or iatrogenic injury to the MCL typically will require increased constraint in the total knee system to allow for adequate stability against valgus deformity. The MCL is also comprised of two separate bundles: the deep fibres and the superficial fibres (dMCL and sMCL respectively). The dMCL is also known as the medial capsular ligament. It is intimately involved with the joint capsule and the medial meniscus. Its primary role includes coronal stability of the knee but also stabilizes the medial meniscus and assists with rotational stability. It attaches to the femoral medial epicondyle just distal to the sMCL insertion and inserts to the proximal aspect of the medial tibial condyle as a part of and just distal to the capsular attachment approximately 6.5mm from the tibial joint line[16]. This femoral attachment is approximately 20mm from the femoral joint line and is about 9.9mm wide and 9.4mm long[16]. There are two sets of fibres, the meniscofemoral fibers and the meniscotibial fibres. These fibres attach to the medial meniscus through the coronary ligaments. The superficial medial collateral ligament is also known as the tibial collateral ligament. It also originates on the medial femoral epicondyle just proximal to the dMCL attachment. This is approximately 31mm from the femoral joint line and is about 11.8mm wide and 9.0mm long[16]. It runs on average 94.8mm long and attaches to the medial aspect of the tibia, running deep to the pes anserinus[17]. The tibial attachment starts between 4.6 and 6.2cm distal from the tibial joint line and has a large distal footprint, approximately 15mm wide and 31mm long[16,17]. The anterior fibres of the sMCL are tightened in the first

90° of flexion, and the posterior fibres of the sMCL are tightened in extension[14]. Complete release of the tibial attachment of the dMCL is routinely carried out to correct varus deformity in TKA. It can also be released simply because the resection of the proximal tibia eliminates the insertion point. The sMCL is essential to maintain coronal stability; it is the primary restraint to valgus force, especially at 30° of knee flexion. Its secondary function is to help stabilize against anterior tibial translation and IR. Partial release is often carried out to help balance the tension across the medial compartment of the knee.

The lateral collateral ligament is also a key structure to coronal stability of the knee. However, in valgus knees it can be released if required, and the knee can maintain stability secondary to the other lateral stabilizing structures. The LCL is also known as the fibular collateral ligament. Its primary function is to resist varus force to the knee and also helps resist ER and posterior displacement of the tibia. Resistance to varus deformity occurs throughout the full range of motion of the knee. During clinical assessment for competence of the LCL, placing the knee in flexion of 30° allows for the largest amount of laxity to be tested[18]. It attaches to the femur near the lateral epicondyle approximately 1.4mm superior and 3.1mm posterior to the epicondyle ridge[19]. It is superior and posterior to the popliteus insertion. It is a very tubular, cord-like structure that is approximately 3-5mm in diameter and 66mm long[14,19]. It attaches distally to the anterolateral aspect of the fibular head and covers approximately 38% of the fibular head width[18].

These ligaments greatly affect the load patterns across the tibiofemoral joint. The pattern in which ligaments respond to stress is explained initially by Blankevort *et al.* through their force displacement curve[20]. The initial load length and reference strain can help us understand the joint contact forces. However, there is great variation in the literature as to what the initial load length, reference strains, and stiffness of each of these ligaments are. In a review article by Peters *et al.* the multitude of values reported for ligament stiffness and reference strains were presented[21]. Through examining the different papers, the ligament models that were used had significant variation as to the age and conditions of the ligaments that were initially examined. We elected in this project to use the stiffness

and reference strains from Smith *et al.* as the specimens that were used in his study were elderly patients who had osteoarthritic changes within their joints[22]. This is likely to represent the patients we are studying more closely. Stiffness is reported in N/strain as strain is mm/mm and is a unitless value. In Smith *et al.* the stiffness for the aPCL and pPCL is 5700N/strain and 2400N/strain respectively, with a reference strain of 0.01% and -0.06% respectively. In the setting of ligament strain, a negative strain does not mean the ligament creates a compressive force. It is an indication that there is no tension across the ligament in the specific reference pose. During flexion or extension from that reference pose the ligament length will vary. When there is tension across the ligament the strain will become a positive value. The sMCL and dMCL have a stiffness of 2200N/strain and 2800N/strain respectively with a reference strain of 0.03% each. The LCL has a stiffness of 1800N/strain and a reference strain of 0.06%[22]. The reference strains, stiffnesses, and zero load lengths for our virtual ligaments were adapted from these values and calculated to match our computational models to give ideal realistic ligamentous properties.

1.2.4 Cartilage

The knee joint articular surface is comprised of hyaline cartilage. Hyaline cartilage is an extremely smooth surface that covers the bone ends to allow the articulating surfaces to glide on each other in a nearly frictionless way. It allows for load distribution throughout the joint. When free of disease or defect, it allows the joint to move in a painless fashion. It is comprised of water (about 80% of its weight), collagen (mostly type II), proteoglycans, and chondrocytes. Articular cartilage is avascular and receives its nutrition from the synovial fluid at the surface and the subchondral bone at its base. Its healing capacity is significantly limited, and thus treatment of cartilage disease or defect is limited. Severe damage to cartilage will occasionally repair with fibrocartilage if the damage is deep (to the subchondral bone), but the body is unable to regrow or heal hyaline cartilage.

1.2.5 Capsule and Synovium

All synovial joints are surrounded by a joint capsule to maintain the synovial fluid within the joint and to aid in joint stability. Ligaments are often intimately involved as

thickenings of the capsule which help maintain the stability of the joint. Lining the inside of the capsule, there is an inner membrane called the synovium. This lining makes synovial fluid through filtering plasma. This allows for the synovial fluid to maintain nutrient exchange from the blood. The synovial fluid acts as a lubricant for the articular surfaces and provides the cartilage with nutrients through diffusion. In diseased states or during inflammation, the synovial lining may become thickened and the synovial production can be increased. This may lead to an enlarged swollen joint as is often seen in osteoarthritis. As the joint capsule contains the effusion, the capsule can become taught and stretched limiting range of motion and causing pain.

Figure 1-9. Location of the capsule and synovial membrane of the knee. (A) Anterior projection. (B) lateral projection. Reprinted with permission from Campbell's Operative Orthopaedics 13th ed.

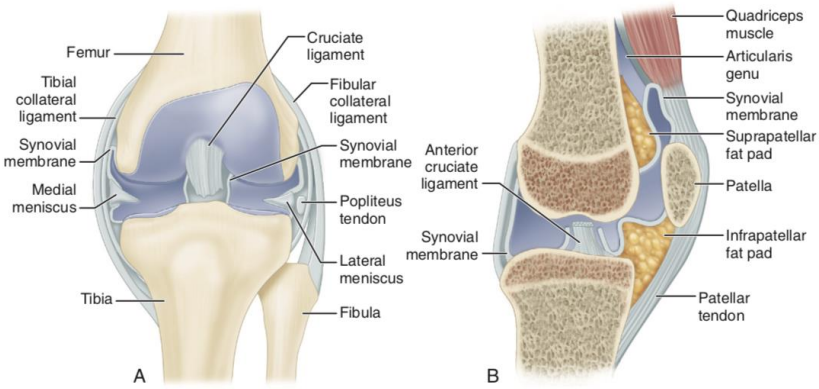

1.2.6 Cutaneous and articular innervation

Superficial sensation over the anterior portion of the knee is provided by a plexus of nerves called the peripatellar plexus. It arises from connections made by branches of the saphenous nerve becoming the infrapatellar branch as it courses medial to anterior. There are also branches from the medial femoral cutaneous, intermediate femoral cutaneous (anterior coverage), and lateral femoral cutaneous. The posterior skin is innervated by the posterior cutaneous nerve of the thigh. During TKA surgery, the anterior skin nerves are cut often leaving patients with a permanent numb patch of skin anterolaterally.

The articular innervation is primarily through the geniculate nerve system. These nerves often run with the geniculate arteries as well. The posterior geniculate nerve arises from a branch of the posterior obturator nerve. The superolateral and inferolateral geniculate nerves branch off of the common peroneal nerve. The superomedial and inferomedial geniculate nerves are branches from the saphenous nerve.

1.2.7 Blood Supply

There is a large network of anastomosing arteries that surround the knee to provide the knee joint with arterial blood flow. This primarily is compromised of the geniculate arteries with a few other supplemental vessels. The descending geniculate artery is the first to supply the knee branching off of the superficial femoral artery. The popliteal artery then provides the superior, middle, and inferior geniculate arteries. The medial and lateral superior geniculate artery branches superficially and deep wrapping from posterior to anterior to supply the anterior portion of the knee. The deep medial superior geniculate arteries anastomose with branches of the descending geniculate artery and the medial inferior geniculate artery. The middle geniculate artery branches off the popliteal artery as well and provides blood flow to the cruciate ligaments and the synovium. The medial and lateral inferior geniculate arteries also branch off the popliteal artery. The lateral inferior geniculate anastomoses with the lateral superior and medial inferior geniculate arteries. There is also anastomoses with the anterior and posterior recurrent tibial arteries, which are branches of the anterior tibial artery, and circumflex fibular artery, which is a branch of the posterior tibial artery.

1.3 Biomechanics of the native knee

The knee is not a simple hinge joint. It is an inherently unstable joint and relies heavily on the dynamic and static stabilizing structures around the knee to keep it stabilized. There is little boney congruity to aid with stabilization. Static stabilizers include: both bundles of the ACL and PCL, sMCL, dMCL, posterior oblique ligament, LCL, arcuate ligament, and iliotibial band. Dynamic stabilizers of the knee include: semimembranosus, semitendinosus, gracilis, sartorius, popliteus, medial and lateral head of gastrocnemius, biceps femoris, vastus medialis and lateralis, and the extensor mechanism.

Knee motion is a complex combination of six degrees of freedom. It is not just flexion and extension, but there is also IR/ER, varus/valgus, anterior/posterior (A/P) translation, medial/lateral translation, and compression/distraction. Flexion and extension are the primary motions of the knee. In order for the knee to fully flex, there needs to be an element of A/P translation. The femur needs to roll back and slide on the tibia to allow deep flexion. Femoral roll back is defined as the combination of shifting the tibial femoral contact point and the joint axis simultaneously[10]. The cruciate ligaments (primarily the PCL) control the roll/glide motion. This is the main reason why TKA implants either retain the PCL or compensate for it. Without posterior translation, deep flexion would be unachievable. Normal range of motion is from -5 to 140-165° of flexion[23]. This means the knee normally goes into 5° of hyperextension and will bend all the way up to 160°. Full range of motion allows for normal function; for example, 93-115° is ideal for getting out of a chair and a minimum of 90° is needed for stair ascent and descent[10,11].

Throughout the full range of motion there is approximately 10-15 total degrees of IR/ER combined. While the knee goes through the swing phase of gait, the tibia is internally rotated. As the foot hits the ground and leg extends into full extension, the "screw home mechanism" caused by the larger more congruent medial femoral condyle (MFC) externally rotates the tibia on the femur. This tightens the cruciate ligaments and stabilizes the knee in the stance phase. In order to "unlock" the knee and initiate knee flexion, the popliteus muscle IRs the tibia loosening the cruciates and allowing the knee to initiate flexion. In relation to the IR/ER throughout the range of motion, there is a helical pattern of motion between the condyles and a varying amount of translation. The medial femoral condyle translates approximately 2mm posteriorly while the lateral femoral condyle (LFC) will translate approximately 21mm on the tibia[11]. More recent studies have shown even higher posterior translation of the MFC up to about 10mm with deep knee bend between 120° to 140° and only 5mm of posterior translation in the LFC – this still results in approximately 5° of IR overall[23,24]. There is also close to 10° of variation in varus and valgus alignment of the knee during gait as can be seen in Figure 1-10 from Campbell's operative orthopedics[11]. The MCL stabilizes the knee to valgus stress and the LCL stabilizes the knee to varus stress. However, in normal knees there can

be 5mm of laxity in both these structures in full extension[10]. Also, as the knee flexes there are different bundles of the collateral ligaments that become taught or loose[25].

Figure 1-10. Biomechanics of the native knee during gait. Reprinted with permission from Campbell's Operative Orthopaedics 13th ed.

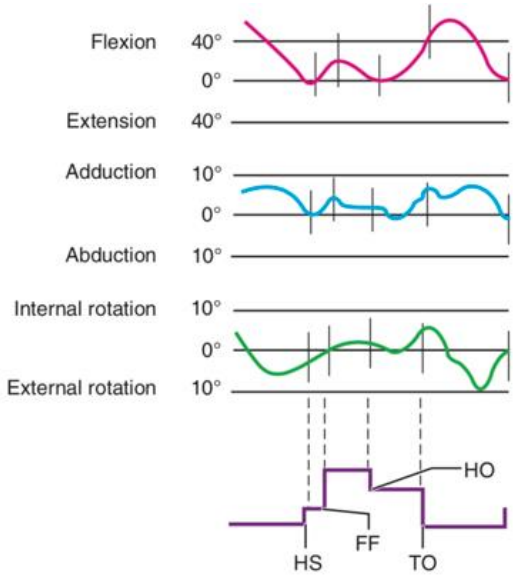

FIGURE 7-12 Triaxial motion of normal knee during walking, as measured by electrogoniometer. Flexion and extension are about 70 degrees during swing phase and 20 degrees during stance phase. About 10 degrees of abduction and adduction and 10 to 15 degrees of internal and external rotation occur during each gait cycle. FF, flatfoot; HO, heel-off; HS, heel-strike; TO, toe-off.

Throughout the range of motion, the static stabilizers or ligaments take on large forces to maintain the joint stability. In normal gait the average maximum forces on these ligaments are: PCL 329N, ACL 154N, MCL 62N, and LCL 235N[14]. Other motions can drastically increase the tension across these ligaments. For example, the PCL force can go up to 1,868N during a two legged squat[14]. Peak ACL forces are at 30-45° of flexion whereas peak PCL forces occur from 90° of flexion and above. Tibiofemoral joint contact pressures vary throughout different activities and can be as high as 5-10 times body weight with stair ascent and descent and jumping activities[11]. Also, in normal gait simulation with normal knee anatomy the medial compartment experiences higher joint contact forces than the lateral compartment does[26].

1.4 Knee Osteoarthritis

Arthritis, in general, is a medical or structural condition causing inflammation and pain within a joint. There are a multitude of causes for arthritis. Some of the most common types of arthritis are: rheumatoid arthritis, seronegative spondyloarthropathies, osteoarthritis, and post-traumatic or secondary osteoarthritis. Arthritis presents with the following signs and symptoms: joint pain, effusion or swelling, stiffness or decreased range of motion, erythema, decreased function, and substantial disability.

In Canada, arthritis is the most common chronic condition affecting about 20% of the population (6 million people). This number is projected to climb to 9 million people by 2040. Arthritis is found predominantly in women, with 23% of women affected and 17% of men being affected[27]. Although arthritis is commonly known to affect the elderly, more than half (55%) of people affected are under the age of 65. In the knee, the most common forms of arthritis are osteoarthritis, rheumatoid arthritis, and post-traumatic arthritis.

Osteoarthritis (OA) can be defined as degenerative disease of synovial joints causing progressive wear, erosion, or deterioration of articular cartilage. The pathophysiology of OA begins with increased water content, disorganized collagen, and subsequent proteoglycan breakdown. Mild synovial inflammation progresses to severe synovial inflammation and thickening. As cartilage breaks down and thins, more stress is transferred to the subchondral bone. Subchondral bone attempts to remodel causing sclerosis and, in late stages, subchondral cysts. Increased pressure on the periarticular bone causes osteophyte formation which can lead to further pain and stiffness. Primary OA is idiopathic and is most common in the elderly population. Secondary OA is due to another underlying condition (most commonly post-traumatic).

Figure 1-11. Normal healthy knee (left) and Osteoarthritic knee (right) with cardinal changes shown of osteophytes (bone spurs), cartilage loss and joint space

narrowing. Reproduced with permission from OrthoInfo © American Academy of Orthopaedic Surgeons. http://orthoinfo.aaos.org

Risk factors for OA are both modifiable and non-modifiable. Some of the modifiable risk factors are: obesity, muscle weakness, metabolic syndrome, occupation (with repetitive knee bending or heavy loads), dyslipidemia, hypertension, and elevated blood sugar levels. Some non-modifiable risk factors are: gender (females>males), increased age, genetics, and race.

People who present with osteoarthritis most commonly complain of pain. Initially it is pain related to activity or weightbearing exercises. They often experience stiffness after sitting or being immobilized and need to "warm up" their joint to have it feel better. With excessive activity they can get severe pain, swelling, and erythema. The pain limits their function and many become unable to tolerate walking significant distances or climbing up and down stairs. OA can be severely debilitating and limit an individual's ability to perform their activities of daily living. As the disease progresses, patients begin to complain of pain at rest and even at night that is severe enough to wake them from sleep. They often become stiff and lose range of motion of the knee. Patients often complain of mechanical symptoms such as grinding, catching, or giving way of their knee. OA can lead to progressive deformity in the lower extremity, with varus deformity at the knee most common. However, patients can present with valgus deformities, flexion

contractures, or recurvatum as well. With severe deformity, the knee can become unstable if ligaments become attenuated to the point where they are incompetent.

Treatment of OA begins with conservative measures, and all conservative measures should be exhausted before TKA should be carried out[28]. Conservative management consists of land-based exercise programs or physiotherapy, topical ointments, nutraceuticals agents can be tried with little harm (eg. chondroitin, glucosamine and turmeric), pharmaceutical agents (eg. NSAIDS, acetaminophen, Tramadol), activity modification, bracing, and walking aids. Intraarticular injections have been proven to be beneficial to patients symptoms, specifically corticosteroid and high molecular weight hyaluronic acid derivatives. Evidence is currently inadequate, but other injections of protein rich plasma and stem cells are gaining popularity. Cannabis products are also becoming popular, but there is no significant amount of evidence to back this up currently. There is no cure for OA other than to cut away and replace the diseased portion of bone in the form of arthroplasty. Arthroplasty can be performed on a portion of the joint (eg. unicondylar arthroplasty or patellofemoral arthroplasty), or the total joint can be replaced.

1.5 Knee Radiographic imaging[10]

Radiographic imaging is fundamental to diagnosis and monitoring progression of OA as well as preoperative planning for arthroplasty. OA can be identified on x-ray with asymmetric joint space narrowing, osteophyte formation, subchondral sclerosis, and subchondral cyst in advanced cases. In order to appropriately assess the knee for OA and alignment, weightbearing films should be used that allow visualization of all three compartments in the knee (medial, lateral, and patellofemoral compartments). The standard views for assessing arthritis are a three-foot standing view or hip-to-ankle view, AP, Tunnel, Lateral, and skyline.

Hip-to-ankle or three-foot standing views are important for overall assessment of the limb alignment. From this view, pre-operative varus or valgus deformity can be calculated. It is also helpful for visualizing extraarticular deformity that may need to be corrected

during the TKA. These views can also be used to mark out mechanical and anatomic axis to help with planning for bone cuts.

Figure 1-12. Example of a 3 foot standing or Hip to ankle view. Allows proper assessment of lower extremity alignment. As can be seen here the Right leg (left of picture) is in slight valgus and the left leg is in slight varus

AP view is routine view of the knee to assess for initial arthritic changes within the knee. It allows for visualization of the medial and lateral compartments of the knee. It gives an indication of the cartilage health which is an extrapolation from the available joint space. This information gives an indication of the weight bearing surface of the distal femur in full extension.

Figure 1-13. Example of AP weightbearing views. Best for assessing distal femoral cartilage health as knees are in full extension. Left knee (right of picture) shows significant medial joint space narrowing

Tunnel views are a PA x-ray with the knees bent to 45°. This gives supplemental information to the AP but allows evaluation of the cartilage on a more posterior portion of the femoral condyles, which is an area that is often more affected by osteoarthritis. This view also helps visualize the joint space between the tibia and the femur as it brings the posterior slope of the tibia into better perspective.

Figure 1-14. Example of a Tunnel view with knees bent to 45°. This allows for better assessment of the posterior condylar cartilage surface. This difference can be seen in the Right knee where there is marked narrowing of the lateral compartment joint space in flexion when compared to the previous AP weightbearing film in Figure 1-13

Skyline view is an x-ray taken with the knee bent to 30° and the x-ray beam directed vertically (from inferior to superior) through the anterior knee. This gives a straight

through shot of the patellofemoral compartment and allows for evaluation of the joint space and cartilage health in the patellofemoral compartment. It also gives information about the patellar tracking preoperatively.

Figure 1-15. Example of a skyline view. This view is taken down the vertical axis of the Patellofemoral joint allowing assessment of the joint space and patellar tracking

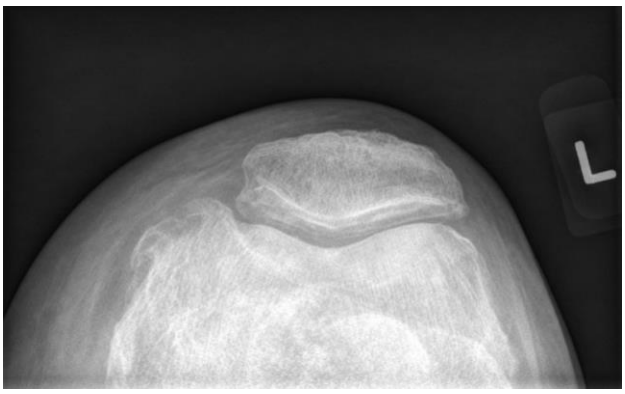

Lateral view is usually done with the knee in approx. 30° of flexion. It allows for assessment of the joint space of all three compartments. However, the information from these compartments is overlapped and not as clear as the AP, Tunnel, and skyline views. The lateral is great for visualizing posterior osteophyte formation, extensor mechanism characteristics, or causes of decreased range of motion. The lateral is also important for preoperative templating and allows for assessment of the AP dimensions of the femoral component. To assess the tibial slope, the lateral view is critical.

Figure 1-16. Example of a Lateral view. This view allows some visualization of all three compartments, posterior osteophytes, tibial slope, extensor mechanism position and is used commonly for pre-op templating

In certain scenarios, CT scans and MRI scans can be used to aid in the diagnosis and preoperative planning. This is especially pertinent in cases where there is significant deformity and a possible large boney defect or soft tissue compromise. There is the possibility that conventional instrumentation may not be able to be used and navigation or patient specific instrumentation is required. Some of these techniques require a preoperative CT or MRI scan for proper surgical planning.

1.6 Knee alignment[10,11]

Knee alignment plays an important role in knee function. There are many diseases (eg. degenerative, inflammatory, trauma, and congenital) that can affect the alignment of the knees. This can lead to pain and decreased function. In the setting of osteoarthritis, the native knee alignment can be disrupted. The most common deformity of alignment is genu varum. This can be the patients normal (physiologic) alignment or caused by intraarticular pathology. A working knowledge of the normal lower extremity alignment is important for surgeons performing TKA. As alignment is often disrupted by osteoarthritis, one of the goals of TKA is to restore alignment.

The normal alignment of the lower extremity is on average 3° of overall valgus as compared to the vertical line of the body. The mechanical axis of the lower extremity is defined by a line from the center of the femoral head to the center of the talus.

The femur has a mechanical axis which is 3° from the vertical line. The mechanical axis of the femur runs from the center of the femoral head to the middle of the intercondylar notch. The anatomic axis of the femur is 9° from the vertical axis of the body. The anatomic axis is defined by a line from the piriformis fossa to the middle of the intercondylar notch running directly thought the middle of the medullary canal. The difference between the mechanical axis and the anatomical axis of the femur is 6+/-2°. The condyles of the distal femur are aligned in 3° of valgus from the mechanical axis. This gives a distal femoral articular surface that is 81° from the anatomical axis.

The tibia has a mechanical axis that matches the anatomical axis. This is defined by a line that runs from the center of the tibial plateau to the center of the tibial plafond. The articular surface of the proximal tibia is in 3° of varus to the mechanical and anatomical axis of the tibia. A summary of these angles can be seen in Figure 1-177 below[11].

Figure 1-17. Summary of the mechanical and anatomic axis of the lower extremity. Reprinted with permission from Campbell's Operative Orthopaedics 13th ed.

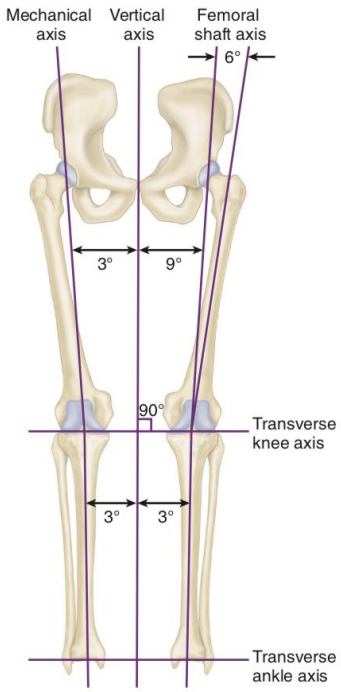

FIGURE 7-18 Mechanical axis of lower limb extends from center of femoral head to center of ankle joint and passes near or through center of knee. It is in 3 degrees of valgus from vertical axis of body. Anatomic axis of femur is in 6 degrees of valgus from mechanical axis of lower limb and 9 degrees of valgus from true vertical axis of body. Anatomic axis of tibia lies in 2 to 3 degrees of varus from vertical axis of body.

There is variation in these numbers among individuals. A 3-foot standing x-ray or hip-to-ankle x-ray can be used to measure these alignment values to help in preoperative planning for TKA and restoration of the lower limb alignment. This x-ray can also be used to measure the alignment at the knee. A line along the mechanical axis of the lower extremity will give an indication if the overall alignment of the leg is in varus or valgus. With neutral alignment the line will pass through the center of the knee. If this line passes through the medial compartment or medial to the knee, the lower extremity is in varus. If the line passes through the lateral compartment or lateral to the knee, the lower extremity is in valgus. Each person's overall limb alignment is specific to them, both in a native or in a diseased state. Recently, the idea of physiologic varus has gained interest. It has been defined as lower limb alignment of 3° of varus or greater. Bellemans et al. first described constitutional or physiologic varus in asymptomatic, healthy individuals. They stated that 32% of males and 17% of females had constitutional varus[29]. More recent literature has indicated that the incidence of physiologic varus among patients with medial OA may

be as high as 46% in males and 23% of females[30,31]. It has also been shown that patients with physiologic varus are at increased risk of developing medial compartment end stage osteoarthritis. This positive correlation between physiologic varus and varus osteoarthritis is more pronounced in the male population compared to females[30].

If the knee is in varus or valgus, the coronal alignment of the knee can be calculated during preoperative planning. This is done by measuring the angle between the mechanical axis of the femur and the mechanical axis of the tibia. Depending on the surgeons preference, one of the aims of the surgery is to restore the normal anatomical alignment of the knee, or to restore the knee to a neutral alignment in reference to the mechanical axis of the lower extremity.

The sagittal alignment of the knee is also important to ensure that the knee does not fall into recurvatum. The distal femoral flexion angle is approximately 3-5° from the mechanical axis. It is important to assess the flexion of the femur on the lateral x-ray and during TKA to place the femoral component in the same anatomical flexion. Extending the femoral component can lead to notching the anterior cortex of the distal femur or anterior translation of the femoral component and subsequent overstuffing of the patellofemoral joint, whereas too much flexion of the component can lead to a tight flexion space. The posterior tibial slope in a normal joint is approximately 7°. Changes to the tibial slope can affect the stability and range of motion of a TKA. It is important to assess a patients normal slope on sagittal x-ray and for a surgeon to know the aim for posterior slope depending on what type of TKA implant used.

1.7 Total Knee Arthroplasty

After conservative measures have been exhausted, total knee arthroplasty is the gold standard surgical management for end stage tricompartmental arthritic pain. TKA (along with THA) is one of the surgical success stories of modern times. It has revolutionized management of arthritic pain and improved the quality of life of countless individuals since its advent. The very first knee arthroplasty was a hinged prosthesis made of ivory, created by a German surgeon, Themistocles Gluck, in 1860[3]. Since then, there has been much improvement in the design. The TKA that we know today really blossomed in the

1970's when the total condylar design began to take root. Over the last 50 years there have been major advances in the design and instrumentation of the TKA. Also, the perioperative protocols have improved, which has drastically improved surgical outcomes. Today many patients benefit from enhanced quality of life and restoration of knee function. It is predicted that 3.48 million TKA procedures will be performed annually by 2030[1].

TKA is a very successful surgery with great outcomes. Despite this, there are still some patients that are dissatisfied postoperatively. This is one of the most common postoperative complaints from patients. The difficulty is the fact that this is a subjective finding and is hard to predict which patients will have persistent pain after their surgery. Approximately 15-20% of patients have difficulty obtaining normal function secondary to pain, limited motion, or arthrofibrosis[2,3]. Although the strongest predictor for dissatisfaction with postoperative pain and function was that the patients expectations were not met [2], the dissatisfaction in TKA function is even higher. As even more patients are dissatisfied with the function, altered knee mechanics may be the source of patient dissatisfaction. TKA is ultimately a mechanical joint and does not exactly reproduce the anatomy or biomechanical function of the native knee. The advancement in surgical technique and component design has brought TKA closer to native joint kinematics, but there still remains a significant amount of people dissatisfied with their function. With altered biomechanical function possibly being a source of patient dissatisfaction, we are therefore endeavoring to look at the biomechanics of different TKA implants and alignments.

Over the history of TKA, the reason for revision has changed. Most recent data shows that aseptic loosening, infection, and instability are the top three reasons for revision[6,7]. Aseptic loosening may be secondary to soft tissue imbalance and improper joint biomechanics. Suffice it to say that with instability still as the third most common reason for revision and aseptic loosening potentially arising from abnormal biomechanics, addressing alignment and ligament balancing to improve TKA stability may help decrease the reasons for revision TKA.

1.8 Surgical Approach

The medial parapatellar approach is the most commonly used surgical approach for knee arthroplasty. There are multiple other options to obtain access to the knee joint. However the medial parapatellar approach gives excellent exposure and allows for efficient use of all instrument techniques and implant options. The medial parapatellar approach also has extensile options to allow adequate exposure for most knee revisions.

Figure 1-18. Example of the medial parapatellar approach, the most common surgical approach to the knee for performing a Total Knee Arthroplasty. Reprinted with permission from Campbell's Operative Orthopaedics 13th ed.

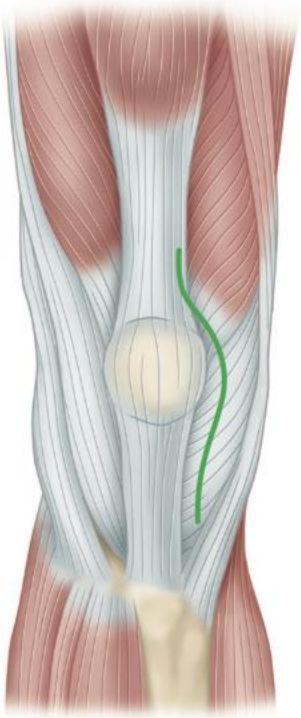

To perform a medial parapatellar approach, the skin is incised midline centered over the patella and extending on average from 10cm above the patella to the medial border of the tibial tubercle. Full thickness skin flaps may be raised if needed to fully expose the extensor mechanism. The proximal portion of the arthrotomy is started longitudinally through the quads tendon and carried distally, hugging closely to the Vastus medialis origin. Careful dissection should be carried out to avoid going into the muscle and

maintaining a sleeve of tendon on the muscle side of the arthrotomy and the superior medial pole of the patella side. This will allow for strong closure of the arthrotomy. From the superior medial corner of the patella, dissection is carried down along the medial side of the patella and patellar tendon to the medial border of the tibial tubercle. This medial parapatellar arthrotomy allows full access to the joint and facilitates carrying out a medial soft tissue release for the most common varus knee deformity. Often a complete release of the deep MCL off the proximal tibia is performed and selectively a partial release of the superficial MCL dependent upon the patients deformity. From this exposure, the arthrotomy can also be extended in the revision setting for better access. This can be carried out with a quads snip, V-Y turndown, or a tibial tubercle osteotomy. The quads snip allows for recovery and quads muscle strength equal to a standard medial parapatellar arthrotomy[11].

Some of the other approach options for knee arthroplasty include: medial midvastus, medial subvastus, lateral parapatellar and far lateral sub vastus. The medial midvastus and subvastus were first described in hopes of reducing patellofemoral complications and expediting quads recovery postop[32,33]. These approaches preserve more of the blood supply to the patella through the supreme genicular artery. Relative contraindications to these approaches include obesity, previous high tibial osteotomy, and knee flexion of 80° or less[11]. Careful hemostasis is necessary as the most common complication with these approaches is postop hematoma. The lateral parapatellar approach is used by some surgeons regularly for valgus knee deformities. The far lateral approach is useful in the setting of distal or total femoral replacement. It is a fully extensile approach that allows for exposure proximally to the hip joint.

Completion of total knee arthroplasty is carried out with various means of instrumentation. The most common instrumentation being used today is the conventional intramedullary and extramedullary cutting jigs that have been used and modified since the advent of TKA. Conventional instrumentation has multiple benefits. It is most familiar to surgeons across the world. It is associated with the lowest cost among the different instrumentation tools. Usually the femoral bone cuts are determined through an intramedullary guide and are based off of the anatomical axis. Rarely the femoral cuts are

determined using an extramedullary jig. On the tibial side, extramedullary guides are used commonly in the primary joint replacement setting and intramedullary guides are used occasionally in primary joint replacement depending on the surgeon's preference. Intramedullary guides are used almost exclusively in revision settings. The conventional instruments require physical reference off boney landmarks to guide the appropriate cuts.

As technology has advanced substantially in the 21st century, newer forms of instrumentation for carrying out TKA have evolved. These include, but are not limited to: navigation, robotics, and patient specific instrumentation. Navigation relies on computer assistance trackers in determining anatomical landmarks in the knee. This then guides the placement of the cutting jigs on the bone, and the alignment is referenced off the values as depicted by the computer. Navigation tools are helpful for establishing coronal plane and sagittal plane cuts. Only some systems are helpful in determining the rotation of either femoral or tibial components. Robotics is a more recent application of technology, with a range of tools and philosophies such as active cutting tools, 3D imaging based navigation, or mounted cutting guides. It is postulated that the surgeon can make precise cuts assisted by a robotic instrument. Patient specific instrumentation (PSI) refers to cutting blocks that are created specifically to the patients anatomy and the preoperative templating carried out by the surgeon. PSI requires either CT or MRI scans prior to surgery to make the cutting blocks and the preoperative templating to be done. There is a significant time delay with PSI because the cutting blocks are made uniquely for each patient. PSI helps perform the initial distal femur and proximal tibial cuts to establish the overall alignment of the lower extremity. However, the balancing and the component rotation is finished with conventional instruments and cutting blocks. No matter which instrumentation technique is used, one of the main goals of TKA is to perform a stable knee through a range of motion with either a neutral mechanical axis or kinematic alignment.

1.9 Surgical alignment technique

Osteoarthritis often leads to significant deformity in the knee. Most commonly a varus deformity is present. The primary goal of TKA is to relieve pain through a stable range of motion, typically with a restoration of the alignment of the knee. Traditionally the

alignment target has been to bring the lower extremity into a neutral alignment. This is accomplished by making bone cuts and subsequently the joint line of the knee perpendicular to the mechanical axis of the lower extremity. This mechanically neutral alignment (MA) was performed ubiquitously since knee replacements originated. Mechanically neutral aligned knees allow for a "biomechanically friendly [to the implant] knee" and align the extensor mechanism helping prevent patellar instability[34]. One major benefit to having the implants perpendicular to the mechanical axis is that this allows for even force distribution across the implant thus allowing for an even wear pattern and decreased risk of component loosening or failure[34]. This was a significant issue with early component designs. However, with the more recent advent of better bearing surfaces, the idea of mechanical alignment has been challenged. It is also thought that mechanical alignment significantly alters the native ligamentous balance of the knee, causing delayed instability and liftoff. There have been a few newly proposed alignment techniques, namely: anatomic alignment (AA), adjusted mechanical alignment (aMA), kinematic alignment (KA), and restricted kinematic alignment. In this thesis, I will focus on mechanical and kinematic alignment.

Kinematic alignment was introduced to potentially improve the natural gait kinematics and functional outcome of TKAs. Kinematic alignment is a patient specific approach attempting to restore the patients native pre-arthritic joint line and alignment. This is challenging because there are some assumptions needed as to what each patients specific pre-arthritic joint line and alignment is. Kinematic alignment is primarily a bone procedure while the ligaments are spared. Only under exceptional circumstances are ligament releases required[35]. The aim is to have totally anatomically positioned components that can be likened to a true resurfacing of the knee joint[36]. This can be accomplished by focusing on three main goals: firstly, to set the alignment of the femoral and tibial components to match the native tibiofemoral articular surface in all 6 degrees of motion; secondly, to restore the native limb and knee joint alignment; and thirdly, to restore the native laxities of the knee[37], which have been previously reported as tighter in extension and looser through flexion[37,38] (however, this may be more a result of the femoral roll back and near subluxation of the tibiofemoral joint[23]). The differences in surgical techniques can be seen in the table from Riviere et al[34].

Table 1-1. Table produced by Riviere et al[34]. Indicating some of the technical differences between performing a Kinematically aligned (KA) TKA or a Mechanically aligned (MA) TKA

Table 1
Technical differences between mechanic and kinematic alignment techniques.

	KA technique "patient specific approach"	MA technique "systematic approach"
F component sagittal rotational positioning (F distal cut)	Follow F bowing (3° flexion relative to the sagittal F mechanical axis)	Follow F bowing (3° flexion relative to the sagittal F mechanical axis)
F component frontal rotational positioning (F distal cut)	Parallel to the frontal femoral slope after correction for wear	Perpendicular to the femoral mechanical axis
F component horizontal rotational positioning (F anterior and posterior cuts}	Neutral rotation relative to PCL Measured resection technique only	External rotation relative to PCL Measured resection or gap-balancing techniques
F component anteroposterior translational positioning	Posterior referencing technique only (compromise done on the trochlear offset)	Posterior or anterior referencing techniques (compromise done on the flexion gap or on the trochlear offset)
F component mediolateral translational positioning	Centered on the notch	Centered on the notch or slightly lateralized to optimize patella tracking
T component frontal rotational positioning (Tcut)	Parallel to the frontal tibial slope after correction for wear (no attention is paid to the ankle)	Perpendicular to the tibial mechanical axis
T component sagittal rotational positioning (T cut)	Parallel to medial plateau slope	Between 2 and 7° posterior slope relative to the sagittal T mechanical axis
T component horizontal rotational positioning	Parallel to lateral plateau axis [no attention is paid to ATT)	Towards ATT
FT soft tissues balancing	No (goal is to restore constitutional knee laxity in flexion and extension)	Often (goal is to obtain rectangular symmetric flexion and extension gaps)
PF soft tissues balancing	No	Often

It has been proposed the KA might be an option to improve functional outcomes for patients post TKA. Some studies have shown that KA allows faster recovery, better functional scores, flexion, feelings of normality, and similar revision rates to MA[34,37]. Total knees with KA minimized abnormal contact kinematics because of the natural alignment of the femoral and tibial components, thus proposing better prognosis for long-term implant survival[36]. However, a recent meta-analysis also shows that there is no significant difference in functional, radiological, and perioperative results or complications between KA versus MA[39]. Also, a systematic review that showed KA may compromise loading vectors, increase risk of aseptic loosening, and FEA (finite element analysis) modelling has shown abnormal bone strain[40]. The potential advantages, clinical improvement, and possible concerns can be seen in the summary table by Riviere et al[34].

Table 1-2. Table produced by Riviere et al[34]. Indicating their ideas of potential advantages, clinical improvements and possible concerns between kinematically aligned and mechanically aligned TKA

Table 4
Advantages, evidence of clinical improvement, and potential concerns of the kinematic alignment technique for total knee arthroplasty (TKA) in comparison with the mechanical alignment technique.

Advantages	Clinical improvements	Potential concerns
Patient-specific implant positioning likely to restore the constitutional femorotibial alignment and laxity → Better femorotibial kinematics Higher surgical reproducibility	Faster recovery Better functional results: higher knee scores; less residual pain; higher flexion; more forgotten knee; higher patient satisfaction Easier revision of medial UKA to TKA	Severe constitutional varus or valgus deformities Severe tibial plateau varus Pathoanatomy favoring patella instability Trochlea design of current TKA implants

UKA: Unicompartmental Knee Arthroplasty.

1.10 Knee balancing in TKA

No matter which alignment technique is chosen for a total knee arthroplasty, balancing the soft tissues is an essential step in the procedure. It has been said that total knee arthroplasty is a soft-tissue procedure with boney work. Soft tissue balancing has been defined as a knee with the following characteristics: 1) Full range of motion, 2) Symmetrical medial and lateral ligament tension in extension and 90° of flexion with rectangular shaped tibiofemoral gap, 3) Correct varus/valgus alignment in both flexion and extension, 4) Well tracking patella throughout the full range of motion, 5) Maximal flexion with the patella reduced and appropriate femoral roll back on the tibia, 6) Correct rotational balance between the femoral and tibial components[41]. Deformity associated with osteoarthritis can lead to irreversible shortening of ligaments on the concave side of the deformity and lengthening of the ligaments on the convex side. Balancing of the soft tissues is usually performed by appropriate bone cuts, removal of all osteophytes, and progressive ligament releases. Rarely repair, transposition, or tightening of slack ligaments is also performed. Balancing the soft tissues around the knee will lead to favorable results with function, alignment, stability, wear, aseptic loosening, increased range of motion, proprioception, and pain. Improvement in all these areas can lessen the risk for revision surgery[41].

There are two main methods for balancing the soft tissues in TKA; the first is measured resection, and the other is gap balancing. In measured resection, the primary goal is to make standardized cuts on the femur and tibia based on boney anatomy and landmarks.

This is to create the space adequate to allow the thickness of the implants to be inserted[41]. In measured resection, the distal femur and proximal tibial are cut perpendicular to the mechanical axis of their respective bones. The posterior slope in the tibia will be determined dependent upon whether a CR or PS component will be used. The femoral rotation is based on measurements off the femoral anatomy. The rotation is usually set parallel to the epicondylar axis, perpendicular to Whiteside's line or in 3° of external rotation in reference to the posterior condylar axis. Once the boney cuts are made, the goal is to have a rectangular flexion and extension gap. If the flexion and extension gaps are not balanced at this point, then osteophytes are resected and subsequent soft tissue releases are carried forward to obtain a balance and rectangular space in both flexion and extension. Soft tissues are released depending on the deformity angle and severity[11].

Gap balancing has a number of variations in steps, with the end goal being that the femoral rotation is performed to create an equal rectangular space in both flexion and extension. Although there is a wide variety in the sequence of steps, it can be performed by making the proximal tibial cut first. The tibial cut must be accurate to the surgical plan as all subsequent cuts will be based off of this initial cut. While the flexion space or the extension space can be balanced first, a tensioning device is used to balance the soft tissues. This may require resection of osteophytes and progressive soft tissue releases to obtain balance. The femoral rotation is done to match the tension of the soft tissues to the balanced tension in extension. Thus the femoral rotation is achieved by the tension across the balanced ligaments and not by anatomical landmarks[11,41].

The vast majority of TKAs performed to date rely on subjective ligamentous or soft tissue balancing intraoperatively[42,43]. Surgeons asses the stability of the knee throughout the full range of motion and aim to create a stable, balanced knee through the range of motion[9]. The varus and valgus stability is also assessed throughout the range of motion by applying a moment of force on the lower leg[44]. A goal of 1-2mm of balanced gaping of the medial and lateral compartment is a reasonable end point[11,45,46]. There are some objective measures that are available to measure soft tissue balancing intraoperatively such as spacers, tensors, computer assisted instruments, and load bearing sensors that quantify the forces across each compartment of the knee[42,43,46,47]. These objective

measures are precise and guide focused soft tissue releases of individual knee structures allowing for patient specific soft tissue balancing[42]. However, controversy is still present. Using these precise intraoperative measurements of joint forces may or may not equate to better functional outcome scores[43,47,48]. Also, the correct magnitude of these forces is still unknown.

Postoperatively, joint stability and soft tissue balancing has been assessed through clinical exam and functional outcome measures. Examples of functional outcome scores are: WOMAC (Western Ontario and McMaster Universities Arthritis index), 6-minute walk, 30-second stair climb, KOOS (Knee injury and Osteoarthritis Outcome Score), International Knee Documentation, Lower Extremity Functional Scale, and UCLA activity-level rating[49]. Physical exam is also used to assess the stability of the knee. Overall alignment of the limb is checked with the patient standing and walking. Varus and valgus forces are applied on the knee throughout the range of motion to assess the collateral ligament integrity in correlation with the patients symptoms. Anterior and posterior translation is also assessed throughout the ROM. Patellar stability and tracking can be assessed with manual distraction force and visualizing the patella through a full range of motion. As part of the postoperative assessment, standing AP, lateral, and skyline x-rays are obtained to assess the component alignment and stability. X-rays can also be helpful in determining asymmetric wear, loosening, or component failure. In situations where overall alignment is a concern, hip-to-ankle standing views can also be obtained.

Scientifically, there have been many studies that have looked at the soft tissue balancing around TKA. The assessment of TKA stability is carried out using biomechanical analysis and kinematic measures. Biomechanics has defined knee stability as the rotation or translation of the joint when a moment or force is applied to the knee. The displacement profile from these applied forces is characterized by the soft tissue laxity and stiffness[50]. The primary outcome measures most frequently assessed are AP translation, IE rotation, and VV moments. These outcomes are often assessed through range of motion testing, gait, or through simulated activities of daily living such as stair ascent and descent[51–55].

1.11 VIVO

Joint motion simulation can be performed using a servo-hydraulic 6 degree of freedom joint motion simulator known as the VIVO[54]. The VIVO is the world's first full speed, full load 6 degree of freedom joint motion simulator that can be used to test prosthetic joints or cadaveric native joint samples. This apparatus can be used in force control or displacement control for all 6 degrees of motion. The 6 degrees of freedom can be individually placed into either force or displacement control depending on what variable is to be controlled or assessed. It can be programmed with custom motions and loads, or it can use pre-programmed simulations such as activities of daily living, motions in sport and even trauma situations. It relies on the Grood and Suntay coordinate system[56], however, adjustments in the coordinates origin and flexion axis can be made to accommodate the prosthesis or cadaveric specimen being tested. There is built within the VIVO and the VIVO sim a multi-fiber ligament model that can capture the 6 degrees of freedom as seen in biological specimens with proper soft tissue restraints. The VIVO sim also allows for visualization of the testing model in 3-D and individual assessment of each ligamentous structure and its strain, tension, and force components. This technology can be coupled to computer generated anatomic models, complete with mechanically and kinematically aligned total knee arthroplasty components and virtually simulated soft tissue constraints.

Figure 1-19. Picture of VIVO during CR TKA joint motion simulation.

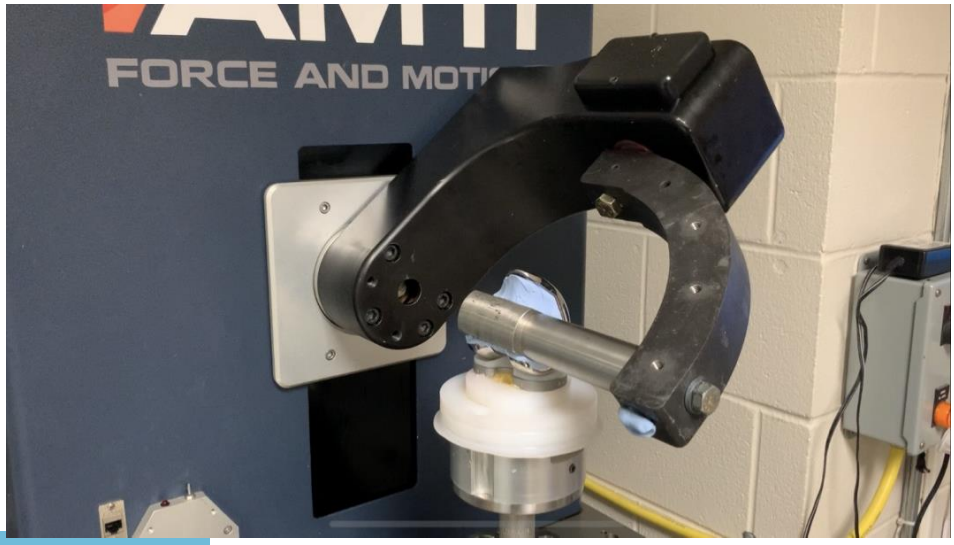

The VIVO is capable of collecting real time data points of the biomechanics occurring on the joint during ROM or ADL testing. This data is collected to an accuracy of 0.1mm and 0.1°; the dynamic load-tracking error can be reduced to less than 10N or 0.5Nm[54]. It is collected at a frequency of 100Hz, resulting in thousands of data points. The data points contain information on forces, moments, displacements, and angular displacements for all degrees of freedom as well as ligament forces and moments in all degrees of freedom.

1.12 References

1. Papas PV, Cushner FD, Scuderi GR. The History of Total Knee Arthroplasty. Tech Orthop. 2018;33(1):2–6.
2. Bourne RB, Chesworth BM, Davis AM, Mahomed NN, Charron KDJ. Patient satisfaction after total knee arthroplasty: Who is satisfied and who is not? Clin Orthop Relat Res. 2010;468(1):57–63.
3. Williams DH, Garbuz DS, Masri BA. Total knee arthroplasty: Techniques and results. B C Med J. 2010;52(9):447–54.
4. Marsh J, Somerville L, Howard JL, Lanting BA. Significant cost savings and similar patient outcomes associated with early discharge following total knee arthroplasty. Can J Surg. 2019;62(1):20–4.
5. Bhandari M, Smith J, Miller LE, Block JE. Clinical and economic burden of revision knee arthroplasty. Clin Med Insights Arthritis Musculoskelet Disord. 2012;5:89–94.
6. Sharkey PF, Lichstein PM, Shen C, Tokarski AT, Parvizi J. Why are total knee arthroplasties failing today-has anything changed after 10 years? J Arthroplasty [Internet]. 2013;29(9):1774–8. Available from: http://dx.doi.org/10.1016/j.arth.2013.07.024
7. Lombardi A V., Berend KR, Adams JB. Why knee replacements fail in 2013: Patient, surgeon, or implant? Bone Jt J. 2014;96B(11):101–4.
8. Fehring TK, Odum S, Griffin WL, Mason JB, Nadaud M. Early failures in total knee arthroplasty. In: Clinical Orthopaedics and Related Research. 2001.
9. Smith T, Elson L, Anderson C, Leone W. How are we addressing ligament balance in TKA? A literature review of revision etiology and technological advancement. J Clin Orthop Trauma [Internet]. 2016;7(4):248–55. Available from: http://dx.doi.org/10.1016/j.jcot.2016.04.001
10. Thompson JC, Netter FHCN-GHSLQRWE 17 T 2010 L use only. Netter's concise orthopaedic anatomy. Netter clinical science. 2010.
11. Azar FM, James H. Beaty, S. Terry Canale. Campbell's Operative Orthopaedics, Thirteenth Edition. Elsevier. 2017;
12. Servien E, Viskontas D, Giuffrè BM, Coolican MRJ, Parker DA. Reliability of bony landmarks for restoration of the joint line in revision knee arthroplasty. Knee Surgery, Sport Traumatol Arthrosc. 2008;
13. Laprade CM, Civitarese DM, Rasmussen MT, Laprade RF. Emerging updates on the posterior cruciate ligament. Am J Sports Med. 2015;43(12):3077–92.
14. McCarty EC, McAllister DR, Leonard JP. Anatomy and biomechanics of the knee. AAOS Compr Orthop Rev 2. 2018;1(1):1353–66.
15. Edwards A, Bull AMJ, Amis AA. The Attachments of the Fiber Bundles of the Posterior Cruciate Ligament: An Anatomic Study. Arthrosc - J Arthrosc Relat Surg. 2007;

16. Liu F, Yue B, Gadikota HR, Kozanek M, Liu W, Gill TJ, et al. Morphology of the medial collateral ligament of the knee. J Orthop Surg Res. 2010;5(1):1–8.

17. LaPrade RF, Engebretsen AH, Ly T V., Johansen S, Wentorf FA, Engebretsen L. The anatomy of the medial part of the knee. J Bone Jt Surg - Ser A. 2007;89(9):2000–10.

18. Grawe B, Schroeder AJ, Kakazu R, Messer MS. Lateral collateral ligament injury about the knee: Anatomy, evaluation, and management. J Am Acad Orthop Surg. 2018;26(6):e120–7.

19. Moorman CT, LaPrade RF. Anatomy and biomechanics of the posterolateral corner of the knee. The journal of knee surgery. 2005.

20. Blankevoort L, Huiskes R. Ligament-bone interaction in a three-dimensional model of the knee. J Biomech Eng. 1991;

21. Peters AE, Akhtar R, Comerford EJ, Bates KT. Tissue material properties and computational modelling of the human tibiofemoral joint: A critical review. PeerJ. 2018.

22. Smith CR, Vignos MF, Lenhart RL, Kaiser J, Thelen DG. The influence of component alignment and ligament properties on tibiofemoral contact forces in total knee replacement. J Biomech Eng. 2016;138(2).

23. Freeman MAR, Pinskerova V. The movement of the normal tibio-femoral joint. J Biomech. 2005;38(2):197–208.

24. Galvin CR, Perriman DM, Newman PM, Lynch JT, Smith PN, Scarvell JM. Squatting, lunging and kneeling provided similar kinematic profiles in healthy knees—A systematic review and meta-analysis of the literature on deep knee flexion kinematics. Knee [Internet]. 2017;25(4):514–30. Available from: https://doi.org/10.1016/j.knee.2018.04.015

25. Park ES, DeFrate LE, Suggs JF, Gill TJ, Rubash HE, Li G. The change in length of the medial and lateral collateral ligaments during in vivo knee flexion. Knee. 2005;12(5):377–82.

26. Lenhart RL, Kaiser J, Smith CR, Thelen DG. Prediction and Validation of Load-Dependent Behavior of the Tibiofemoral and Patellofemoral Joints During Movement. Ann Biomed Eng. 2015;43(11):2675–85.

27. Badley EM, Wilfong JM, Millstone D, Perruccio A V. National Report on the Status of Arthritis in Canada. 2018;(August):1–32.

28. Feeley BT, Gallo RA, Sherman S, Williams RJ. Management of osteoarthritis of the knee in the active patient. J Am Acad Orthop Surg. 2010;18(7):406–16.

29. Bellemans J, Colyn W, Vandenneucker H, Victor J. The chitranjan ranawat award. Is Neutral Mechanical Alignment Normal for All Patients? The Concept of Constitutional Varus. Clin Orthop Relat Res. 2012;470(1):45–53.

30. Vandekerckhove PJTK, Matlovich N, Teeter MG, MacDonald SJ, Howard JL, Lanting BA. The relationship between constitutional alignment and varus

osteoarthritis of the knee. Knee Surgery, Sport Traumatol Arthrosc. 2016;25(9):2873–9.

31. Lanting BA, Williams HA, Matlovich NF, Vandekerckhove PJ, Teeter MG, Vasarhelyi EM, et al. The impact of residual varus alignment following total knee arthroplasty on patient outcome scores in a constitutional varus population. Knee [Internet]. 2018;25(6):1278–82. Available from: https://doi.org/10.1016/j.knee.2018.08.019

32. Engh GA, Holt BT, Parks NL. A Midvastus Muscle-Splitting Approach for Total Knee Arthroplasty. J Arthroplasty. 1997;12(3).

33. Gore DR, Sellinger DS, Gassner KJ, Glaeser ST. Subvastus approach for total knee arthroplasty. Orthopedics. 2003;

34. Rivière C, Iranpour F, Auvinet E, Howell S, Vendittoli PA, Cobb J, et al. Alignment options for total knee arthroplasty: A systematic review. Orthop Traumatol Surg Res [Internet]. 2017;103(7):1047–56. Available from: http://dx.doi.org/10.1016/j.otsr.2017.07.010

35. Blakeney W, Clément J, Desmeules F, Hagemeister N, Rivière C, Vendittoli PA. Kinematic alignment in total knee arthroplasty better reproduces normal gait than mechanical alignment. Knee Surgery, Sport Traumatol Arthrosc [Internet]. 2019;27(5):1410–7. Available from: http://dx.doi.org/10.1007/s00167-018-5174-1

36. Howell SM, Roth JD, Hull ML. Kinematic Alignment in Total Knee Arthroplasty Definition, History, Principle, Surgical Technique, and Results of an Alignment Option for TKA What is Kinematic Alignment in TKA? Arthropaedia. 2014;(1):44–53.

37. Lee YS, Howell SM, Won YY, Lee OS, Lee SH, Vahedi H, et al. Kinematic alignment is a possible alternative to mechanical alignment in total knee arthroplasty. Knee Surgery, Sport Traumatol Arthrosc. 2017;25(11):3467–79.

38. Roth JD, Howell SM, Hull ML. Native Knee Laxities at 0°, 45°, and 90° ofFlexion and Their Relationship to the Goal of the Gap-Balancing Alignment Method of Total Knee Arthroplasty. J Bone Jt Surg. 2015;97:1678–84.

39. Luo Z, Zhou K, Peng L, Shang Q, Pei F, Zhou Z. Similar results with kinematic and mechanical alignment applied in total knee arthroplasty. Knee Surgery, Sport Traumatol Arthrosc [Internet]. 2019;(0123456789). Available from: https://doi.org/10.1007/s00167-019-05584-2

40. Vandekerckhove PJ, Lanting B, Bellemans J, Victor J, MacDonald S. The current role of coronal plane alignment in Total Knee Arthroplasty in a preoperative varus aligned population: An evidence based review. Acta Orthopaedica Belgica. 2016. p. 129–42.

41. Babazadeh S, Stoney J, Lim K, Choong P. The relevance of ligament balancing in total knee arthroplasty: how important is it? A systematic review of the literature. Orthop Rev (Pavia). 2009;1(26):70–8.

42. Gustke KA, Golladay GJ, Roche MW, Elson LC, Anderson CR. A Targeted

Approach to Ligament Balancing Using Kinetic Sensors. J Arthroplasty [Internet]. 2017;32(7):2127–32. Available from: http://dx.doi.org/10.1016/j.arth.2017.02.021

43. Gustke KA. Soft-tissue and alignment correction: The use of smart trials in Total knee replacement. Bone Jt J. 2014;96B(11):78–83.

44. Mihalko WM, Whiteside LA, Krackow KA. Comparison of ligament-balancing techniques during total knee arthroplasty. In: Journal of Bone and Joint Surgery - Series A. 2003.

45. Deep K, Picard F, Clarke J V. Dynamic Knee Alignment and Collateral Knee Laxity and Its Variations in Normal Humans. Front Surg. 2015;2(November):1–6.

46. Aunan E, Kibsgård T, Clarke-Jenssen J, Röhrl SM. A new method to measure ligament balancing in total knee arthroplasty: Laxity measurements in 100 knees. Arch Orthop Trauma Surg. 2012;132(8):1173–81.

47. Shelton TJ, Howell SM, Hull ML. Is There a Force Target That Predicts Early Patient-reported Outcomes after Kinematically Aligned TKA? Clin Orthop Relat Res. 2019;477(5):1200–7.

48. Gustke KA, Golladay GJ, Roche MW, Elson LC, Anderson CR. Primary TKA patients with quantifiably balanced soft-tissue achieve significant clinical gains sooner than unbalanced patients. Adv Orthop. 2014;

49. Bourne RB. Measuring tools for functional outcomes in total knee arthroplasty. Clin Orthop Relat Res. 2008;466(11):2634–8.

50. Siston RA, Maack TL, Hutter EE, Beal MD, Chaudhari AMW. Design and cadaveric validation of a novel device to quantify knee stability during total knee arthroplasty. J Biomech Eng. 2012;134(11):1–7.

51. Willing R, Moslemian A, Yamomo G, Wood T, Howard J, Lanting B. Condylar-Stabilized TKR May Not Fully Compensate for PCL-Deficiency: An In Vitro Cadaver Study. J Orthop Res. 2019;

52. Shimizu N, Tomita T, Patil S, Yamazaki T, Kurita M, D'Lima D, et al. Comparison of TKA kinematics between cruciate retaining insert and condylar stabilized insert. In: Transactions of the Annual Meeting of the Orthopaedic Research Society. 2013.

53. Song EK, Lim HA, Joo SD, Kim SK, Lee KB, Seon JK. Total knee arthroplasty using ultra-congruent inserts can provide similar stability and function compared with cruciate-retaining total knee arthroplasty. Knee Surgery, Sport Traumatol Arthrosc. 2017;25(11):3530–5.

54. Willing R, Walker PS. Measuring the sensitivity of total knee replacement kinematics and laxity to soft tissue imbalances. J Biomech [Internet]. 2018;77:62–8. Available from: https://doi.org/10.1016/j.jbiomech.2018.06.019

55. Borque KA, Gold JE, Incavo SJ, Patel RM, Ismaily SE, Noble PC. Anteroposterior Knee Stability During Stair Descent. J Arthroplasty. 2015;

56. Grood ES, Suntay WJ. A joint coordinate system for the clinical description of

three-dimensional motions: Application to the knee. J Biomech Eng. 1983;105(2):136–44.

57. Keeney JA, Clohisy JC, Curry M, Maloney WJ. Revision total knee arthroplasty for restricted motion. Clin Orthop Relat Res. 2005;(440):135–40.

58. Fehring TK, Valadie AL. Knee instability after total knee arthroplasty. In: Clinical Orthopaedics and Related Research. 1994.

59. Insall JN, Binazzi R, Soudry M, Mestriner LA. Total knee arthroplasty. Clin Orthop Relat Res. 1985;

Chapter 2

2 Thesis Objectives

The aim of this work is to understand the effects that the three most commonly used total knee arthroplasty implant designs (Cruciate Retaining, Cruciate Sacrificing, and Posterior Stabilized) have on the soft tissue balance of the knee. The effects of soft tissue balance will be assessed through passive flexion and extension of the knee as well as during simulated activities of daily living. This will be performed via gate kinematic analysis of ligamentous and soft tissue balancing in the three different TKA constructs of a single implant system using a servo-hydraulic 6 degree of freedom joint motion simulator (VIVO)[1] in conjunction with virtual simulations of joint anatomy and soft tissue constraints.

The first objective will be to determine the joint kinematics of each of the TKA constructs in the current standard of mechanical alignment. We will explore in our second objective the effects of different alignments of the lower extremity on ligamentous balance. Using the same implants, we will adjust our alignment on the VIVO through our virtual ligaments to look specifically at mechanical alignment verses kinematic alignment. Simulation of mechanical aligned and kinematic aligned TKAs will be carried forward on the VIVO machine. Gait kinematic analysis and soft tissue balance will be monitored. In future works using the normative data from the previous investigations, we will compare the effects of misaligned or unbalanced components. Misalignment of the implant components will be simulated by relocating them on the VIVO and adjusting the virtual ligaments according to commonly made errors which lead to instability or unbalance TKAs. We will then measure the effects of misalignment on soft tissue balancing. Again, we will assess the overall TKA balance and stability by looking at biomechanical measures and kinematic evaluation.

The primary outcome measures are anterior/posterior translation, internal/external rotation, and varus/valgus (AP, IE and VV) kinematics of passive flexion/extension and activities of daily living (ADL). We will also look at ligament laxity testing throughout

the knee range of motion. Specifically we will examine AP laxity, varus laxity and valgus laxity each broken down into the individual ligament components.

The hope is that this information will give us a better understanding of how to best achieve ideal alignment and soft tissue balancing. This will lead to a change in surgical objectives and ultimately the contact kinematics in specific modelled functional situations. We will gather information to best direct surgeons in appropriate alignment and soft tissue balancing specific to the implants which they use. This would allow for optimum TKA stability for patients which will allow for possible improved patient satisfaction and implant survival.

2.1 References

1. Willing R, Walker PS. Measuring the sensitivity of total knee replacement kinematics and laxity to soft tissue imbalances. J Biomech [Internet]. 2018;77:62–8. Available from: https://doi.org/10.1016/j.jbiomech.2018.06.019

Chapter 3

3 Biomechanical analysis of soft tissue balancing in mechanically aligned total knee arthroplasty (TKA) using TKA implants linked to a virtual ligament model.

3.1 Abstract

Total knee arthroplasty (TKA) is a very successful surgery, but improvements in stability, soft tissue balance, joint kinematics and overall patient satisfaction may lead to a decrease in TKA revisions. It is still unclear what the optimal soft tissue tension, balance or alignment is to provide superior patient outcomes. Computational models provide a means to effectively parameterize ligaments and simulate multiple scenarios of TKA. This work used an amalgamation of a sophisticated 6 degree of freedom joint motion simulator with a virtual soft tissue model representative of the static soft-tissues used to balance TKAs. Through testing joint kinematics and soft tissue laxity through 90° of neutral flexion and extension and simulated Activities of Daily Living (ADLs) we were able to reproduce a model that elicited joint kinematics in a balanced TKA similar to what has been shown in the literature. We looked specifically at Cruciate Retaining, Cruciate Sacrificing and Posterior Stabilized components. We found that a CS poly does not adequately compensate for the lack of a PCL in neutral flexion and extension, but does properly compensate during ADLs. The Posterior Cruciate Ligament (PCL) plays a protective role in offloading some of the forces in the superficial Medial Collateral Ligament (sMCL). Also posterior tibial slope can have a significant effect on the soft tissue tensions. Ligament properties for computational modeling need to be refined to better match anatomical properties. This study also offers a baseline computational model that reproduces appropriate TKA joint kinematics and laxities, which can then be used for future studies providing better understanding of total knee arthroplasty.

3.2 Introduction

Total knee arthroplasty has revolutionized the quality of life for individuals suffering from end stage knee arthritis. Joint replacement has come close to mimicking natural knee kinematics[1], but there still remains a significant amount of people dissatisfied with their results.[2,3]. Poorly balanced knees or knees with unequal soft tissue tension, may cause residual pain or overall dissatisfaction. Dissatisfied TKA patients have lower quality of life and higher health care resource burdens[4]. Occasionally, a revision operation is carried out to improve their symptoms, function and quality of life. TKA revision places an enormous burden on patients, hospitals, surgeons and the healthcare system[5]. With TKA surgeries projected to increase[1] it is likely the number of revision surgeries will subsequently be increasing. Research efforts have been ongoing to eliminate or decrease the main reasons for revision to effect patient outcomes and quality of life as well as substantially decreasing the economic burden of TKA revision surgery.

Instability is one of the top three most common reasons for TKA revision[6,7]. Approximately 63% of TKA failures occur in the first 5 years post op[8]. Of these failures that occur in the first 5 years, 35% of them can be attributed to soft tissue imbalance[9]. Proper ligament balancing and alignment is considered a requirement for achieving good functional outcomes and long-term survival of total knee arthroplasty. It is still unclear as to what the optimum soft tissue balancing or alignment is for implant survival and superior patient satisfaction, as this may differ with various implant designs. There have been well defined properties of intact knees and the ultimate goal of a TKA system would be to replicate the functional properties of intact knees. The aim of this work is to understand how Cruciate Retaining, Cruciate Sacrificing and Posterior Stabilized components effect the soft tissue balance, stability and knee joint kinematics. This is in relation to the current standard of mechanical alignment TKA.

3.3 Methods

3.3.1 Virtual Model Development and Anatomical Coordinate System

The virtual knee model, complete with anatomic ligaments and mechanically aligned TKA implants, was created first. An in depth description of the virtual model can be found in an excerpt from a previous work by Montgomery et al and can be found in Appendix A. Using cadaveric CT scans from a previous work, isolated distal femoral and proximal tibial 3-D models were also created.

Each 3-D model was assigned an individual set of coordinates based off the previously described Grood and Suntay coordinate system[11]. The origin of the femoral coordinate system was defined by the midpoint between the sphere-fit center of the condyles. The z-axis was equivalent to the mechanical axis of the femur (positive in the superior direction), the x-axis was defined 90° to the z-axis in the coronal plane and colinear with the trans epicondylar axis (referenced 3° externally rotated off the posterior condylar axis and positive to the right), the y-axis was defined as the cross product of the z and x-axis along the sagittal plane (positive in the anterior direction). The origin of the tibial coordinate system was centered between the intercondylar eminences. The z-axis was equivalent to the mechanical or anatomic axis of the tibia (positive in superior direction), the x-axis was defined 90° to the z-axis in the coronal plane (positive to the right), the y-axis was defined as the cross product of the z and x-axis along the sagittal plane (positive in the anterior direction). The finalized 3-D models were then saved as triangle tessellated stereolithographic surface models (.stl) files to be used in CAD software.

Surface model files of the Stryker Triathlon® (Stryker Corp., Mahwah, NJ) femoral, tibial and polyethylene components were used. A coordinate system was then applied to the femoral and tibial components respectively. All directions of the component coordinates matched the 3D model axes. The origin of the femoral component coordinate system was defined at the midpoint between the two condylar sphere-fit centres, Figure 3-1. The x-axis was defined as a line connecting the two sphere-fit centres, the z-axis was perpendicular to the x-axis and a horizontal line taken from the distal articulating surface

of the component, and the y-axis was a cross product of the z-axis and x-axis. The origin of the tibial component was centered at the front edge of the central hole of the implant, Figure 3-1. The x-axis was defined as a line parallel to the back edge of the components, the y-axis perpendicular to this line and the z-axis was a product of the y and x axes.

Figure 3-1. Images displaying origins of individual component coordinate systems. (A) Femoral Component. (B) Tibial component.

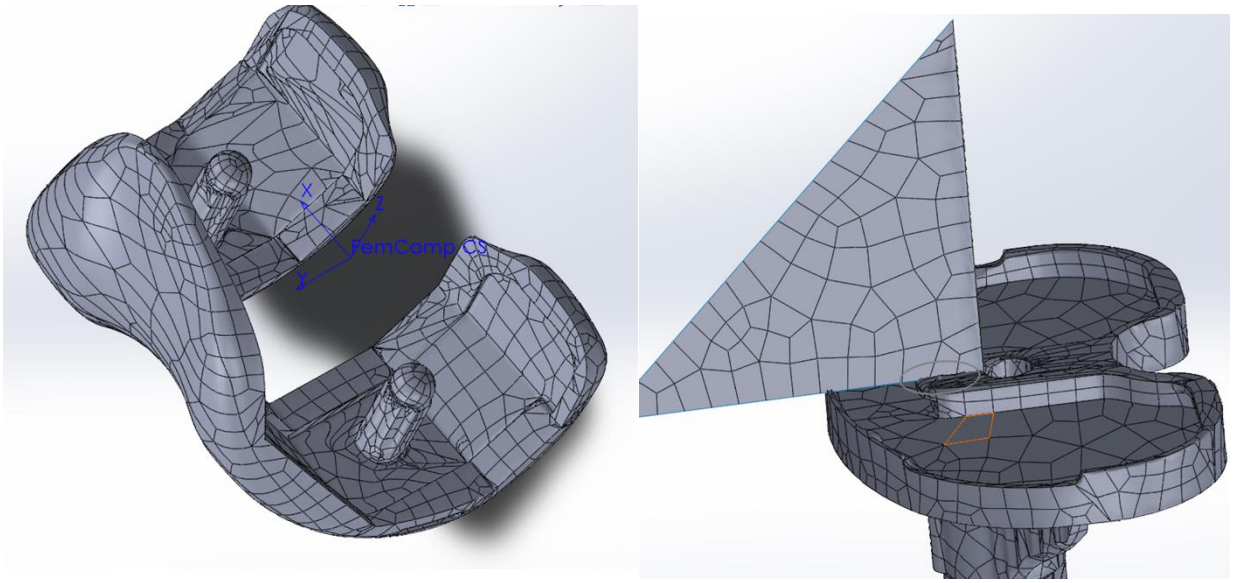

A **B**

3.3.2 Virtual TKA Operation

The Stryker Triathlon® (Stryker Corp., Mahwah, NJ) femoral and tibial components were placed on the respective 3D anatomical models using SOLIDWORKS 2018®. References created for all axes and corresponding planes for both the anatomical models and TKA components were linked. A virtual TKA operation was carried out, resulting in appropriate bone cuts to produce a mechanically aligned TKA. The component sizes were determined from the TKA performed on the same cadaveric specimens used in a previous study. The previous TKA and sizing of the components was performed by a

board-trained orthopedic surgeon specializing in arthroplasty. The distal femur was cut perpendicular to the mechanical axis with 8mm of bone resection depth and neutral flexion. The anterior, posterior and chamfer cuts were made to fit a size 5 Triathlon® (Stryker, Mahwah, NJ) femur, with the anterior cut flush with the anterior cortex. The femoral rotation was set parallel to the x-axis of the femoral anatomical model which was aligned with the approximated trans epicondylar axis (TEA), measured as 3° externally rotated off the posterior condylar axis. The proximal tibia was cut perpendicular to the mechanical axis of the tibia with 5° of posterior slope for the CR/CS components and 3° of posterior slope for the PS component. This equated to 8mm of resection measured off the anterior surface of the tibia. The tibia was also sized to size 5. The tibial component was placed on the proximal tibia with the center of anterior portion of the implant lining up with the medial 1/3rd portion of the tibial tubercle. A 9mm poly was then placed into the virtual tray to produce the finished virtual TKA. Images of the final mechanically aligned virtual TKA model can be seen in Figure 3-2.

Figure 3-2. Image displaying final computational model of mechanically aligned CR knee. Anterior (A) and Posterior (B) views allow visualization of all ligament insertions and bundles.

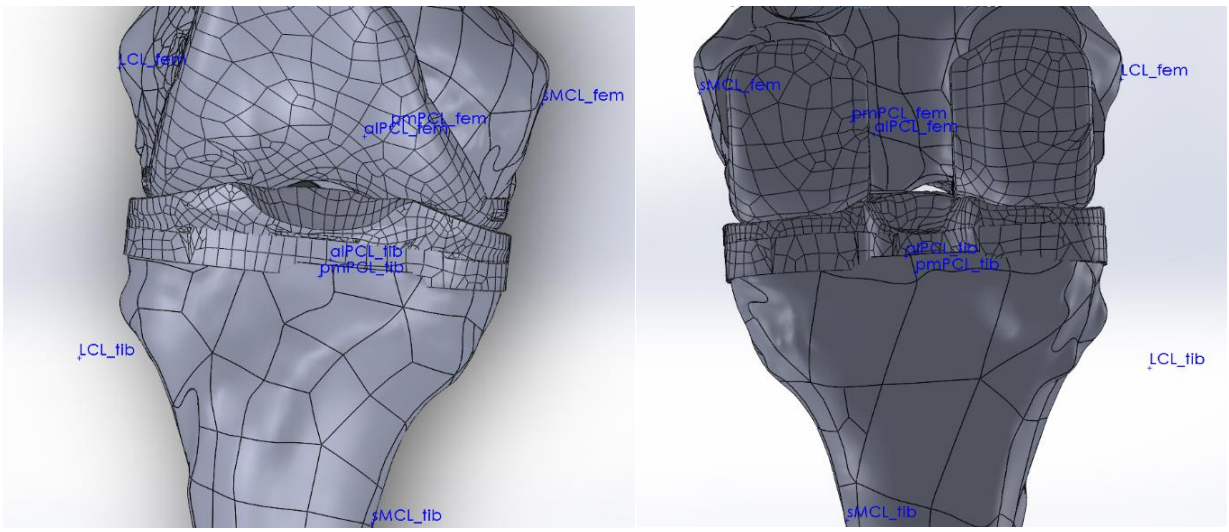

A **B**

3.3.3 Virtual Ligament Model

We simulated soft tissue restraints by applying the virtual ligaments most commonly addressed during balancing of a TKA. The Posterior Cruciate Ligament (PCL), the superficial Medial Collateral Ligament (sMCL) and the Lateral Collateral Ligament (LCL) were used. The ACL and deep MCL were not used as these are routinely released in most TKAs as part of the soft tissue dissection required for exposure or boney resection. The insertion points were determined from previous anatomic studies and linked to our anatomic models[12–19]. Once the anatomical models had the anatomic insertion points, the model points were linked to the coordinate system within the VIVO and co-registered to the coordinate system on the femoral component. The insertion points were related to the femoral component, this allowed poly changes without affecting insertion points. The femoral component coordinate system was also centered to the VIVO coordinate origin during joint motion simulation.

Ligament properties including stiffness, reference strain, reference length and zero load length were adapted from the literature and calculated to fit with our virtual model. A combination of computational TKA models and native knee properties were used to create the ideal ligamentous properties in our work[15,20–24]. The femoral component was used as the reference for all the ligament insertion points and thus the ligament properties were specific to the CR and the PS femoral components that were used. Ligament properties had to be defined with respect to a distinct pose, or starting position on the VIVO. This reference pose was defined at 0° of extension, all remaining position variables were obtained by applying a 100N compressive load across the joint and recording the resulting equilibrium pose. With the knee in full extension, each ligament's length can be defined from our models and ligament insertion points. Using this pose we are able to calculate the reference strain of each ligament. We used the native ligament length at the same pose and the strain on each ligament, as reported in the literature, to calculate the values for zero load length or slack length. The following calculation for the reference strain of each ligament was used: ([current length – original length] / original length, x 100%). Qualitatively this defines the amount of deformation in the ligament at full extension due to the tension placed on the ligaments. For example; the PCL in

mechanical alignment has a reference strain of -3.42% which equates to approximately 1.3mm of slack in the ligament (zero load length of 37.9mm vs mechanically aligned load length of 36.6mm). Another example is the sMCL in mechanical alignment has a reference strain of 2.73% which equates to the ligament being on stretch by approximately 2.4mm beyond its slack length. The ligament properties of stiffness, reference strain, and ligament length used for each alignment are shown in Table 3-1.

Table 3-1. Ligament properties adapted from literature and calculated to fit our virtual ligament model. All lengths are in millimeters, reference (ref.) strains are given as a percentage of zero-load length, stiffness is in units of Newtons per unit strain. (A) CR femoral component, (B) PS femoral component. ***MA=Mechanically Aligned, KA = Kinematically Aligned***

Ligament CR Component	Zero-Load Length (mm)	MA Length (mm)	MA Ref. Strain (%)	Stiffness (N/ε)
PCL	37.93	36.63	-3.42	9000
sMCL	89.75	92.21	2.73	2200
LCL	63.25	64.61	2.14	1800

A

Ligament PS Component	Zero-Load Length (mm)	MA Length (mm)	MA Ref. Strain (%)	Stiffness (N/ε)
sMCL	89.75	92.38	2.93	2200
LCL	63.25	64.91	2.62	1800

B

3.3.4 Biomechanical Testing

Joint motion simulation was performed using a servo-hydraulic 6 degree of freedom VIVO joint motion simulator (AMTI VIVO, Watertown, MA, USA)[25]. We tested isolated implant components mounted on the VIVO. This was performed with the Stryker

Triathlon® knee system. The femoral component was mounted to the upper actuator arm via a mounting axle. Two separate axles were used for the CR and PS femoral components because of the different geometries of the femoral components. The femoral component was mounted to the mounting axle with poly methyl methacrylate cement (Bosworth Fastray; Keystone Industries GmbH, Singen, Germany). It was mounted to align as closely parallel to the flexion axis of the VIVO machine. There was a slight variation in the rotation of the femur at the attachment to the mounting axel and this was corrected through adjusting the coordinate systems accordingly. The tibial component was attached to the lower actuator via a mounting platform. The tibial baseplate component was anchored into place using dental model stone (Modern Materials Golden Denstone Labstone; Modern Materials, Kulzer GmbH, Hanau, Germany). The desired polyethylene liner was then snapped into place on the tibial baseplate. This allowed easy interchangeability of the tibial articulating component. The mounted TKA on the VIVO can be seen in Figure 3-3.

Figure 3-3. Complete physical set up of the TKA mounted to the VIVO.

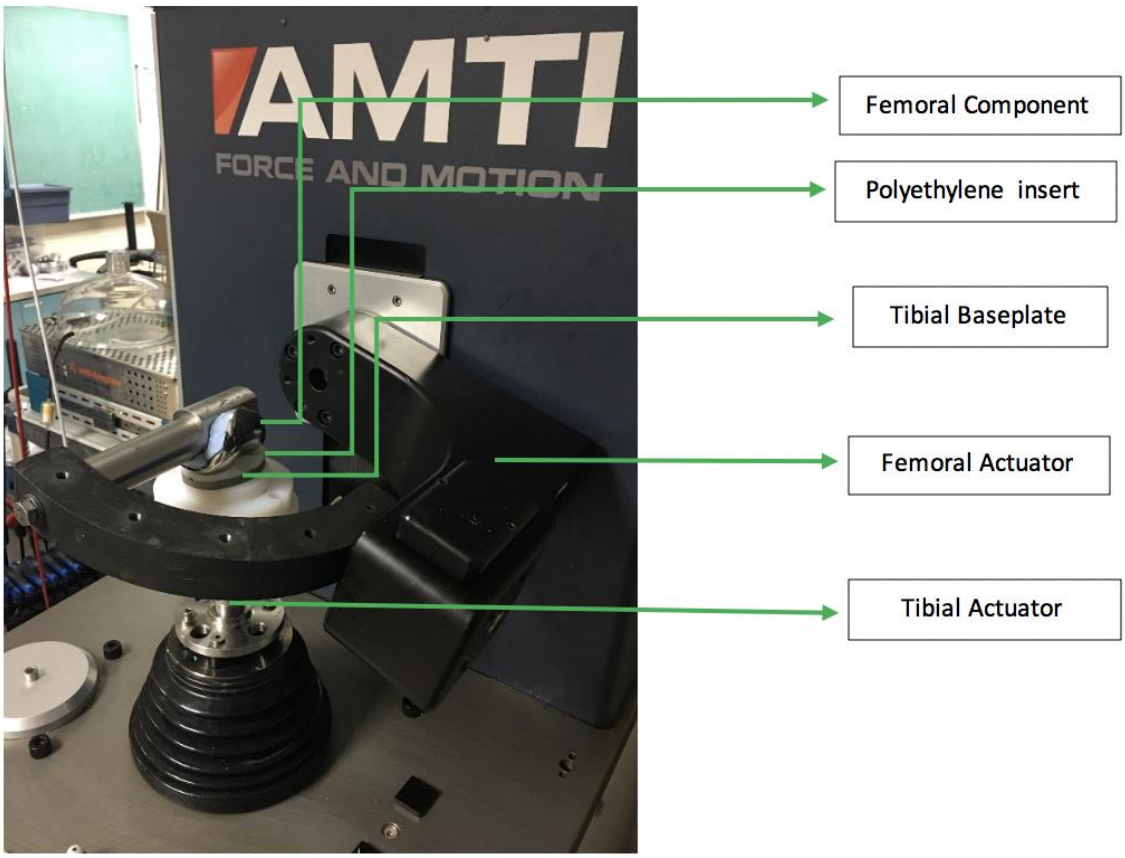

The VIVO machine expressed implant kinematics in the Grood and Suntay coordinate system[11], thus adjustments in the coordinates origin and flexion axis were made to align the mounted prosthesis and VIVO coordinates. Forces and kinematics were reported with respect to the VIVO's coordinate system; positive superior z axis, positive x axis to the right, and positive anterior y axis. There is built within the VIVO the capability to simulate the force contributions of virtual ligaments which are modeled as 1D point-to-point springs with a non-linear force versus strain response[22]. We used this technology to couple our computer-generated anatomic model, complete with mechanically aligned total knee arthroplasty components and virtual simulations of soft tissue constraints, with the VIVO joint motion simulator. This complete model was made to capture the 6 degrees of freedom as seen in biological specimens with proper soft tissue restraints.

The 6 degrees of freedom can be individually placed into either force or displacement control depending on what variable is to be controlled or assessed. The femoral actuator is responsible for flexion/extension and adduction/abduction. The tibial actuator is responsible for superior/inferior movement, internal/external rotation, medial/lateral movement, and anterior/posterior movement. It was programmed with custom motions and loads for assessment of 0-90° of neutral flexion and extension. The flexion/extension of the knee was placed in force control and regulated by the femoral actuator from 0-90°. The remaining 5 degrees of freedom were placed and displacement control and were recorded by the VIVO. This was performed for the CR and CS component with virtual ligaments representing an intact PCL, LCL and sMCL. We then removed the virtual PCL for assessment with the CS component without a PCL (CS-xPCL) and the PS component. This cyclical flexion and extension motion was monitored over 4 separate cycles at a rate of 25 s/cycle. We also simulated activities of daily living (ADLs) by importing gait and stair ascent/descent loads and motions. The programmed load and motion data for these activities were obtained from previous work within the same lab[26]. For this work the AVER75 (average loads in subjects with 75kg body weight) motion parameters were used. The original data files were acquired from the Orthoload website database (https://orthoload.com/)[27]. For the gait files, the load cycle begins at flat foot and goes through the gait cycle (flat foot, heel off, toe off, swing phase, heel strike, flat foot etc.). This splits the gait cycle into the first 60% stance phase and the last 40% swing phase. The stair ascent and descent load cycles both begin and end with the middle of swing phase. This splits the stair ascent and decent into the first and last 20% swing phase and the middle 60% as stance phase[27]. Throughout joint motion simulation we used a polydimethylsiloxane (silicone)-based lubricant (HAS0001-OS, Horizon Fitness, Cottage Grove, WI) to lubricate the articulating surface. Kinematic data was obtained every other cycle using the VIVO Control program's data logging features. The primary outcome measures were anterior/posterior translation, internal/external rotation and varus/valgus (AP, IE and VV) kinematics as well as total joint compressive forces. We also measured ligament laxity throughout the knee range of motion. AP laxity was measured by applying 100N of posteriorly directed force starting at 0° and at 15° increments up to 90°, and then extending back to 0°. This entire motion was completed over a period of 50

seconds. In the same manner, VV laxity was performed by applying a 10Nm varus or valgus torque on the femur at the same 15° increments. Laxity was defined as the absolute value of the difference between motion limits, with AP laxity being the difference between the anterior motion limit and the posterior motion limit and VV laxity was the measured difference between both varus and valgus motion limits. Laxity testing was repeated for four cycles. For all neutral flexion and laxity tests, there was a 10 N compressive force applied along the z axis. During the ADL testing, normal joint compression loads for an average 75kg person were applied. The outcomes measured for the ADL testing was the AP translation, IE rotation and VV kinematics.

3.3.5 Data aquisition

The kinematics and force data were recorded during the last flexion/extension cycle at a sampling rate of 100 samples per second. This data was smoothed using a low-pass Butterworth filter followed by a spline interpolation function in Matlab (The MathWorks, Natick, MA), and then down-sampled to only include data at 15° intervals of flexion and only during the flexion phase of the complete flexion/extension motion. During the ADL testing the joint motion was sampled in 5% increments of the cycle. We extracted the AP, IE, VV kinematic data and the net ligament forces in each of the 6 degrees of freedom during the kinematic testing. We also collected posterior, varus, valgus motion limits and the net ligament forces in each of the 6 degrees of freedom at these limits. The smoothed and processed data was then analysed and statistically compared. For each dataset, a two tailed paired T-test was used to compare each TKA variation to the other variations in a paired fashion. A statistical significance level of $p<0.01$ was used.

3.4 Results

3.4.1 Joint Kinematics

Looking at the kinematics for neutral flexion/extension testing seen in Figure 3-4A, the PCL has a significant effect on the femoral roll back as seen in the CR and CS AP kinematics. Both these poly's have a maximum AP translation of 10.59mm and 10.30mm respectively (AP - CR:CS, $p<0.001$). Without the PCL, it is apparent that the CS poly does not provide the same degree of femoral roll back as seen with an intact PCL. The CSxPCL had a maximum AP translation of 6.39mm (AP - CR:CSxPCL, $p=0.01$; AP – CS:CSxPCL $p=0.03$). Although statistically insignificant, the pattern is clear. Also the PS poly, although having a more anterior starting position in extension, doesn't fully compensate for the lack of a PCL, providing only 3.55mm of roll back (AP - CR:PS, $p<0.001$; AP - CS:PS, $p<0.001$; AP - CSxPCL:PS, $p<0.001$). As seen in Figure 3-4B, the PS component does, however, compensate for the lack of a PCL by constraining the IE kinematics to be more similar to the CR and CS components with an intact PCL (IE - CR:PS, $p=0.69$; IE - CS:PS, $p=0.54$). The maximal internal rotation of the tibia for the CR, CS and PS components are 7.1°, 7.4° and 8.3° respectively. This occurred at mid flexion between 30-45° of flexion. This graph shows us the significant role PCL plays in limiting internal rotation in deeper flexion. The CS component without a PCL is unable to compensate for the internal rotation moment. This is seen where the maximal IR in the CSxPCL is 8.1° starting at approximately 45° of flexion. Also in deep flexion at 90°, the IR end point for CR and CS, are 0.8°, 0.4° with the PS ending in slight ER of 0.3° respectively. Whereas the CSxPCL at 90° of flexion is 4.8° of IR (IE - CR:CSxPCL, $p=0.01$; IE - CS:CSxPCL, $p=0.03$; IE - PS:CSxPCL, $p<0.001$). In Figure 3-4C we can see that the VV kinematics are not affected by the loss of the PCL in the CS poly. There is no significant difference in the VV kinematics between the CR and CSxPCL polys and a near identical trend between the CR/CS, CS and CSxPCL polys (VV - CR:CS, $p=0.001$; VV - CR:CSxPCL, $p=0.08$; VV - CS:CSxPCL, $p<0.001$). The PS component doesn't show significant difference statistically, but the trend shows an obvious increase in constraint to VV kinematics. As the knee flexes up to 90° there is only 1.1° of overall change in varus/valgus angle. Whereas the CR, CS and CSxPCL poly's have a much

higher net change of 3.2°, 3.2° and 3.2° in varus/valgus angle respectively (VV - CR:PS, p=0.10, VV - CS:PS, p=0.14, VV - CSxPCL:PS, p=0.07).

Figure 3-4. Kinematic testing for CR, CS, CSxPCL and PS components through 0-90° of neutral flexion. (A) AP kinematics, (B) IE Kinematics, (C) VV kinematics.

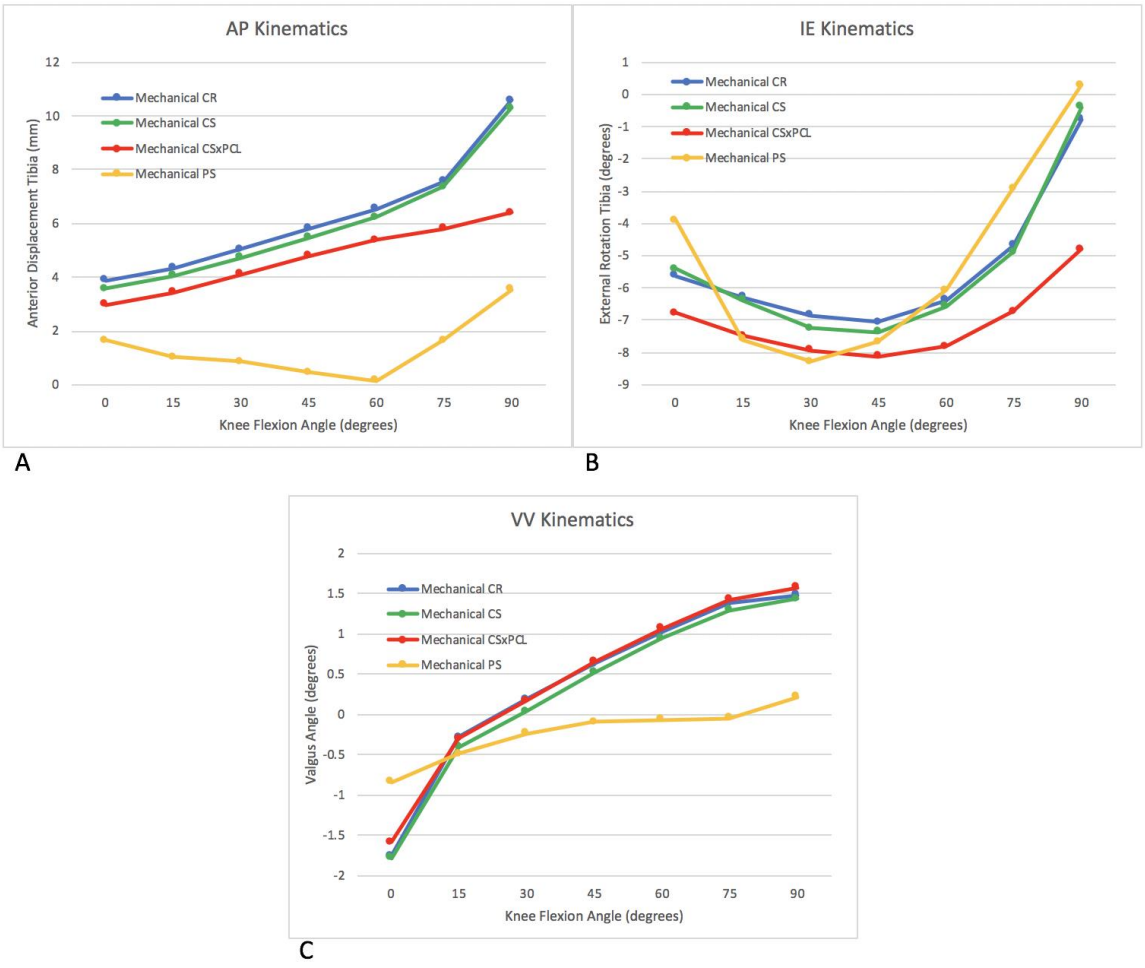

During neutral flexion and extension we measured the joint compression forces as generated by the virtual soft tissue envelope and the articular geometries. Figure 3-5 shows the total inferior/superior joint contact forces that occur using each poly during neutral flexion and extension cycle. It is clear that the CR, CS and CSxPCL polys

produce similar total joint compressive forces. The maximum compressive force are 160.5N, 160.6N and 166.1N for CR, CS and CSxPCL respectively. These forces peak at 60° of flexion and there is no statistical difference found (JCF - CR:CS, p=0.27; JCF - CR:CSxPCL, p=0.87; JCF - CS:CSxPCL, p=0.08). The PS component produces much greater joint compression forces. The maximum compressive force is 222.9N and this occurs at 90° of flexion. This is statistically significant compared to the CR and CS, but only near significance with the CSxPCL (JCF - PS:CR, p=0.009; JCF - PS:CS, p=0.009; JCF - PS:CSxPCL, p=0.016).

Figure 3-5. Total joint compressive forces during kinematic testing for CR, CS, CSxPCL and PS components through 0-90° of neutral flexion.

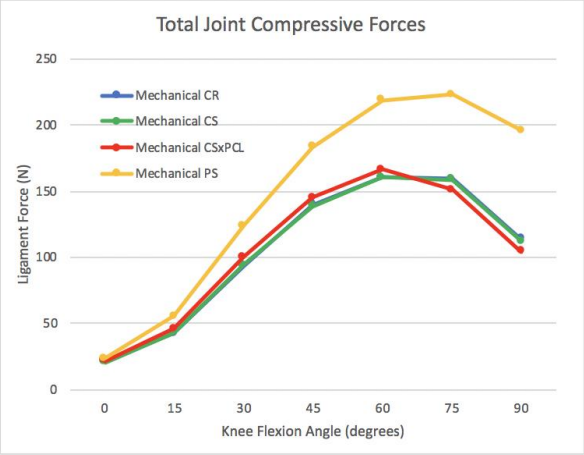

Looking at the separate ligaments it is evident that the increase in total joint contact forces in the PS component is primarily due to the significant tension in the collateral ligaments. Figure 3-6 shows the tensions across each separate ligament bundle during neutral flexion and extension. Figure 3-6A shows the PCL has no effect in extension and then initiates the femoral roll back by increasing tension at 60° of flexion. It's also at 60° of flexion that there is a trend down in tension for the sMCL and LCL in the CR, CS and CSxPCL components (Figure 3-6B&C). Whereas the collateral tensions continue to increase in the PS component comparatively. Whether it's in CR or CS polys there is no

significant difference in the tensions of the PCL (PCL - CR:CS, p=0.24). The sMCL has higher tension in the PS component after 60° of flexion and has 52.9N at 90°. Whereas the sMCL tension for the CR, CS and CSxPCL is 32.6N, 30.3N and 28.0N at 90°. This is not statistically significant though (sMCL - PS:CR, p=0.09; sMCL - PS:CS, p=0.03; sMCL - PS:CSxPCL, p=0.21). The LCL has a very similar force pattern with the CR, CS and CSxPCL (LCL - CR:CS, p=0.04; LCL - CR:CSxPCL, p=0.01; LCL - CS:CSxPCL, p=0.03) where the tension increases nearly linearly until 60° of flexion and then tapers off. The CR, CS and CSxPCL max out at 109.2N, 110.8N and 112.6N respectively. Whereas the LCL in the PS component behaves similarily, but is much tighter maxing out at 171.8N at 75° of flexion. Although the force pattern is very different between PS and CR, CS and CSxPCL the overall difference in force throughout the 90° of motion is significant only for the CR component and near significance for the CS and CSxPCL (LCL - PS:CR, p=0.009; LCL - PS:CS, p=0.01; LCL - PS:CSxPCL, p=0.01).

Figure 3-6. Individual ligament (PCL, sMCL, LCL) forces during kinematic testing for CR, CS, CSxPCL and PS components through 0-90° of neutral flexion.

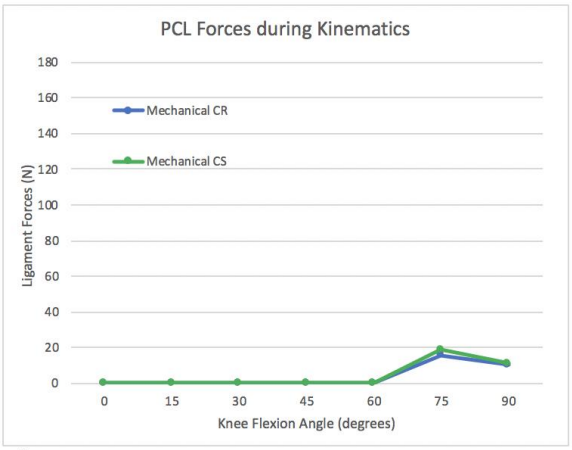

A

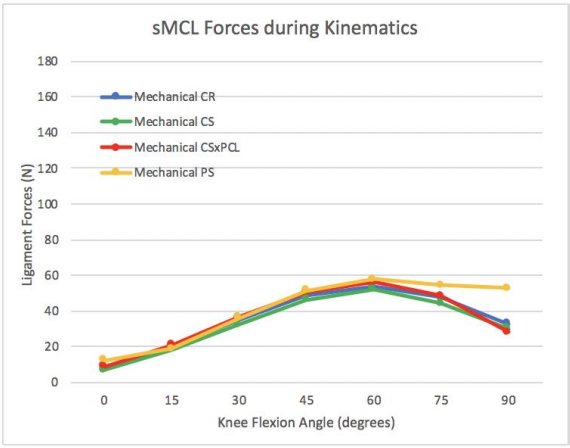

B

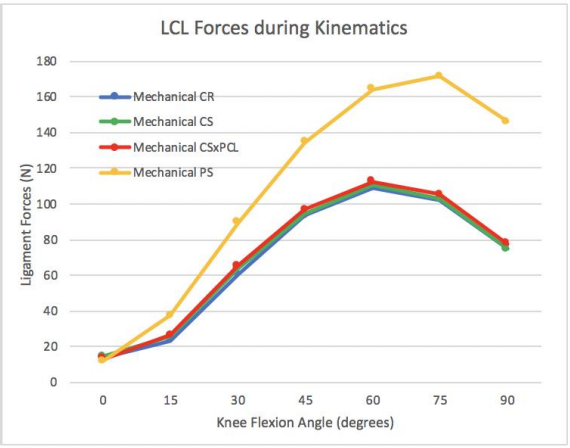

C

When looking at joint kinematics during ADLs there is no longer any difference between the CS and CSxPCL joint kinematics. This can be seen in the Gait AP, IE and VV kinematics, the graphs show in Figure 3-7A, B & C nearly identical kinematic patterns between CS and CSxPCL (AP - CS:CSxPCL, $p=0.17$; IE - CS:CSxPCL, $p=0.01$; VV - CS:CSxPCL, $p<0.001$). Comparing CR poly to the other poly's there is a statistically significant difference between each ($p<0.001$), except for CR vs PS in Gait AP kinematics (AP - CR:PS, $p=0.015$). During Gait AP kinematics there is overall less tibial displacement with the PS component (AP - PS:CR, $p=0.015$; AP - PS:CS, $p=0.122$; AP - PS:CSxPCL, $p=0.096$). The maximum posterior tibial translation occurs in the middle of the stance phase and the maximum anterior tibial translation occurs in the end of the swing phase. The total AP translation during gait is 11.08mm, 14.68mm, 15.21mm and

14.84mm for PS, CSxPCL, CS and CR respectively. In terms of gait IE kinematics, during the last third of stance phase and just over half of the swing phase, the CR poly has more constraints against IE movement compared to the two CS poly's. During this portion of the gait pattern the PS poly limits the IE kinematics the most. The maximum internal rotation occurs immediately prior to the initiation of the swing and is 12.6°, 16.1°, 18.8° & 19.2° for PS, CR, CSxPCL & CS respectively. The IE kinematics are statistically significantly different between each poly ($p<0.001$ and IE - CS:CSxPCL, $p=0.008$). In terms of Gait VV kinematics statistical analysis, there is a statistical difference between all polys ($p<0.001$); however, the pattern of the CR, CS and CSxPCL is very similar. The most striking feature graphically is that during the stance phase the PS component is persistently in a more varus position by about 0.5°. Also during the swing phase the PS component levels off at around 0° demonstrating more VV constraint than the other three components.

Figure 3-7. Kinematic testing for CR, CS, CSxPCL and PS components during normal Gait. Gait cycle begins with flat foot and goes to heel off then finishes with heel strike and flat foot. (A) Gait AP kinematics, (B) Gait IE Kinematics, (C) Gait VV kinematics.

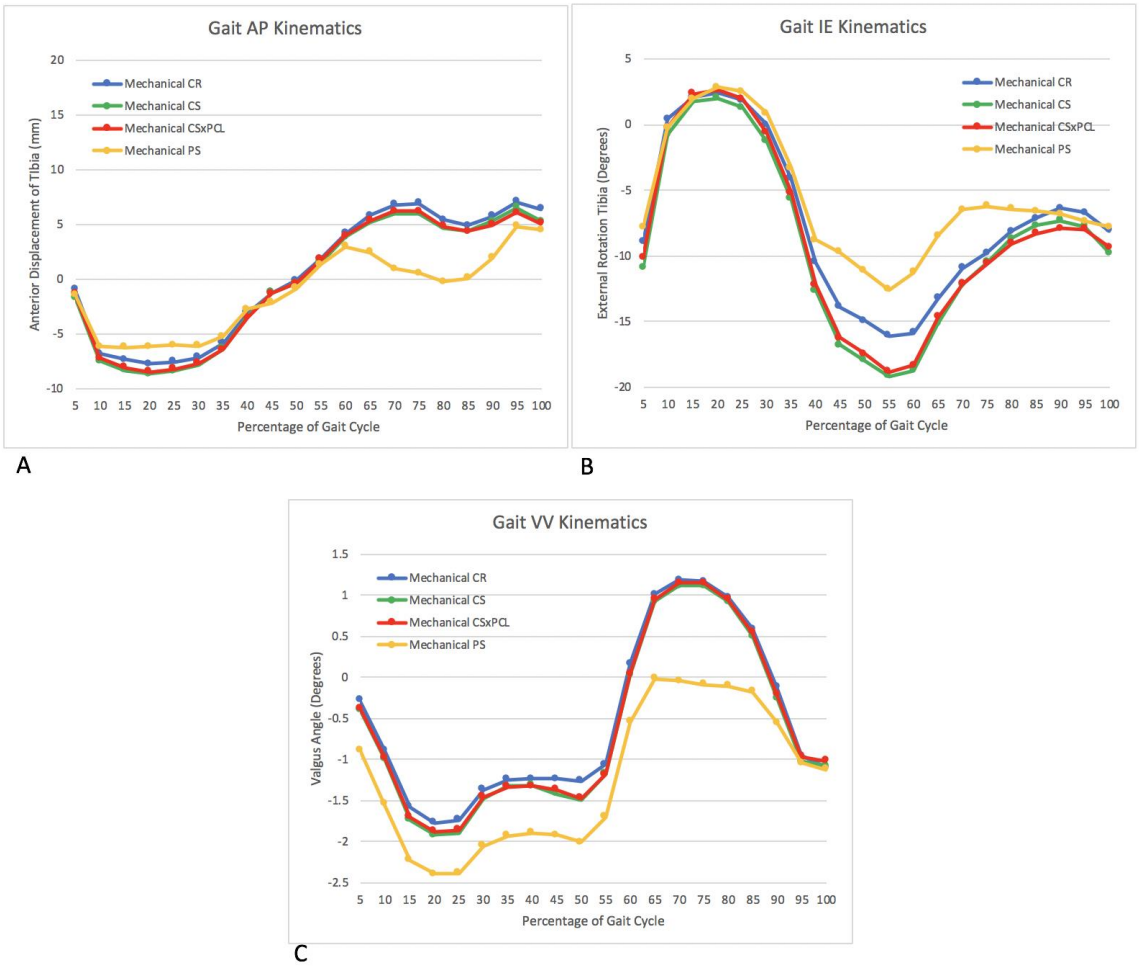

The kinematic pattern comparing CS and CSxPCL is nearly identical for Stair Descent as seen in Figure 3-8A, B & C. There are no statistically significant differences in the AP, IE or VV kinematics during Stair Descent (AP - CS:CSxPCL, p=0.97; IE - CS:CSxPCL, p=0.12; VV - CS:CSxPCL, p=0.39). During the Stair Descent AP kinematics the CR poly also behaves similar to the CS and CSxPCL although p<0.001. The PS component causes the joint to behave significantly different throughout the whole AP kinematic cycle, with the anterior displacement of the tibia being kept lower compared to the CR, CS and CSxPCL components (p<0.001). In measuring IE Kinematics the CR is significantly different than the CS and CSxPCL, averaging 2° less internal rotation at each point throughout the cycle (p<0.001). The PS component is also significantly different to the CS and CSxPCL component being more constrained overall (IE - PS:CS, p=0.001; IE. –

PS:CSxPCL, p=0.002). When comparing the PS to CR poly they respond more similarly to each other overall when compared to the CS and CSxPCL poly. However there is a significant difference in the IR limit of this motion which occurs during the last half of the stance phase. The CR is much less constrained compared to the PS during this portion of the stair descent having a maximum IR of 15.7° and 11.7° respectively. The PS is more constrained having less overall IE rotation. As the CR and PS components cross over they average out to have a non-significant overall difference (IE – PS:CR, p=0.06). The CR, CS and CSxPCL components all behave similarly during VV kinematics, although the subtle differences between the CR and CS/CSxPCL are statistically significant (VV - CR:CS, p<0.001; VV - CR:CSxPCL, p<0.001). The range of VV motion is 2.7°, 2.8°, 2.8° and 2.0° for the CR, CS, CSxPCL and PS components, respectively. The VV kinematics of the PS component is much more constrained as would be expected with the geometry of the PS post on the poly (VV - PS:CR, p<0.001; VV - PS:CS, p=0.002; VV - PS:CSxPCL, p=0.001). It also maintains a slightly more varus position throughout the stair descent cycle ranging from 0.3° to 1.5° more varus during different stages of stair descent.

Figure 3-8. Kinematic testing for CR, CS, CSxPCL and PS components during Stair Descent. Stair Descent begins and ends with the middle of swing phase. (A) Stair Descent AP kinematics, (B) Stair Descent IE Kinematics, (C) Stair Descent VV kinematics.

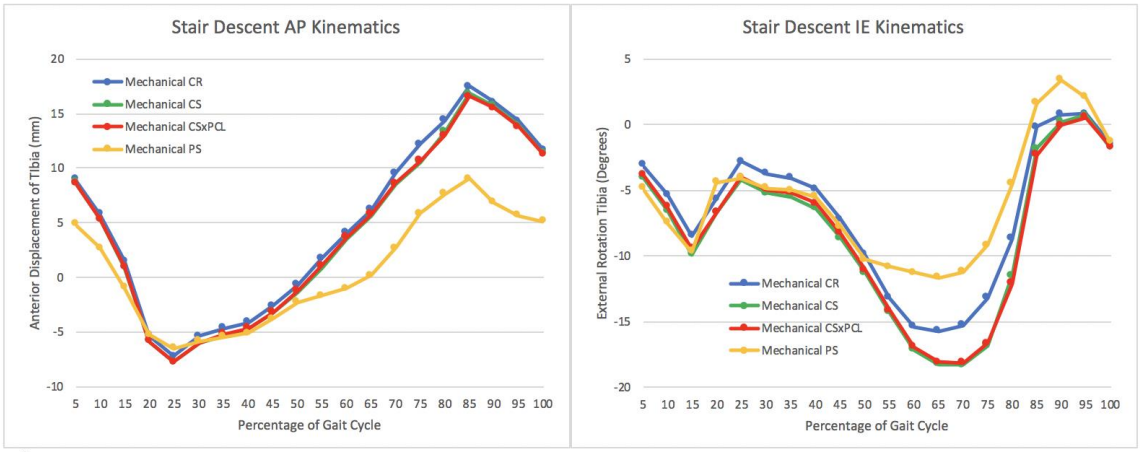

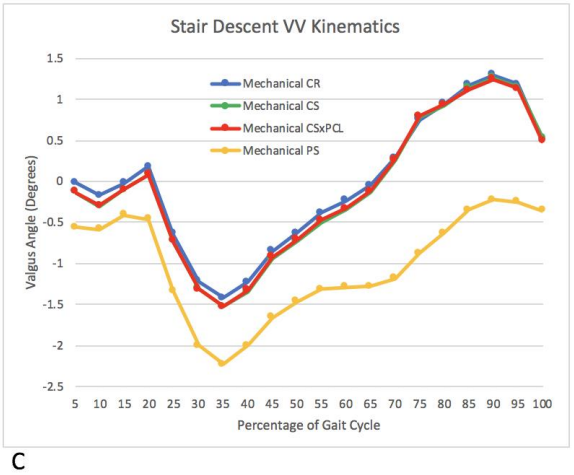

The graphed kinematics comparing CS and CSxPCL are nearly identical for Stair Ascent as seen in Figure 3-9A, B & C. However the statistical analysis does show a significant difference between CS and CSxPCL for Stair Ascent AP and VV kinematics, and there is no difference in the IE Kinematics (AP - CS:CSxPCL, $p=0.004$; IE - CS:CSxPCL, $p=0.18$; VV - CS:CSxPCL, $p<0.001$). The CR poly also produces very similar graph patterns to the CS and CSxPCL for stair ascent AP and VV kinematics, but is much different with regards to IE kinematics. However, when comparing CR with CS statistically, there is a significant difference of $p<0.001$ for all CR vs CS values except for VV - CR:CSxPCL, $p=0.05$. The PS poly performs differently to all the other polys ($p<0.003$) during stair ascent except for the CR component during IE kinematics where the overall behavior is more similar. The PS poly limits the AP translation at the joint

significantly with maximum anterior displacement of the tibia 8.22mm this is compared to the CR, CS and CSxPCL at 15.70mm, 15.52mm and 15.41mm respectively (AP - PS:CR, $p<0.001$; AP - PS:CS, $p=0.003$; AP - PS:CSxPCL, $p=0.003$). The PS and CR poly behave more similarly to each other compared to the CS/CSxPCL poly during IE kinematics (IE – PS:CR, $p=0.16$). This was seen by the PS and CR poly maintaining on average a more externally rotated position throughout the stair ascent, this was most pronounced during the swing portion of the gait. The minimal IR for the PS, CR, CS and CSxPCL was 0.2°, 2.0°, 2.8° and 3.0° respectively. The maximal IR for the PS, CR, CS and CSxPCL was 11.2°, 11.3°, 12.7°, 12.5° respectively. This gave and average IR for the PS, CR, CS, CSxPCL of 5.6°, 6.2°, 7.4°, 7.5° respectively (IE – CR:CS, $p<0.001$; IE – CR:CSxPCL, $p<0.001$; IE – PS:CS, $p<0.001$; IE – PS:CSxPCL, $p<0.001$). The CS and CSxPCL behave almost identically during the IE kinematics of stair ascent (IE – CS:CSxPCL, $p=0.18$). With regards the Stair Ascent VV kinematics for each poly variation, there was a statistically significant difference to the other polys with a $p<0.001$ except for the CR and CSxPCL (VV – CR:CSxPCL, $p=0.05$). Despite this the CR, CS, and CSxPCL seem to behave very similarly. The most prominent difference is the constraint of the PS poly limiting the VV motion and the overall more varus position maintained by the PS poly. This can be seen with the total VV range of 1.8° for the PS and 2.4°, 2.5° and 2.5° for the CR, CS and CSxPCL respectively. Also the average varus position for the PS component was 1.0° whereas the CR, CS and CSxPCL maintained an average valgus position of 0.1°, 0.1°, 0.1° respectively.

Figure 3-9. Kinematic testing for CR, CS, CSxPCL and PS components during Stair Ascent. Stair Ascent begins and ends with the middle of swing phase. (A) Stair Ascent AP kinematics, (B) Stair Ascent IE Kinematics, (C) Stair Ascent VV kinematics.

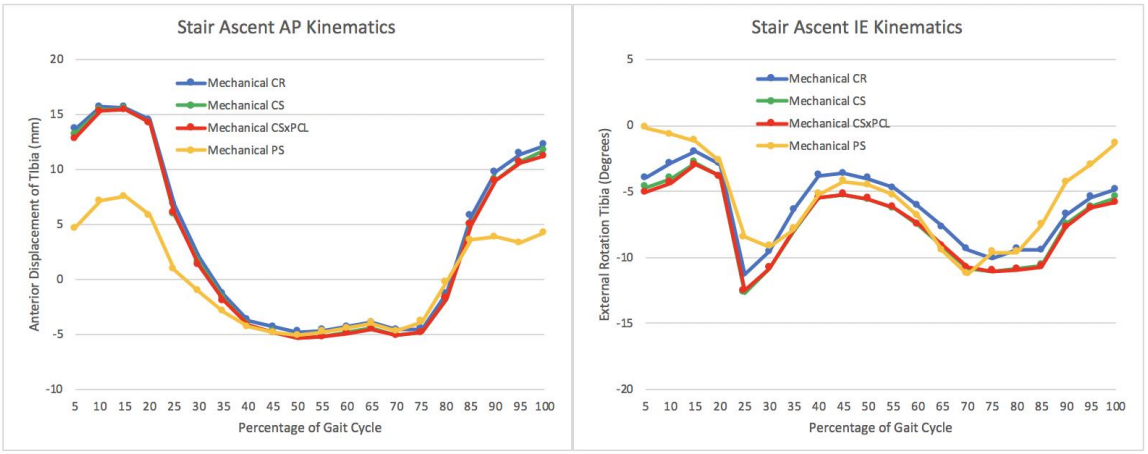

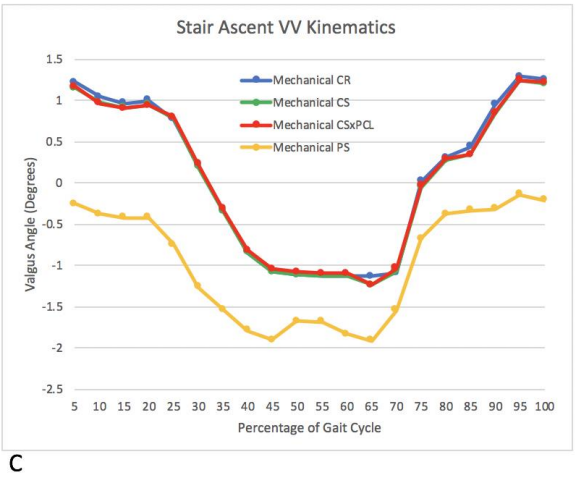

3.4.2 Joint Laxity

During AP laxity testing in neutral flexion and extension, the CSxPCL does not fully compensate for the lack of a PCL, as shown in Figure 3-10A. The CSxPCL poly decreases posterior tibial translation slightly as the knee flexes, but overall maintains a much greater posterior tibial displacement compared to the other polys. In contrast, the CR, CS and PS decrease in posterior translation as restrained by the PCL or the PS post geometry as the knee flexes. Also, the PS post produces more constraint than the PCL in this scenario. The posterior translation of the tibia at 90° of flexion is 11.0mm, 3.3mm, 3.5mm and 1.4mm for the CSxPCL, CS, CR and PS respectively (AP - CSxPCL:CR, p=0.02; AP - CSxPCL:CS, p=0.01; AP - CSxPCL:PS, p=0.002). The PS poly has a more persistant drop in AP translation compared to the variable nature of the CR and CS poly

(AP - PS:CR, p=0.006; AP - PS:CS, p=0.01). When looking at the VV laxity as seen in Figure 3-10B all the poly components behave quite similarly. There is no statistically significant difference among the polys (p>0.01) except for between the PS and CR poly (VV – CR:PS, p=0.005). In all polys there is a steady decrease in VV displacement until 60° of flexion. It is at this point that the CSxPCL poly trends upward slightly more rapidly than the CS, CR and PS polys. This indicates the PCL aids in VV constraint in deeper flexion but does not add as much constraint as the PS post.

Figure 3-10. Joint laxity during neutral motion testing for CR, CS, CSxPCL and PS components through 0-90° of flexion. (A) AP laxity when 100N of posterior force applied. (B)VV laxity when 10Nm moment applied to tibial actuator.

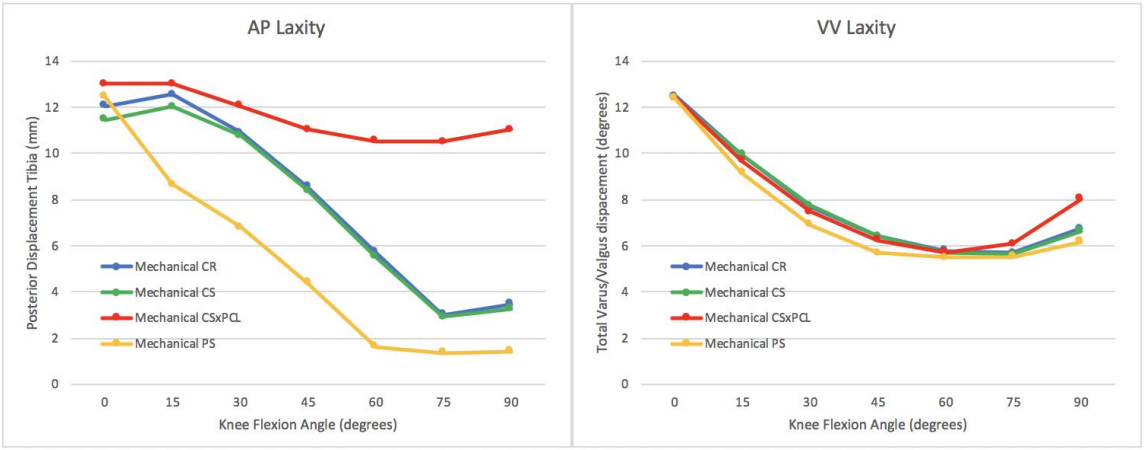

A B

We also looked at the tensions across each ligament during the laxity testing. Figure 3-11 shows the individual ligament forces during the AP laxity test. As would be expected the forces in the PCL during AP laxity testing are greater than they were in neutral flexion and extension without any loads or external forces. The PCL had 0N force on it in the first 60° of kinematic testing and then engages to assist with femoral roll back and increases to a maximum of 16.0N and 18.9N for CR and CS respectively. During the AP laxity testing the PCL is engaged immediately at 0° of flexion and increases throughout

the 90° of flexion. The PCL starts at 82.4N and 50.4N, it reaches a maximum of 163.4N and 169.5N for CR and CS respectively. As in the neutral flexion and extension the CR and CS polys with a PCL intact during AP laxity testing, behave very similarly (PCL AP - CR:CS, $p=0.23$). In Figure 3-11C the sMCL has significantly higher initial forces in the CSxPCL and the PS component compared to the CR and CS polys. The sMCL forces in the CSxPCL maintains a significantly higher tension, whereas the PS component quickly drops in the first 15° of flexion to match the CR and CS components more closely. This is again evidence that the CSxPCL doesn't compensate fully for the lack of a PCL (sMCL AP – CSxPCL:CR, $p<0.001$; sMCL AP – CSxPCL:CS, $p<0.001$; sMCL AP – CSxPCL:PS, $p<0.05$; sMCL AP – PS:CR, $p=0.29$; sMCL AP – PS:CS, $p=0.21$). In Figure 3-11D the overall difference among each poly compared to the other ones is mostly insignificant with a $p>0.01$ except for comparing CSxPCL to the CR and CS poly (LCL AP – CSxPCL:CR, $p=0.002$; LCL AP – CSxPCL:CS, $p=0.002$). The PS poly, however, initiates with a slight decrease in the LCL forces during early flexion, which then steadily increase to produce the greatest tension across the LCL. In contrast, the CR, CS and CSxPCL increase LCL forces initially then taper off after 60° of flexion. The CSxPCL maintains higher tension compared to the CR and CS poly. The maximum LCL tension for each poly is 119.6N, 117.1N, 142.7N and 170.0N for the CR, CS, CSxPCL and PS poly respectively.

Figure 3-11. Individual ligament (PCL, sMCL, LCL) forces during AP laxity testing for CR, CS, CSxPCL and PS components. AP laxity testing was applied through 0-90° of neutral flexion, having 100N of posterior force applied at 15° increments.

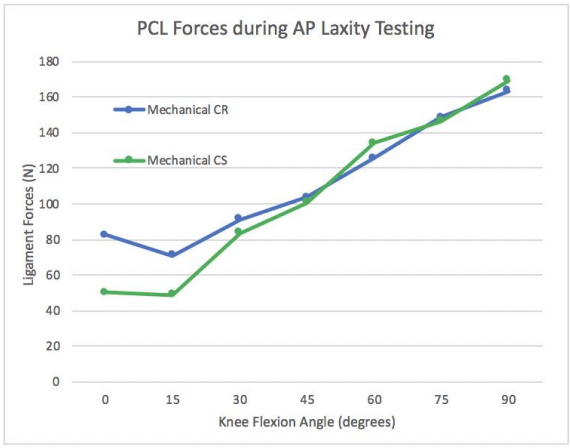

A

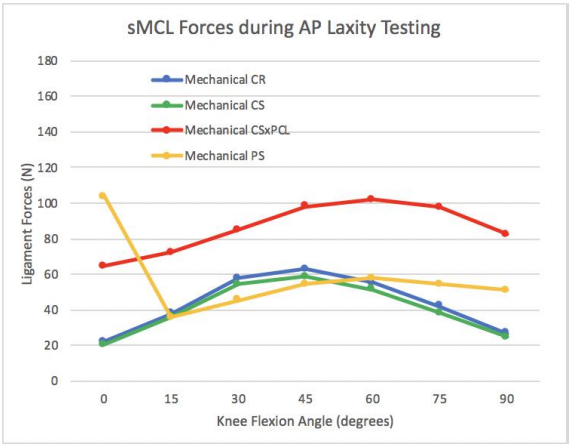

B

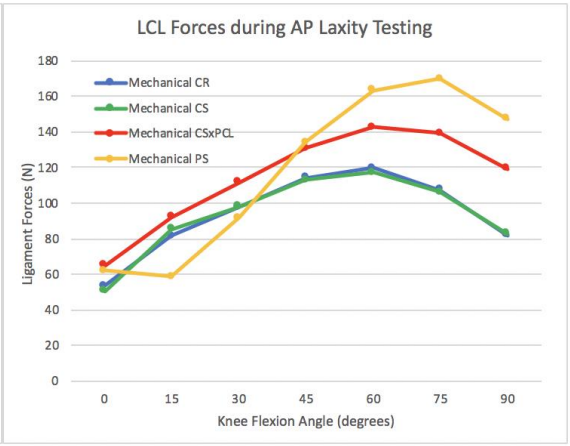

C

Figure 3-12 shows the individual ligament forces during valgus stress testing. The PCL as seen in Figure 3-12A generates tension in the first 15° of flexion and then again after 45°, but it produces much lower forces in the Valgus laxity test (max tension of 56.5N and 65.5N in the CR and CS respectively) as compared to the AP laxity test. The CR and CS poly's have a similar pattern of reactive force (PCL Valgus - CR:CS, p=0.3). As expected the force generated by the sMCL is greatly increased during the valgus stress as can be seen in Figure 3-12B. The sMCL ligament forces in all the poly components increase by about three to fourfold compared to the neutral tests. The CR, CS and CSxPCL were not statistically different to each other (sMCL Valgus - CR:CS, p=0.99; sMCL Valgus - CR:CSxPCL, p=0.04; sMCL Valgus - CS:CSxPCL, p=0.07). However the PS was statistically different to the CR, CS and CSxPCL (sMCL Valgus - CR:PS, p=0.002;

sMCL Valgus – CS:PS, p=0.004; sMCL Valgus – CSxPCL:PS, p<0.001). The PS component produced persistently higher tension in the sMCL which can be seen in their maximum tensions of 145.1N, 145.3N, 151.2N and 177.3N for CR, CS, CSxPCL and PS respectively. In Figure 3-12C the forces across the LCL are substantially decreased as they are on the concave side of the valgus angle. The average force in each poly is about 33% decreased compared to neutral testing. Again the CR, CS and CSxPCL behave almost identically although the CR and CS have a statistically difference (LCL Valgus – CR:CS, p=0.007; all others p>0.01). The PS poly produces a persistently higher tension across the LCL however this not statistically significant. The maximum tension on the LCL is 72.4N, 73.6N, 75.8N and 126.5N for CR, CS, CSxPCL and PS respectively.

Figure 3-12. Individual ligament (PCL, sMCL, LCL) forces during Valgus laxity testing for CR, CS, CSxPCL and PS components. Valgus laxity testing was applied through 0-90° of neutral flexion, having a 10Nm valgus torque applied at 15° increments.

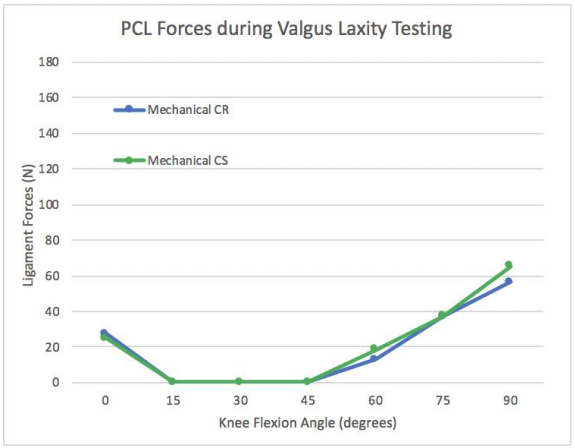

A

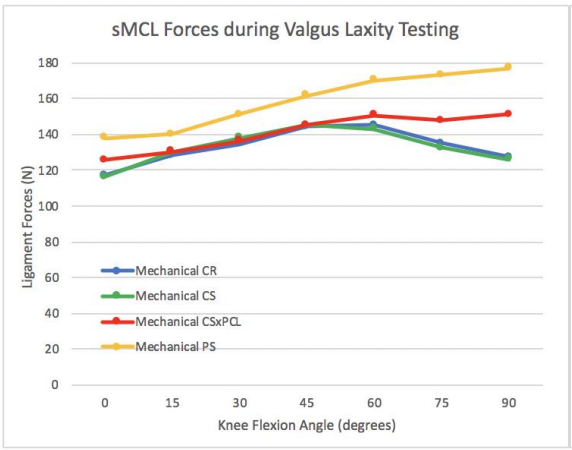

B

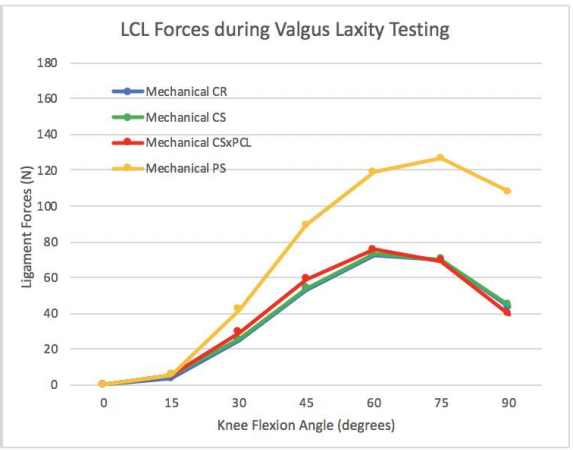

C

During Varus testing as seen in Figure 3-13A the PCL has very minimal force generated in it. This is because the PCL is considered a medial structure and is on the concavity of varus angle. The PCL has minimal and decreasing force during the first 15° then has 0N of force across it till 60° of flexion where it increases to only 24.0N and 22.8N for the CR and CS respectively (PCL Varus - CR:CS, p=0.6). In all polys the overall sMCL forces are substantially decreased. They are decreased by about 33% in the all polys compared to neutral flexion tests. The sMCL force in the PS component is slighty more taught throughout the flexion cycle and is most pronounced after 60° of flexion. However, the are no statistically significant differences among all the polys for the sMCL tension ($p>0.01$). The LCL experiences much higher forces during the varus stress. For all different polys the forces exponentially increased in the first 45° of flexion. In the second

45° of flexion there was still about 50% more tension in the CR, CS and CSxPCL polys and about 10% increase in the PS poly. There was a more consistent state of tension in the CR, CS, and CSxPCL polys, with less than 15N of variation over the 90° of flexion. There was more variation in the LCL tension with the PS poly, but comparing all the polys, they were not statistically different to one another with p>0.01.

Figure 3-13. Individual ligament (PCL, sMCL, LCL) forces during Varus laxity testing for CR, CS, CSxPCL and PS components. Varus laxity testing was applied through 0-90° of neutral flexion, having a 10Nm varus torque applied at 15° increments.

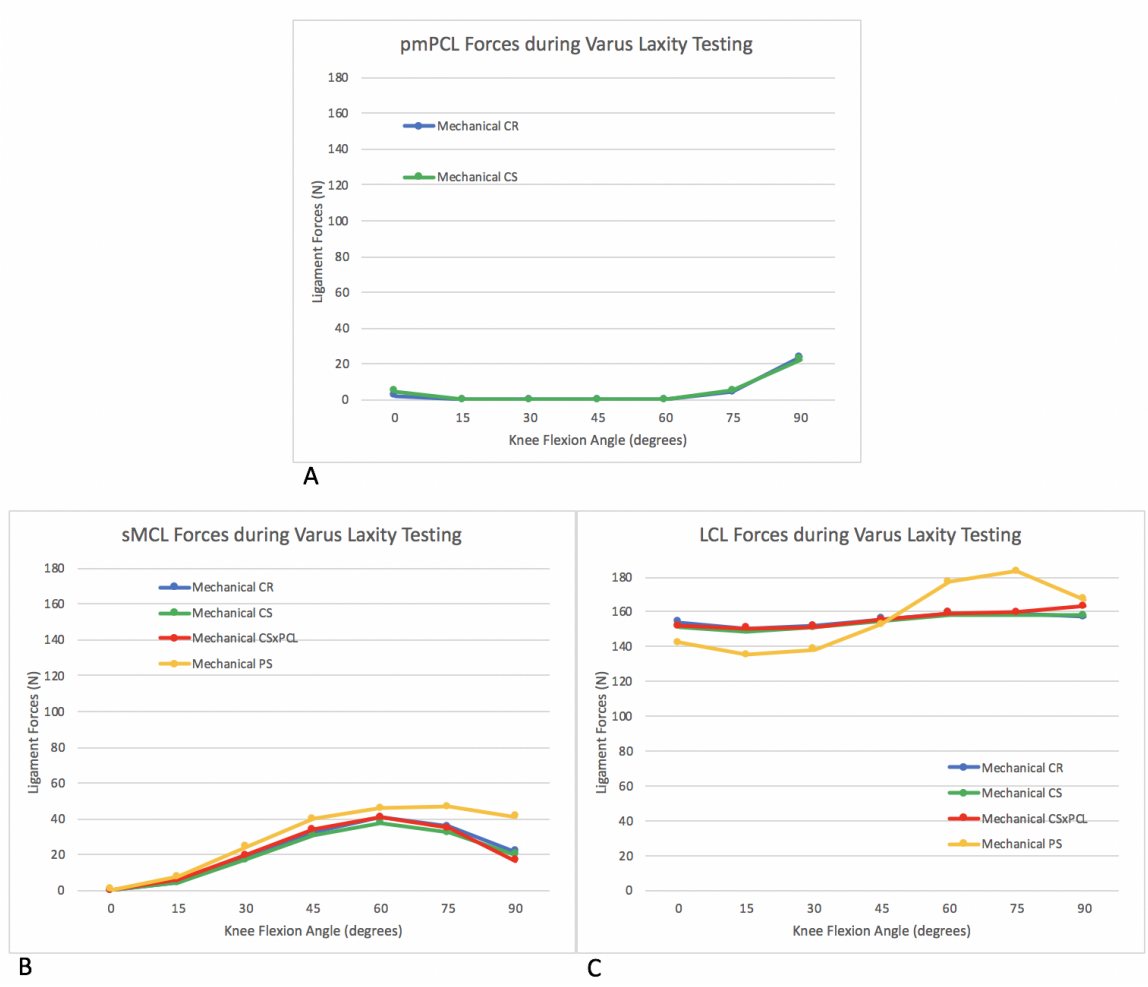

3.5 Discussion

The main objective of this work is to understand how Cruciate Retaining, Cruciate Sacrificing and Posterior Stabilized components effect the soft tissue balance, stability and knee joint kinematics. The most striking difference was the manner in which the CSxPCL poly behaved compared to the CS poly with a PCL or the CR and PS poly. There are periods where the CSxPCL poly behaves just like the CS poly as would be expected, but there are also periods where the CSxPCL poly behaves more like the PS poly. As shown by Willing et al. we also found that the CS poly without a PCL does not fully compensate for the lack of a PCL[26]. This can be seen in Figure 3-4A where the AP joint kinematics are significantly different and the CSxPCL does not produce as much femoral roll back as the CR and CS polys with a PCL. Also Figure 3-4B show the lack of constraint the CSxPCL poly has to resisting IE especially in deep flexion. It is known that in deeper flexion the PCL has a significant role in limiting internal rotation[12] and this can be seen in the lack of constraint the CSxPCL demonstrates in Figure 3-4B. When looking at the AP laxity testing (Figure 3-10A) it was very evident that the CSxPCL poly could not compensate for the lack of PCL. The AP translation in the CSxPCL was not constrained at all as the knee flexed. In the CR, CS and PS poly's there was a steady decrease in AP translation as the knee flexed and the PCL became more engaged or as the PS post aided in femoral roll back; whereas, the CSxPCL allowed for nearly consistent posterior translation of the tibia (between 10.5-13.0mm) throughout the whole 90° cycle. Interestingly, in the ADL simulation the CSxPCL behaved very similar to the CR and CS with a PCL. As seen in Figure 3-7, Figure 3-8 and Figure 3-9, the CSxPCL and CS polys followed near identical motion patterns. Furthermore, for most of the motion patterns the CR poly also behaved similarly to the CS and CSxPCL components. Although there were some statistical differences it appears that during gait, stair ascent and stair descent the CSxPCL poly does fully compensate for the lack of a PCL when compared to the CR and CS polys. The likely reason for the ADL simulations to show a more similar kinematic pattern between the CSxPCL and the CR/CS polys, is likely because there is not significant deep flexion performed in these motion cycles. Also the compressive forces generated by the simulated 75kg person will allow the geometry of the CS poly to perform better in substituting the role of the PCL. This result was contrary to what

Willing et al. found in the stair ascent and descent group[26]. They found the CSxPCL still did not compensate fully however they only applied 25% of the appropriate loads during the cycle to protect their specimen. This work does prove the Willing et al. speculation that if the loads were increased to normal the CS poly geometry would be able to compensate appropriately during ADLs.

The AP kinematics in Figure 3-4A also show that our overall AP translation in the CR and CS poly's are quite large compared to native knee AP translation (maximum 7-10mm in native knees versus 10.3-10.6mm in the CR and CS TKAs)[26,28]. However complete sectioning of the PCL has been shown to cause 11.4 and 11.7mm of tibial translation at 90° of flexion in the native knee[12]. Also the AP translation of the CR and CS poly is similar to the AP translation seen in the TKA simulations in Willing et al. and Lutzner et al[26,28]. In the AP kinematics the CSxPCL and PS poly produce translations more similar to the native knee[26]. The significant femoral roll back seen could be a result of over tensioned or error in the PCL properties. However our results showed a general increase in PCL force starting at 60° of flexion. The PCL is expected to be engaged between 30° and 60° in order to initiate femoral rollback[29]. When looking at the AP kinematics for the ADL testing the only significant difference is the PS component behaves much differently compared to the other polys. This is likely due to the PS post which does not generate as significant posterior roll back as the PCL itself. This can be seen in Figure 3-7A, Figure 3-8A and Figure 3-9A, which shows that there is less anterior tibial translation in the gate cycles where there is more flexion and in parts of the motion where the knee is less flexed the PS poly behaves more similar to the CR, CS and CSxPCL.

The VV kinematics consistently show that there is more constraint with the PS poly as would be expected due to the significantly different articular geometries. This is most effected in areas of deeper flexion where the PS post would be more engaged. This can be seen very obviously in Figure 3-7C. There is a near plateau in the VV motion during the most flexed position in the swing phase of gait. VV kinematics in a "balanced knee" has defined as less than 2° of motion in varus and valgus[30]. In our VV kinematic testing during neutral flexion we have shown the CR, CS and CSxPCL VV kinematics to be in the 3.2° range and the PS component to be in the 1.1° range, which would prove to be a

balanced knee. Also during the ADL VV kinematic testing the overall degree of VV motion has been similar. In Figure 3-7C the CR, CS and CSxPCL VV kinematics are in the 2.9-3.0° range and the PS is near the 2.3° range. This is the similar in Figure 3-8C the CR, CS and CSxPCL VV kinematics are in the 2.7-2.8° range and the PS is near the 2.0° range. There is slightly less VV motion in Figure 3-9C the CR, CS and CSxPCL VV kinematics are in the 2.4-2.5° range and the PS is near the 1.8° range. Overall the VV kinematics are within expected parameters.

As expected the PS component performs differently as a whole or in part of nearly all testing situations. This is likely due to the significantly different articular geometries. However one area where it may not be due to the PS geometry is the ligament tensions. In Figure 3-5 we see that the total joint compressive forces is different for the PS poly compared to the others. The CSxPCL does have a slightly more rapid decrease in total compressive forces after 60° of flexion when compared to the CR and CS. This is likely due to the fact that the PCL has been sacrificed and as seen in Figure 3-6A, at 60° is also where the PCL becomes significantly engaged. Yet despite the PS poly not having a PCL the compressive forces continue to increase in the PS TKA beyond 60° of flexion. As seen in Figure 3-6B&C the collateral ligaments continue to become significantly taught with the PS but in the CR, CS and CSxPCL the collateral ligaments increase in tightness till 60° and then begin to slacken off. In the CR, CS and CSxPCL the overall joint compression forces (Figure 3-5) are higher at 90° of flexion than at 0°, but there is this consistent pattern of becoming tight and then relaxing after 60° of flexion. In Figure 3-6B&C we can see that the sMCL and the LCL maintains the pattern of tightening through the first 60° of flexion and then tapering off to result with higher tensions at 90° of flexion compared to extension. The LCL however does this with higher amplitude of tension and change. There is significant ligament forces generated by the collateral ligaments during flexion. This is contrary to what Willing et al. and Aunan et al. have published, namely that collateral ligaments should be tight in extension and loosen in flexion[25,31]. However Park et al. has indicated in native knees that different bundles of the collateral ligaments will tighten or loosen with flexion[32]. This can be seen in the fact that our sMCL is closer to the same tension in flexion and extension whereas our LCL is

tighter in flexion than extension. This may also be a limitation to the single point position of our ligament insertion points, and the fact that we are not attaching the ligaments as multiple bundles over a geographical footprint. It is likely that different ligament bundles can behave contrary to another depending upon where their origin and insertion points are. This also is an indication that our point to point insertions can have different properties depending on where within the ligament footprint the have been placed. Ligament insertion points can definitely be a reason why the PS poly continues to have significantly higher compressive forces as well, but the insertion points are identical between the PS and the other 3 polys. Thus there needs to be another explanation for this. Figure 3-6 also shows that the collateral ligaments both behave very differently in the PS TKA. The sMCL maintains its tension in the PS poly after 60° of flexion and doesn't slacken off like the CR,CS and CSxPCL polys. The LCL has much higher forces in it and contrary to the other 3 polys, in the PS poly the LCL is tighter in flexion than in extension. Other than the geometry of the poly there is only one other technical difference in the PS group compared to the CR,CS and CSxPCL group that could explain this persistent tightness. That is the change in the posterior slope of the tibia to 3° compared to the 5°. This shows the significant difference just 2° of slope in the tibia can have in affecting the biomechanics and tightness of the soft tissues around the knee. Other studies have shown tibial slope can affect biomechanics, ligament tension, range of motion and component longevity[33–36]. This would be an important future area to study with this protocol as this area is still not well understood as to what the ideal posterior tibial slope is[33]. Also it is likely one of the least accurately reproduced cuts made in the TKA procedure with conventional instruments and arguably also using more sophisticated guides such as navigation or robotics.

When comparing the laxity testing as discussed previously the CSxPCL does not fully compensate for the lack of the PCL. Another common theme is the increased constraint of the PS poly and a transfer of more of the ligament forces to the collateral ligaments especially the sMCL. The PS poly behaves differently to the other 3 except for the CSxPCL which behaves more like the PS poly by transferring significantly increased forces to the sMCL during AP laxity and Valgus laxity testing (Figure 3-11B & Figure

3-12B). This is likely due to the fact that the PCL is a medial based structure and thus when it is fully release it is no longer able to supplement the sMCL. The fact that the PCL is a medial based structure can also be seen in its ligament behavior during each laxity testing. In Figure 3-11A we can see the significant increase in forces of the PCL as the PCL tries to resist the posterior force of the tibia. As previously shown by Laprade et al. the alPCL bundle does not have as significant role in resisting posterior translation compared to the pmPCL[12] and in our ligament insertions for the PCL, this point to point ligament is more representative of the pmPCL bundle. In Figure 3-12A we see how the PCL is still engaged in resisting valgus forces. However when compared to Figure 3-13A there is very minimal forces seen in the PCL during a varus stress. This significant difference indicates the PCL has a role in resisting valgus forces as a medial based structure. Figure 3-11B&C show that the sMCL has significantly lower forces in the CR and CS poly when there is a PCL to help mitigate the forces. The sMCL also has lower forces in the CR and CS poly when compare to the LCL ligament forces. This is an indication that the PCL and sMCL work together to balance the knee on the medial side compared to the LCL on the lateral side. Whereas the CSxPCL has close to equal forces in the sMCL and LCL throughout the 90° of flexion. The PS TKA has slightly higher LCL forces compared to the sMCL however the ligament behaviour of tight in extension, loosening for the first 15° of flexion and then steadily tightening up again till 90° of flexion is well balanced. In Figure 3-12B&C during valgus force as expected the sMCL forces increase substantially to resist the 10Nm torque. As expected the CSxPCL and PS constructs have even higher sMCL forces than the CR and CS to compensate for the lack of the PCL. The LCL still exhibits similar behaviour as seen in the neutral flexion and AP laxity test but at much lower forces as the ligament is not being stressed during the valgus force. In Figure 3-13B&C during varus stress the LCL has much higher forces across it compared to neutral flexion or AP laxity. The interesting point here is that there is no significant difference at all between the polys as there is no PCL or lack of PCL on the lateral side of the knee to augment the stress on the LCL. The LCL also has around 130-180N of force during the varus stress which is similar to the 130-180N seen in sMCL of the CSxPCL and PS during valgus stress. Whereas the CR and CS polys during valgus stress have around 110-145N of force as they are supplemented with the PCL sharing

some of that force. The compensation of the sMCL may be a reason why patients describe the CR knee as feeling more physiologic[37]. Overall the Laxity testing shows that all TKA constructs are well balanced.

Some limitations to this study include using point to point ligaments rather than bundles of ligaments to fully represent the native ligament properties and origin/insertion footprints. Nearly all studies addressing ligament properties have referenced Blankevoort et al. as one of the foundational papers for ligament properties[22]. Unfortunately each human knee is unique in their ligament properties including zero load lengths, reference strains, stiffness and insertion points. Since Blankevoort et al. there have been many other papers written to try to establish accurate ligament properties, such as the ones we used to help guide our ligament properties[20,21]. Despite all the work that has been done to identify accurate ligament properties there is still a significant variation in the literature as to what the actual ligament properties should be as seen in table 5 of the systematic review performed by Peters et al[24]. A limitation with all computational models are the necessary approximations and assumptions made to simplify the complexity of the human knee to something that can be represented computationally. Therefore assuming ligaments to be point-to-point springs with origins and insertions simply within the anatomic footprint, using ligament properties that aren't exact and only including the three main ligaments addressed in TKA balancing for our soft tissue model limit the overall accuracy of the physical/virtual construct. Another limitation is the ADL simulation loading parameters are based off of TKA parameters using PS polys[27]. This could affect the response of our CR and CS TKA constructs. However there have been other computational studies that show the applicability of the same ADL simulation loading patterns in CR components[38]. Another possible limitation is that we used polydimethylsiloxane (silicone)-based lubricant (HAS0001-OS, Horizon Fitness, Cottage Grove, WI) as a joint lubricant. It has been shown previously that during joint motion simulation a mixture of bovine serum and hyaluronic acid (HA) to lubricate the articulating surface is superior[39]. Reproducing the data with this lubricant may or may not change the results. It is low likelihood as the bovine serum and HA is ideal for higher repetitious wear studies and is likely to have minimal effect on our low velocity, low volume study.

In Summary, the CR, CS, CSxPCL and the PS TKA constructs reproduced balanced TKA motion with joint kinematics similar to previously reported data. Obviously there will be distinct differences as the polys are designed to perform differently. The most striking difference was that the CSxPCL construct did not fully compensate for the lack of a PCL. This was evident in the neutral flexion kinematic and laxity testing. However during the ADLs with full load simulation, the CSxPCL was able to fully compensate for the lack of a PCL producing balanced reproducible kinematics similar to the CR and CS with PCL constructs. Femoral roll back in our study was on the higher end of normal as published by other authors, but when compared to motions in native knees with section PCL the tibial translation was appropriate. It's difficult to know if this is an error in our PCL ligament properties as the literature is so conflicted currently on the appropriate ligament properties. This also applies to the collateral ligaments. However our study does show that there is likely to be differences in kinematics and forces within the different bundles even in the collateral ligaments. Future studies should be done with soft tissue ligament models that more closely represent the anatomical insertions and properties of the ligaments involved in balancing knees. This work produced similar VV and IE kinematics to what has been previously published for TKAs. The posterior tibial slope may have a significant role in the balance of TKAs; a better understanding and technique for performing accurate posterior tibial slope would likely be beneficial to patient outcomes. The laxity testing did show the knees to be well balanced throughout the 90° of flexion, however where the PCL is sacrificed it necessitates that the sMCL picks up the slack to maintain balance in the joint. Having an intact PCL is protective to the sMCL and helps offload forces through the sMCL. This study also offers a baseline computational model that reproduces appropriate TKA joint kinematics and laxities, which can then be used for future studies providing better understanding in total knee arthroplasty.

3.6 References

1. Papas PV, Cushner FD, Scuderi GR. The History of Total Knee Arthroplasty. Tech Orthop. 2018;33(1):2–6.
2. Bourne RB, Chesworth BM, Davis AM, Mahomed NN, Charron KDJ. Patient satisfaction after total knee arthroplasty: Who is satisfied and who is not? Clin Orthop Relat Res. 2010;468(1):57–63.
3. Williams DH, Garbuz DS, Masri BA. Total knee arthroplasty: Techniques and results. B C Med J. 2010;52(9):447–54.
4. Marsh J, Somerville L, Howard JL, Lanting BA. Significant cost savings and similar patient outcomes associated with early discharge following total knee arthroplasty. Can J Surg. 2019;62(1):20–4.
5. Bhandari M, Smith J, Miller LE, Block JE. Clinical and economic burden of revision knee arthroplasty. Clin Med Insights Arthritis Musculoskelet Disord. 2012;5:89–94.
6. Sharkey PF, Lichstein PM, Shen C, Tokarski AT, Parvizi J. Why are total knee arthroplasties failing today-has anything changed after 10 years? J Arthroplasty [Internet]. 2013;29(9):1774–8. Available from: http://dx.doi.org/10.1016/j.arth.2013.07.024
7. Lombardi A V., Berend KR, Adams JB. Why knee replacements fail in 2013: Patient, surgeon, or implant? Bone Jt J. 2014;96B(11):101–4.
8. Fehring TK, Odum S, Griffin WL, Mason JB, Nadaud M. Early failures in total knee arthroplasty. In: Clinical Orthopaedics and Related Research. 2001.
9. Smith T, Elson L, Anderson C, Leone W. How are we addressing ligament balance in TKA? A literature review of revision etiology and technological advancement. J Clin Orthop Trauma [Internet]. 2016;7(4):248–55. Available from: http://dx.doi.org/10.1016/j.jcot.2016.04.001
10. Montgomery L. Testing Mechanical Alignment and Kinematic Alignment in TKR Knees Using a Virtual Ligament Knee Model. 2020.
11. Grood ES, Suntay WJ. A joint coordinate system for the clinical description of three-dimensional motions: Application to the knee. J Biomech Eng. 1983;105(2):136–44.
12. Laprade CM, Civitarese DM, Rasmussen MT, Laprade RF. Emerging updates on the posterior cruciate ligament. Am J Sports Med. 2015;43(12):3077–92.
13. Edwards A, Bull AMJ, Amis AA. The Attachments of the Fiber Bundles of the Posterior Cruciate Ligament: An Anatomic Study. Arthrosc - J Arthrosc Relat Surg. 2007;
14. Hosseini A, Qi W, Tsai TY, Liu Y, Rubash H, Li G. In vivo length change patterns of the medial and lateral collateral ligaments along the flexion path of the knee. Knee Surgery, Sport Traumatol Arthrosc. 2015;23(10):3055–61.
15. Nasab SHH, List R, Oberhofer K, Fucentese SF, Snedeker JG, Taylor WR.

Loading patterns of the posterior cruciate ligament in the healthy knee: A systematic review. PLoS One. 2016;11(11):1–28.

16. Serra Cruz R, Olivetto J, Dean CS, Chahla J, LaPrade RF. Superficial Medial Collateral Ligament of the Knee: Anatomic Augmentation With Semitendinosus and Gracilis Tendon Autografts. Arthrosc Tech [Internet]. 2016;5(2):e347–52. Available from: http://dx.doi.org/10.1016/j.eats.2016.01.011

17. LaPrade RF, Engebretsen AH, Ly T V., Johansen S, Wentorf FA, Engebretsen L. The anatomy of the medial part of the knee. J Bone Jt Surg - Ser A. 2007;89(9):2000–10.

18. Bedi A, Laprade RF, Burrus MT. Knee Ligaments Landmarks Anatomy. 2018;1241–50.

19. Saigo T, Tajima G, Kikuchi S, Yan J, Maruyama M, Sugawara A, et al. Morphology of the Insertions of the Superficial Medial Collateral Ligament and Posterior Oblique Ligament Using 3-Dimensional Computed Tomography: A Cadaveric Study. Arthrosc - J Arthrosc Relat Surg [Internet]. 2017;33(2):400–7. Available from: http://dx.doi.org/10.1016/j.arthro.2016.07.030

20. Smith CR, Vignos MF, Lenhart RL, Kaiser J, Thelen DG. The influence of component alignment and ligament properties on tibiofemoral contact forces in total knee replacement. J Biomech Eng. 2016;138(2).

21. H. Bloemker K. Computational Knee Ligament Modeling Using Experimentally Determined Zero-Load Lengths. Open Biomed Eng J. 2012;

22. Blankevoort L, Huiskes R. Ligament-bone interaction in a three-dimensional model of the knee. J Biomech Eng. 1991;

23. Chen Z, Zhang X, Ardestani MM, Wang L, Liu Y, Lian Q, et al. Prediction of in vivo joint mechanics of an artificial knee implant using rigid multi-body dynamics with elastic contacts. Proc Inst Mech Eng Part H J Eng Med. 2014;228(6):564–75.

24. Peters AE, Akhtar R, Comerford EJ, Bates KT. Tissue material properties and computational modelling of the human tibiofemoral joint: A critical review. PeerJ. 2018.

25. Willing R, Walker PS. Measuring the sensitivity of total knee replacement kinematics and laxity to soft tissue imbalances. J Biomech [Internet]. 2018;77:62–8. Available from: https://doi.org/10.1016/j.jbiomech.2018.06.019

26. Willing R, Moslemian A, Yamomo G, Wood T, Howard J, Lanting B. Condylar-Stabilized TKR May Not Fully Compensate for PCL-Deficiency: An In Vitro Cadaver Study. J Orthop Res. 2019;

27. Bergmann G, Bender A, Graichen F, Dymke J, Rohlmann A, Trepczynski A, et al. Standardized loads acting in knee implants. PLoS One. 2014;9(1).

28. Lützner J, Firmbach FP, Lützner C, Dexel J, Kirschner S. Similar stability and range of motion between cruciate-retaining and cruciate-substituting ultracongruent insert total knee arthroplasty. Knee Surgery, Sport Traumatol Arthrosc. 2015;

29. Dennis DA, Komistek RD, Colwell CE, Ranawat CS, Scott RD, Thornhill TS, et al. In vivo anteroposterior femorotibial translation of total knee arthroplasty: A multicenter analysis. In: Clinical Orthopaedics and Related Research. 1998.

30. Matsuda Y, Ishii Y, Noguchi H, Ishii R. Varus-valgus balance and range of movement after total knee arthroplasty. J Bone Jt Surg. 2005;87(6):804–8.

31. Aunan E, Kibsgård T, Clarke-Jenssen J, Röhrl SM. A new method to measure ligament balancing in total knee arthroplasty: Laxity measurements in 100 knees. Arch Orthop Trauma Surg. 2012;132(8):1173–81.

32. Park ES, DeFrate LE, Suggs JF, Gill TJ, Rubash HE, Li G. The change in length of the medial and lateral collateral ligaments during in vivo knee flexion. Knee. 2005;12(5):377–82.

33. Seo SS, Kim CW, Kim JH, Min YK. Clinical Results Associated with Changes of Posterior Tibial Slope in Total Knee Arthroplasty. Knee Surg Relat Res. 2013;25(1):25–9.

34. Bellemans J, Robijns F, Duerinckx J, Banks S, Vandenneucker H. The influence of tibial slope on maximal flexion after total knee arthroplasty. Knee Surgery, Sport Traumatol Arthrosc. 2005;

35. Okazaki K, Tashiro Y, Mizu-uchi H, Hamai S, Doi T, Iwamoto Y. Influence of the posterior tibial slope on the flexion gap in total knee arthroplasty. Knee. 2014;

36. Kang KT, Koh YG, Son J, Kwon OR, Lee JS, Kwon SK. Influence of Increased Posterior Tibial Slope in Total Knee Arthroplasty on Knee Joint Biomechanics: A Computational Simulation Study. J Arthroplasty. 2018;

37. Scott DF. Prospective Randomized Comparison of Posterior-Stabilized Versus Condylar-Stabilized Total Knee Arthroplasty: Final Report of a Five-Year Study. J Arthroplasty [Internet]. 2018;33(5):1384–8. Available from: https://doi.org/10.1016/j.arth.2017.11.037

38. Freed RD, Simon JC, Knowlton CB, Orozco Villaseñor DA, Wimmer MA, Lundberg HJ. Are Instrumented Knee Forces Representative of a Larger Population of Cruciate-Retaining Total Knee Arthroplasties? J Arthroplasty. 2017;

39. Scholes SC, Joyce TJ. In vitro tests of substitute lubricants for wear testing orthopaedic biomaterials. Proc Inst Mech Eng Part H J Eng Med. 2013;227(6):693–703.

Chapter 4

4 Biomechanical analysis of Mechanically versus Kinematically aligned Total Knee Arthroplasty (TKA) using TKA implants linked to a virtual ligament model

4.1 Abstract

Total Knee Arthroplasty (TKA) has been a revolutionary surgery, improving the patient's quality of life. However, increasing numbers of TKAs means increasing numbers of TKA revisions. It is still unclear what the optimal soft tissue tension, balance, or alignment is to provide superior patient outcomes. Improving these TKA properties and overall patient satisfaction may lead to a decrease in TKA revisions. Computational models effectively simulate TKAs in an array of scenarios. This work implemented a sophisticated 6-degree of freedom joint motion simulator merged with a virtual soft tissue model, eliciting the soft-tissues properties used to balance TKAs. We compared mechanically aligned (MA) and kinematically aligned (KA) TKAs through joint kinematics and soft tissue laxity testing. This was carried out during 90° of neutral flexion and extension and simulated Activities of Daily Living (ADLs). We found that there was no statistically significant difference in all joint motion simulations between the MA and KA TKA constructs. Additionally, the same differences among CR, CS and PS polys used in MA knees are seen in the same polys of KA knees. When comparing MA to KA TKAs, there are slight increases in joint reaction forces and soft tissue tensions in the KA knees. It is unclear if this is advantageous or detrimental to the function or outcomes of TKAs. Considering the similarity in joint kinematics and laxity testing between MA and KA knees, it is probable that patients will have similar results with regard to functional outcome and longevity of implants.

4.2 Introduction

Total Knee Arthroplasty has revolutionized the quality of life for individuals suffering from end-stage knee arthritis. Mechanical alignment has been the standard of care for knee arthroplasty for decades. Recent literature, however, has challenged the idea that neutral or mechanical alignment is ideal for all patients[1]. Knee replacement has come close to mimicking natural knee kinematics,[2] and with recent innovations in alignment strategies, this has the potential to improve. The primary goal of TKA is to provide a painless, stable knee with appropriate range of motion and good function. There is current controversy as to whether mechanical or kinematic alignment will best accomplish this goal.

Despite all the advances in TKA since its advent, a significant amount of people remain dissatisfied with their results[3,4]. Patients with residual pain or overall dissatisfaction may be suffering due to unequal soft tissue tension or poorly balanced knees. These dissatisfied TKA patients have lower quality of life and higher health care resource burdens[5]. Occasionally, a revision operation is carried out to improve symptoms, function, and quality of life. TKA revision causes enormous stress on patients, hospitals, surgeons, and the healthcare system[6]. As TKA surgeries are projected to increase,[2] this will also result in an increase of revision surgeries. Ongoing research efforts, including a recent surge in kinematic alignment work, are working to eliminate or decrease the main reasons for revision. Hopefully, this will lead to better patient outcomes and quality of life, as well as substantially decrease the economic burden of TKA revision surgery.

A stable knee is one of the goals of TKA whether it is mechanically or kinematically aligned. However, instability is currently one of the top three most common reasons for TKA revision[7,8]. Approximately one third of early TKA failures are due to soft tissue imbalance, and close to two thirds of these early failures occur in the first five years post operation[9,10]. Medical professionals agree that correct ligament balancing and stability are prerequisites for achieving good functional outcomes and long-term survival of TKA, but the optimum soft tissue balance or alignment for implant survival and superior patient satisfaction remains unclear[11]. These optimal conditions may even differ with various implant designs.

There have been well-defined properties of intact knees, and if a TKA system would be able to replicate the functional properties of intact knees, it may lead to better patient outcomes. The aim of this work is to understand how mechanically aligned versus kinematically aligned Cruciate Retaining, Cruciate Sacrificing and Posterior Stabilized TKA constructs affect the soft tissue balance, stability and knee joint kinematics.

4.3 Methods

4.3.1 Virtual Model Development and Anatomical Coordinate Systems

Mechanically and kinematically aligned virtual TKA models, complete with anatomic ligament insertions, were created. An in-depth description of the virtual model can be found in an excerpt from a previous work by Montgomery et al. and can be found in Appendix A. Using cadaveric CT scans, isolated distal femoral and proximal tibial 3-D bone models were reconstructed.

Each 3-D model was assigned an anatomical coordinate system based off the previously described work of Grood and Suntay[12]. We used the midpoint between the centers of spheres fit to the posterior aspects of the femoral condyles to define the origin of the femoral coordinate system. The z-axis was coincident with the mechanical axis of the femur (positive in the superior direction). The coronal plane was defined as the plane containing the mechanical axis and the condylar axis. The x-axis was defined as orthogonal to the z-axis in the coronal plane and colinear with the trans-epicondylar axis (referenced 3° externally rotated off the posterior condylar axis and positive to the right). The y-axis was defined by a vector orthogonal to both the z- and x-axes, calculated using their cross product (positive in the anterior direction). The sagittal plane was defined as the plane containing the y- and z-axes. For the tibia, a point centered between the intercondylar eminences defined the origin of the tibial coordinate system. The z-axis was coincident with the mechanical or anatomic axis of the tibia (positive in superior direction), the x-axis was defined 90 degrees to the z-axis in the coronal plane (positive to the right), the y-axis was defined as the cross product of the z- and x-axes along the

sagittal plane (positive in the anterior direction). The finalized 3-D models were then saved as triangle tessellated stereolithographic surface model (.stl) files to be used in CAD software.

A coordinate system was then applied to the surface model files of the femoral and tibial implant components, respectively. The origin of the femoral component coordinate system was defined at the midpoint between the centres of two spheres fit to the posterior condyles for both the CR and PS femoral components. See Figure 4-1A for the CR depiction. The x-axis was defined as a line connecting the centres of the spheres fit to the condyles, the z-axis was perpendicular to the x-axis and a horizontal line taken from the distal articulating surface of the component, and the y-axis was calculated based on the cross product of the z-axis and x-axis. The origin of the tibial component was centered at the front edge of the central hole of the implant, Figure 4-1B. The x-axis was defined as a line parallel to the back edge of the components, the y-axis perpendicular to this line, and the z-axis was a product of the y- and x-axes.

Figure 4-1. Images displaying origins of individual component coordinate systems. (A) Femoral Component. (B) Tibial component.

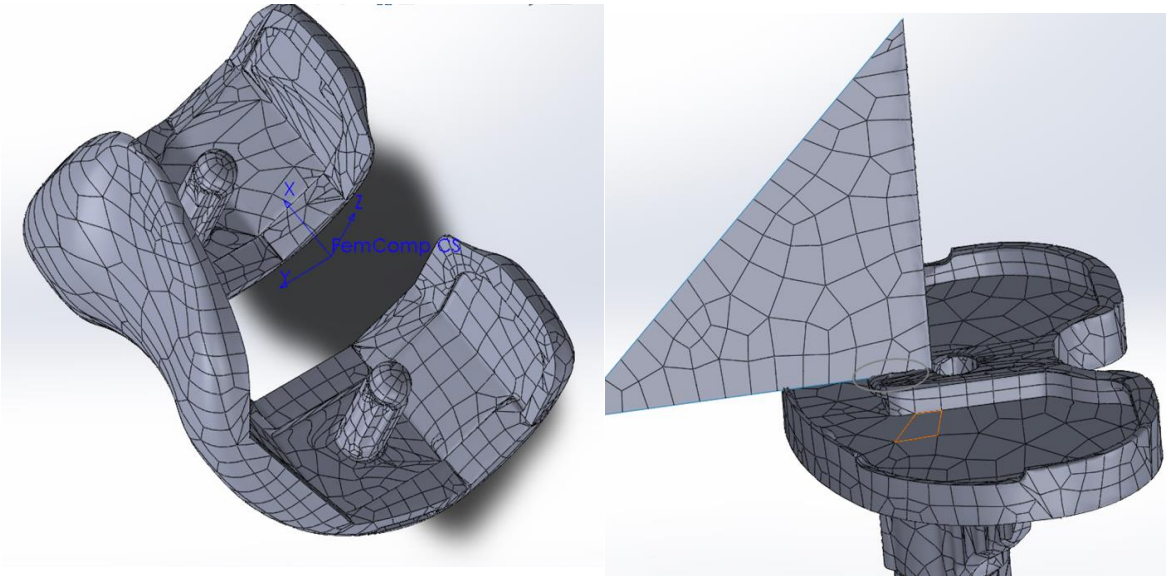

A **B**

4.3.2 Virtual TKA Operation

The Stryker Triathlon® (Stryker Corp., Mahwah, NJ) femoral and tibial components were placed on the respective 3-D anatomical models using SOLIDWORKS 2018®. References were created for all axes, and corresponding planes for both the anatomical models and TKA components were linked. A virtual TKA operation was carried out to create two separate TKA models. This resulted in appropriate simulated bone cuts to produce a Mechanically Aligned (MA) as well as a Kinematically Aligned (KA) TKA. The component sizes were based on those used in a previous experimental study on the same cadaveric specimens, where a board-trained orthopaedic surgeon specializing in TKA chose the implant size based on measurement and trialing. For the MA TKA, the distal femur was cut perpendicular to the mechanical axis, whereas the KA distal femur was cut at 3° of valgus compared to the mechanical axis. Both alignments had an 8mm bone resection depth and neutral flexion. The anterior, posterior and chamfer cuts were made to fit a size 5 Triathlon® (Stryker, Mahwah, NJ) femur, with the anterior cut flush with the anterior cortex. The femoral rotation for the MA model was set parallel to the x-axis of the femoral anatomical model, which was aligned with the approximated trans-epicondylar axis; this was determined by externally rotating 3° from the posterior condylar axis. In the KA TKA model, the femoral rotation was set to align parallel with the posterior condylar axis. The MA proximal tibia was cut perpendicular to the mechanical axis of the tibia, and the KA proximal tibia was cut with a 3° varus cut. Initial bone cut images of the different MA and KA models can be seen in Figure 4-2.

Figure 4-2. Images displaying initial bone cuts of mechanically and kinematically aligned CAD models. (A) Mechanical distal femur, (B) Mechanical proximal tibia, (C) Kinematic distal femur, (D) Kinematic proximal tibia.

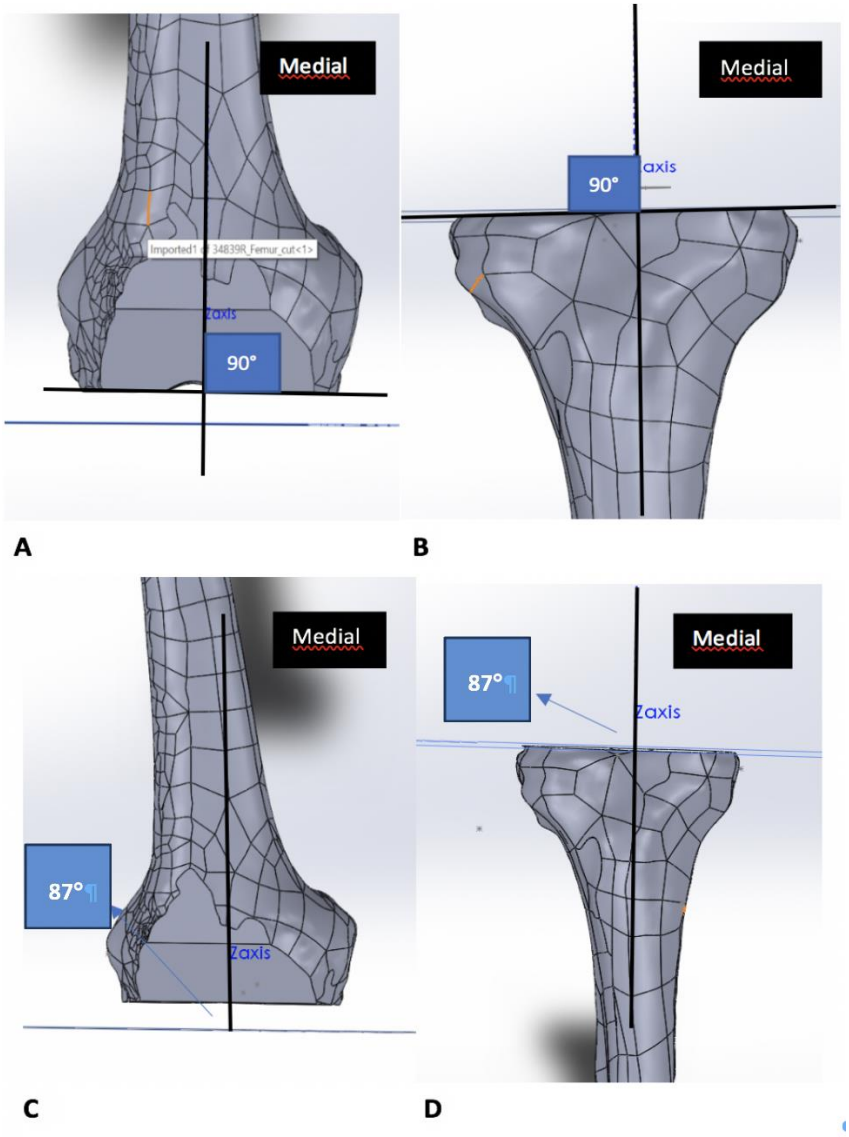

In both the MA and KA models, 5° of posterior tibial slope was cut for the CR/CS components and 3° of posterior slope for the PS component. There was approximately 8mm of resection taken off the proximal tibia. As per the previous cadaver study, the tibia was also sized to size 5. The tibial component rotation was set to align the center of anterior portion of the implant with the medial one third portion of the tibial tubercle. A

9mm poly was then placed into the virtual tray to produce the finished virtual TKA. Images of the final mechanically aligned virtual TKA model can be seen in Figure 4-3.

Figure 4-3. Image displaying final computational model of mechanically aligned CR knee. Anterior (A) and Posterior (B) views allow visualization of all ligament insertions and bundles.

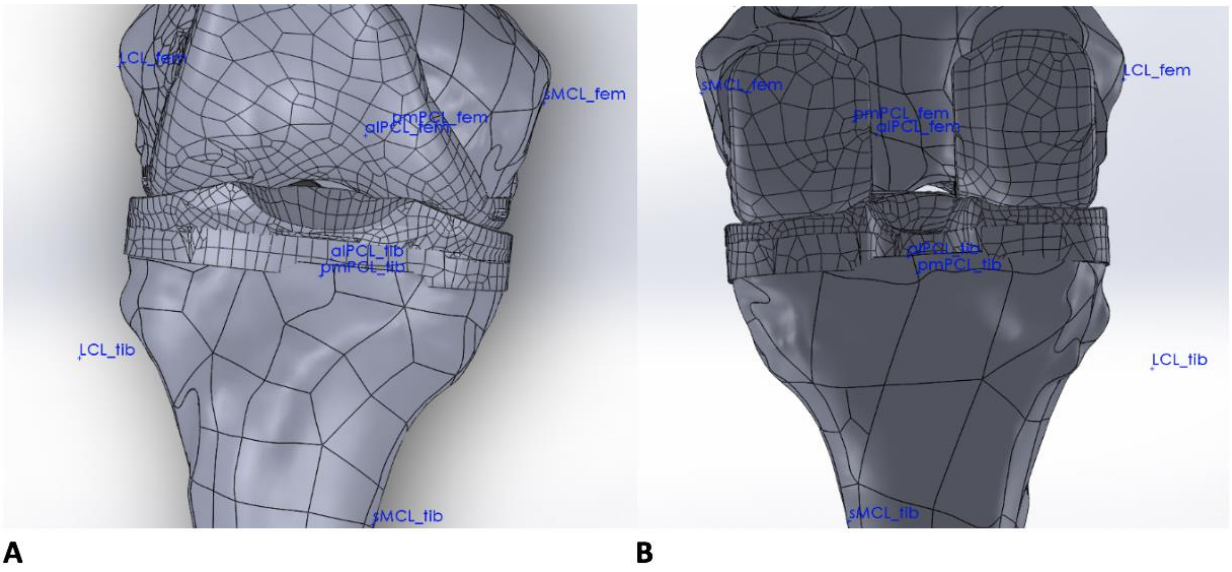

4.3.3 Virtual Ligament Model

We simulated soft tissue balancing that is performed during TKA by applying virtual ligaments that recreate the soft tissues used to balance TKAs. The PCL, the sMCL and the LCL were included in the virtual soft tissue envelope. The ACL and dMCL were not used, as these are routinely released in most TKAs as part of the soft tissue dissection required for exposure or boney resection. The ligament insertion points were determined from previous anatomic studies and defined on our anatomic models[13–20]. Once defined on the model, it was possible to determine the relative position of the ligament insertions with respect to the local coordinate systems of the implant components. The same real implant components were mounted onto a joint motion simulator, and it was then possible to determine the coordinates of the insertion points with respect to the simulator axes based on knowing the position of the implant components on the machine. The

insertion points were referenced in relation to femoral component, which allowed poly changes without affecting insertion points. However, switching between MA and KA, the ligament insertion points were adjusted accordingly to simulate the change in implant component alignment.

Ligament properties including stiffness, reference strain, reference length and zero load length were adapted from the literature and calculated to fit with our virtual model. A combination of computational TKA models and native knee properties were used to create the ideal ligamentous properties in our work[16,21–25]. Ligament properties had to be defined with respect to a distinct pose, or starting position, on the VIVO. This reference pose was defined at 0° of extension with the application of a 100N compressive load across the joint. This position was used to record the resulting equilibrium pose. With the knee in full extension, the ligament's length can be defined from our models and ligament insertion points. Using this pose, we can calculate the reference strain of each ligament. We used the native ligament length at the same pose and strain on each ligament, as reported in the literature, to calculate the values for zero-load length or slack length. The following calculation for the reference strain of each ligament was used: (current length – original length) / original length x 100%. Qualitatively, this defines the amount of deformation in the ligament at full extension due to the anatomical force placed on the ligaments. For example, the PCL in mechanical alignment has a reference strain of -3.42%, which equates to approximately 1.3mm of slack in the ligament (zero-load length of 37.9mm vs mechanical load length of 36.6mm). Another example is the sMCL in mechanical alignment that has a reference strain of 2.73%, which equates to the ligament being on stretch by approximately 2.4mm from its slack length. The ligament properties of stiffness, reference strain, and ligament length used for each alignment are shown in Table 4-1.

Table 4-1. Ligament properties adapted from literature and calculated to fit our virtual ligament model. All lengths are in millimeters, reference (ref.) strains are given as a percentage of zero-load length, stiffness is in units of Newtons per unit

strain. (A) CR femoral component MA and KA, (B) PS femoral component MA and KA. ***MA=Mechanically Aligned, KA = Kinematically Aligned***

Ligament CR Component	Zero-Load Length (mm)	MA Length (mm)	MA Ref. Strain (%)	KA Length (mm)	KA Ref. Strain (%)	Stiffness (N/ε)
PCL	37.93	36.63	-3.42	37.29	-1.67	9000
sMCL	89.75	92.21	2.73	92.45	3.00	2200
LCL	63.25	64.61	2.14	64.26	1.60	1800

A

Ligament PS Component	Zero-Load Length (mm)	MA Length (mm)	MA Ref. Strain (%)	KA Length (mm)	KA Ref. Strain (%)	Stiffness (N/ε)
sMCL	89.75	92.38	2.93	92.58	3.15	2200
LCL	63.25	64.91	2.62	64.59	2.12	1800

B

4.3.4 Biomechanical Testing

A servo-hydraulic 6 degrees of freedom (6-DoF) VIVO joint motion simulator (AMTI, Watertown, MA, USA) was used to simulate TKA motion[26]. We used the Stryker Triathlon® knee system to test isolated TKA components mounted to the VIVO. The femoral component was mounted to the upper actuator arm via a mounting axle. Two separate axles were used for mounting the CR and PS femoral components. Both femoral components were mounted using poly-methyl methacrylate cement (Bosworth Fastray; Keystone Industries GmbH, Singen, Germany). The femoral component was aligned such that the flexion axis of the implant (calculated based on the femoral posterior condyles) was as close to the flexion axis of the VIVO as possible. The tibial baseplate component was anchored into a lower mounting fixture using dental model stone (Modern Materials Golden Denstone Labstone; Modern Materials, Kulzer GmbH, Hanau, Germany). With the locking ring removed for ease of poly change, the appropriate poly liner was docked into the tibial baseplate. The mounted TKA on the VIVO can be seen in Figure 4-4.

Figure 4-4. Complete physical set up of the TKA mounted to the VIVO.

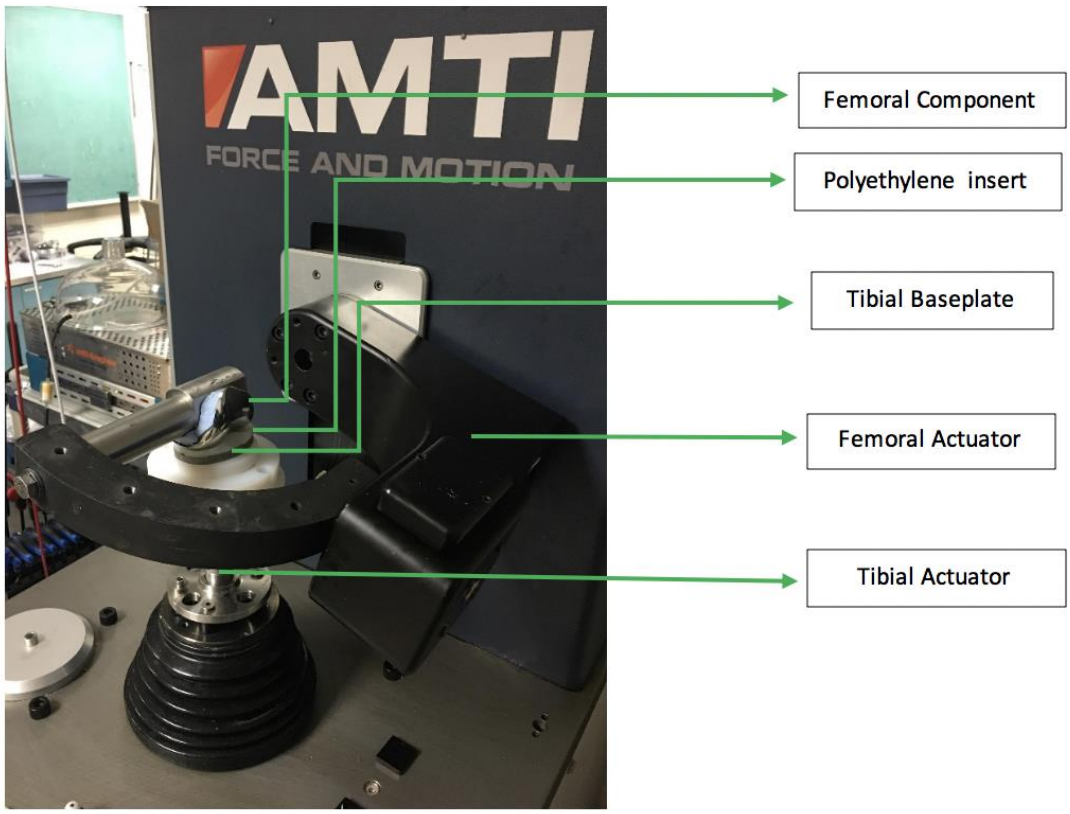

Forces were applied and resulting kinematics were reported in the Grood and Suntay coordinate convention. The coordinate directions have a positive superior z-axis, positive x-axis to the right, and positive anterior y-axis. The VIVO has the capability of incorporating the force contributions of virtual ligaments that are modeled as 1-D point-to-point springs with a non-linear force versus strain response[23]. We used this technology to couple our computer-generated anatomic model, complete with mechanically aligned total knee arthroplasty components and virtual simulations of soft tissue constraints, with the VIVO joint motion simulator. This complete model was made to assess the 6-DoF kinematics as seen in biological specimens with proper soft tissue restraints.

Each of the 6 degrees of freedom can be individually placed into either force or displacement control, depending on what variable is to be controlled or assessed. The

femoral actuator is responsible for flexion/extension and adduction/abduction. The tibial actuator is responsible for superior/inferior movement, internal/external rotation, medial/lateral movement, and anterior/posterior movement. The VIVO was programmed with custom motions and loads for characterization of 0-90° of neutral flexion and extension. Joint simulations with the CR and CS component were performed with all virtual soft tissues applied. The virtual PCL was then removed for assessment of the CS component without a PCL (CS-xPCL) and then the PS component. Cyclical flexion and extension over 90° of motion was repeated for four separate cycles at a rate of 25 s/cycle. Simulated activities of daily living (ADLs) were then performed using imported gait and stair ascent/descent load and motion data. These previously programmed motion data files were obtained from previous work within the same lab[27]. For this work, the AVER75 motion parameters were used. The original data files were acquired from the Orthoload website database (https://orthoload.com/)[28]. For the gait files, the load cycle begins at flat foot and goes through the gait cycle (flat foot, heel off, toe off, swing phase, heel strike, flat foot etc.). This splits the gait cycle into the first 60% stance phase and the last 40% swing phase. The stair ascent and descent load cycles both begin and end with the middle of swing phase. This splits the stair ascent and descent into the first and last 20% swing phase and the middle 60% as stance phase[28]. We used a polydimethylsiloxane (silicone)-based lubricant (HAS0001-OS, Horizon Fitness, Cottage Grove, WI) as an articulation lubricant and applied it consistently throughout the duration of the experiment. Kinematic data was acquired using the VIVO Control program's data logging features. The primary outcome measures were anterior/posterior translation, internal/external rotation and varus/valgus (AP, IE and VV) kinematics. We also measured joint laxity throughout the knee range of motion. Posterior laxity was measured by applying 100N of posteriorly directed force starting at 0° and increasing at 15° increments up to 90° and back to extension over 50sec. VV laxity was performed in a similar fashion by applying a 10Nm varus or valgus torque at the same 15° increments. Laxity was defined as the absolute value of the difference between motion limits, with AP laxity being the difference between the anterior motion limit and the posterior motion limit and VV laxity as the measured difference between both varus and valgus motion limits. Laxity testing was repeated for four cycles. For all tests, there was a 10N

compressive force applied along the z-axis. During the ADL testing, normal joint compression loads for an average 75kg person were applied. The outcomes measured for the ADL testing were the AP translation, IE rotation and VV kinematics.

4.3.5 Data acquisition

The kinematics and force data were recorded during the last flexion/extension cycle at a sampling rate of 100 samples per second This data was smoothed using a low-pass Butterworth filter followed by a spline interpolation function in Matlab (The MathWorks, Natick, MA) and then down-sampled to only include data at 15° intervals of flexion, and only during the flexion phase of the complete flexion/extension motion. During the ADL testing, the joint motion was sampled in 5% increments of the cycle. We extracted the AP, IE, VV kinematic data and the net ligament forces in each of the 6 degrees of freedom during the kinematic testing. We also collected posterior, varus, valgus motion limits and the net ligament forces in each of the 6 degrees of freedom at these limits, and we measured these motion limits during our laxity testing. The smoothed and processed data was then analysed and statistically compared. For each dataset, a two tailed T-test was used. This was a two-sample equal variance T-test to compare each TKA variation to the other coinciding variation in a one-to-one fashion. We primarily focused on the statistical analysis comparing the mechanical alignment with the kinematic alignment of the identical polys. However, all the differently aligned TKA compilations can be compared to each other, as seen in appendix B. A statistical significance level of $p<0.01$ was used.

4.4 Results

4.4.1 Joint Kinematics

Looking at the kinematics for neutral flexion/extension testing seen in Figure 4-5A, the kinematically aligned (KA) CR and CS have slightly more femoral roll back compared to

the mechanically aligned (MA) CR and CS. The total AP translations of these polys are 10.59mm and 10.30mm for the MA CR and CS poly compared to 11.06mm and 10.80mm for the KA CR and CS poly, respectively. Despite having more overall femoral roll back associated with the kinematic alignment, there is no statistically significant difference (AP – MA CR:KA CR, p=0.88; AP – MA CS:KA CS, p=0.67). The MA CSxPCL and the KA CSxPCL also behaved similarly with the KA CSxPCL having slightly more overall tibial translation (MA CSxPCL 6.39mm vs KA CSxPCL 7.11mm), but there was no statistically significant difference (AP – MA CSxPCL:KA CSxPCL, p=0.85). This was true as well for the PS poly (MA PS 3.54mm vs KA PS 3.67mm; AP – MA PS:KA PS, p=0.96). Interestingly, there was a trend of more femoral roll back in each of the KA polys compared to the MA polys, although not statistically significant. When looking at the IE kinematics as seen in Figure 4-5B, there is no overall significant difference between mechanical and kinematic alignment, with $p>0.01$ for all components. All the components behave similarly in that they start with increasing internal rotation for the first 30-45° and then begin to externally rotate in the second half of flexion. They all end in more externally rotated positions than they started. Again, it is noted that in both the MA and KA constructs, the components with a PCL tend to have less internal rotation, especially in deep flexion. This indicates the role the PCL plays in limiting IR in deeper flexion and the PS post also acting as a constraint against IR in deeper flexion. It is interesting, though, that there is a very clear pattern between MA and KA components. The MA components all start in a more IR position and end in a more ER position compared to the corresponding KA components that begin more ER-ed and end more IR-ed. The cross over point is between 45° and 60° of flexion. This can be seen in the end position of each component, MA vs KA: CR - 0.38°IR vs 2.72°IR, CS – 0.38°IR vs 2.20°IR, CSxPCL – 4.81°IR vs 6.08°IR and PS – 0.30°ER vs 1.81°IR. When looking at the VV kinematics in Figure 4-5C, it is apparent that the PS polys behave very differently from the other CR, CS and CSxPCL polys. As was seen in the MA aligned TKA, the KA aligned TKA also has more overall constraint with the PS poly. There are no statistical differences between the MA and KA CR, CS, CSxPCL and PS (VV – MA CR:KA CR, p=0.83; VV – MA CS:KA CS, p=0.71; VV – MA CSxPCL:KA CSxPCL, p=0.82; VV – MA PS:KA PS, p=0.35). Overall, though, there is a trend in that the KA components

maintain a slightly more varus alignment throughout the 90° of flexion. This difference is quite small, however, with the average increase in varus of 0.17°.

Figure 4-5. Kinematic testing for both Mechanically and Kinematically aligned CR, CS, CSxPCL and PS components through 0-90° of neutral flexion. (A) AP kinematics, (B) IE Kinematics, (C) VV kinematics.

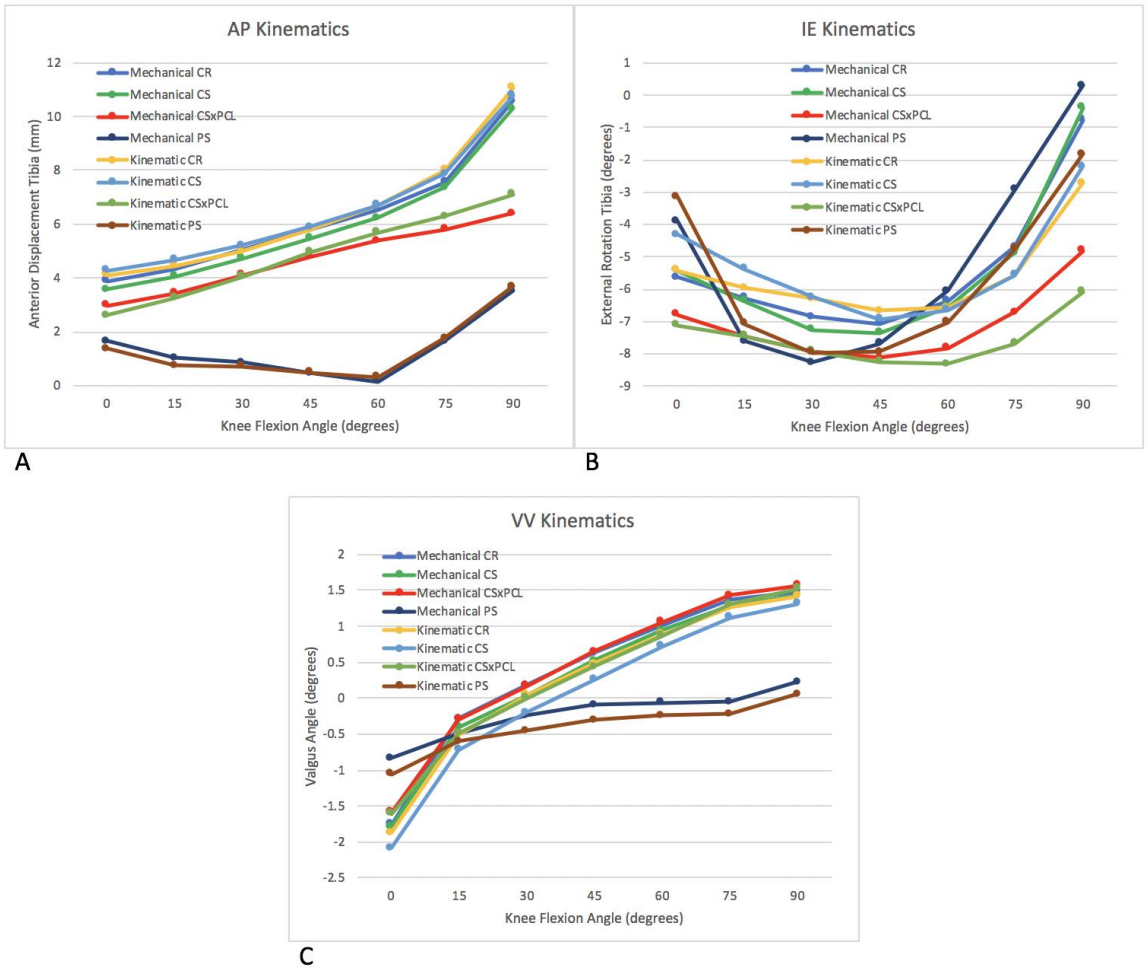

We measured the joint compression forces as generated by the virtual soft tissue envelope and the articular geometries during neutral flexion and extension through 90°. In Figure 4-6 we see the total axial load joint contact forces that occur in each TKA construct during the neutral flexion/extension cycle. There is a consistent pattern of slightly increased compression forces with the KA knees compared to the MA knees. However, there is no significant difference in the joint contact forces between MA and KA

components for CR, CS, CSxPCL and PS, with p>0.01 for each. As seen in the MA knees, the joint compression forces in the KA knees are significantly higher in the PS poly compared to the CR, CS and CSxPCL poly with a maximum compression force of 160.5/169.3N, 160.6/166.7N and 166.1/175.3N for MA/KA CR, CS and CSxPCL, respectively. This compares to the PS component maximum compressive force of 222.9/233.1N MA/KA.

Figure 4-6. Total joint compressive forces during kinematic testing for Mechanically and Kinematically aligned CR, CS, CSxPCL and PS components through 0-90° of neutral flexion.

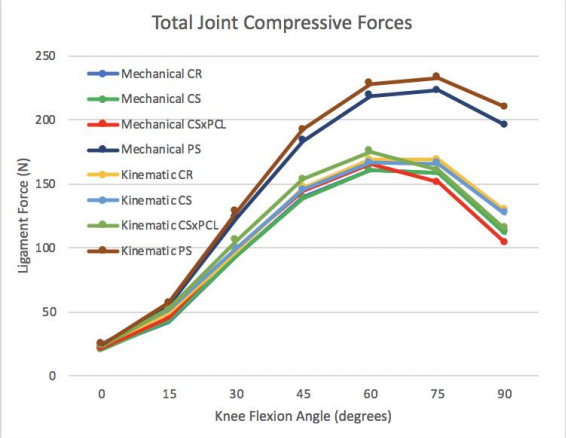

Figure 4-7 shows the tensions across each separate ligament bundle during neutral flexion and extension. As seen in the MA knees, there is a significantly higher tension across the collateral ligaments in the PS components. This disparity is more significant in the LCL, as the PCL being a medial based structure can supplement the sMCL forces in the CR and CS components. In Figure 4-7A, the MA and KA CR and CS knees behave virtually identically with no significant difference in the tensions observed across the PCL. The PCL begins to engage at 60° of flexion in both alignments and produces similar tensions (PCL – MA CR:KA CR, p=0.81; PCL – MA CS:KA CS, p=0.93). In Figure 4-7B, the KA sMCL has a pattern similar to the MA sMCL tensions, increasing until 60° of flexion, and then tapering off until 90° of flexion. The CR, CS and CSxPCL components

taper off faster, leaving the PS components to have higher tensions at 90° of flexion. Although not statistically significant, there is a higher peak in sMCL tensions in the KA polys compared to the MA polys. Maximum sMCL tensions for KA polys are 77.5N, 73.1N, 78.8N and 81.7N compared to MA polys which are 54.0N, 52.5N, 56.1N, and 57.6N for CR, CS, CSxPCL and PS, respectively ($p>0.01$). The opposite is true for the tension across the LCL when comparing MA to KA as seen in Figure 4-7C. Here, the MA polys have higher peak tensions (109.2N, 110.8N, 112.6N and 171.8N), whereas the peak LCL tensions in the KA polys are 94.2N, 96.0N, 98.9N, and 163.5N for CR, CS, CSxPCL and PS, respectively ($p>0.01$). Although not statistically significant, the LCL does experience, on average, higher tensions than the sMCL but a similar peak around 60° or 75°. Despite this, the proportionate difference between KA and MA shows a greater increase in soft tissue tension in the KA knees.

Figure 4-7. Individual ligament (PCL, sMCL, LCL) forces during kinematic testing for Mechanically and Kinematically aligned CR, CS, CSxPCL and PS components through 0-90° of neutral flexion.

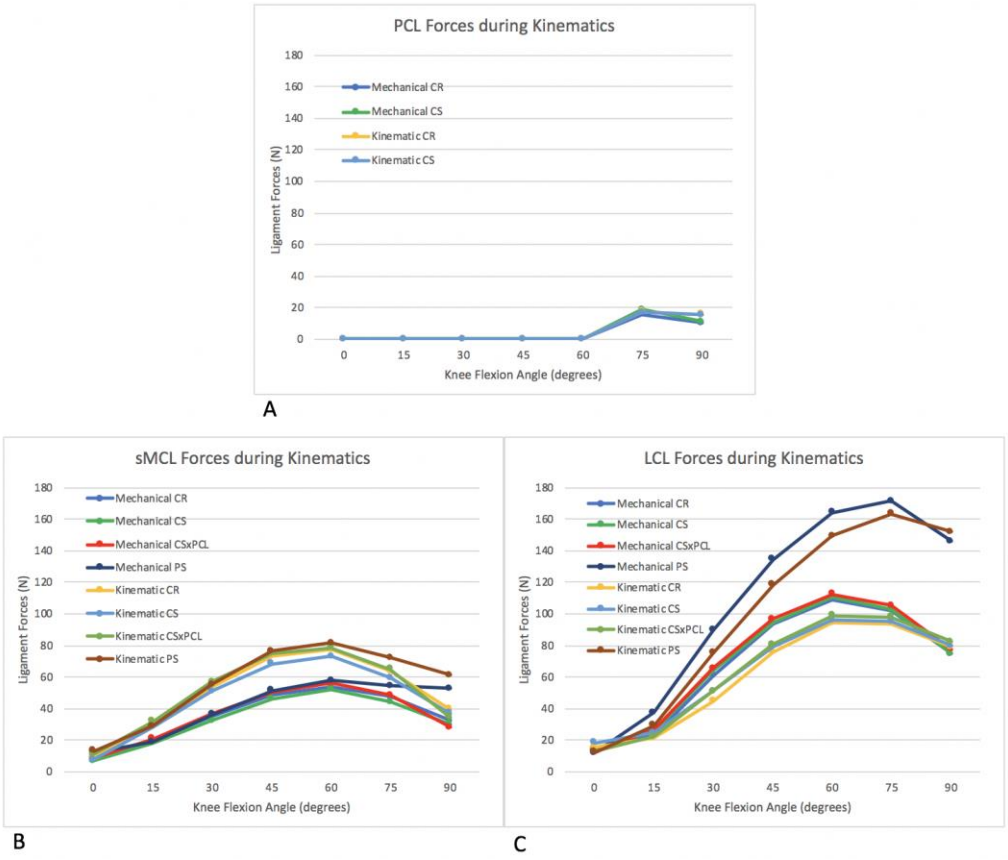

When looking at both MA and KA joints during ADLs, the differences previously observed between the CS and CSxPCL are mostly negated. In Figure 4-8 each component was tested during simulated gait. Clearly, there is virtually no difference in the joint kinematics when comparing MA and KA knees. This is true for AP kinematics, IE kinematics and VV kinematics, with $p>0.01$ for all alignment comparisons. Although there is no significant difference between the MA and KA components, the same patterns appear, as seen previously with the MA polys, when comparing the different polys with each other. In Figure 4-8A, the PS poly shows a more constrained pattern with less overall AP translation. However, this is considered not statistically significant with $p>0.01$. In Gait IE kinematics (Figure 4-8B), during the last third of stance phase and just over half of the swing phase, the PS poly limits the IE kinematics the most. The CR poly

also has slightly more constraints against IE movement compared to the two CS polys during this portion of the gait pattern. In Figure 4-8C, again it is seen that there is no statistically significant difference among the polys, with p>0.01. However, the pattern of the PS poly producing more VV constraint is again observed here. During the stance phase, the PS component is persistently in a more varus position by about 0.5°. Also, during the swing phase, as the knee flexes more, the PS component doesn't go beyond 0°, demonstrating more VV constraint compared to the other constructs.

Figure 4-8. Kinematic testing for Mechanically and Kinematically aligned CR, CS, CSxPCL and PS components during normal Gait. Gait cycle begins with flat foot and goes to heel off then finishes with heel strike and flat foot. (A) Gait AP kinematics, (B) Gait IE Kinematics, (C) Gait VV kinematics.

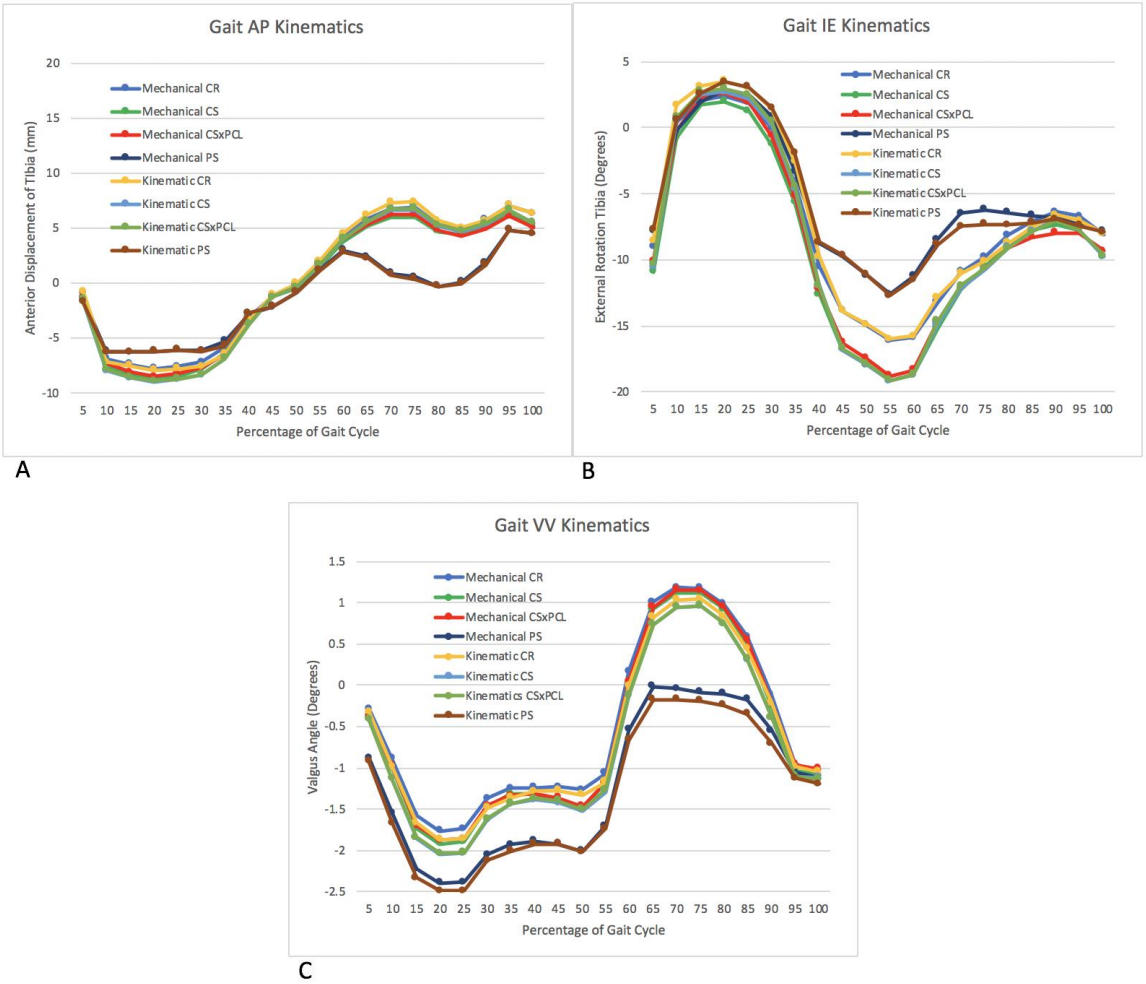

The AP Kinematics pattern observed during stair descent in Figure 4-9A is nearly identical between the two different alignments ($p>0.01$). Again, the anterior translation of the tibia is less in the PS component for both MA and KA knees when comparing it to the other polys and alignments. When looking at IE kinematics in Figure 4-9B, there is no statistically significant difference between MA and KA, with $p>0.01$ for each poly. However, there is an interesting pattern in the IE rotation at the commencement of stance phase and the commencement of the swing phase. At these points, there is a slight difference between the MA and KA polys. At approximately 25% of the gait cycle, which coincides with the commencement of the stance phase, the MA polys have slightly more internal rotation compared the KA aligned ones (CR – 2.67°MA:1.49°KA; CS – 4.16°MA:2.94°KA; CSxPCL – 4.02°MA:2.86°KA; PS – 4.07°MA:3.33°KA). On the contrary, at 90% gait cycle, near the start of the swing phase, the exact opposite is seen: there is more internal rotation with the KA than the MA polys (CR – ER0.77°MA:IR0.88°KA; CS – ER0.21°MA:IR1.61°KA; CSxPCL – IR0.03°MA:IR1.84°KA; PS – ER3.41°MA:ER1.10°KA). In the comparison between MA and KA for VV kinematics as seen in Figure 4-9C, there is a trend for the KA knees to have a slightly more varus position throughout the stair descent cycle. This is not statistically significant, with a $p>0.01$. There is still observed, however, a statistically significant difference between the MA and KA PS components when compared to all the MA and KA aligned CR, CS and CSxPCL polys ($p<0.001$). Here, there is less overall variation in VV angle with the PS components, as well as a more varus-maintained position throughout the stair descent cycle. The varus position of the PS poly in both MA and KA ranges from 0.3° to 1.5° more varus during different stages of stair descent.

Figure 4-9. Kinematic testing for Mechanically and Kinematically aligned CR, CS, CSxPCL and PS components during Stair Descent. Stair Descent begins and ends

with the middle of swing phase. (A) Stair Descent AP kinematics, (B) Stair Descent IE Kinematics, (C) Stair Descent VV kinematics.

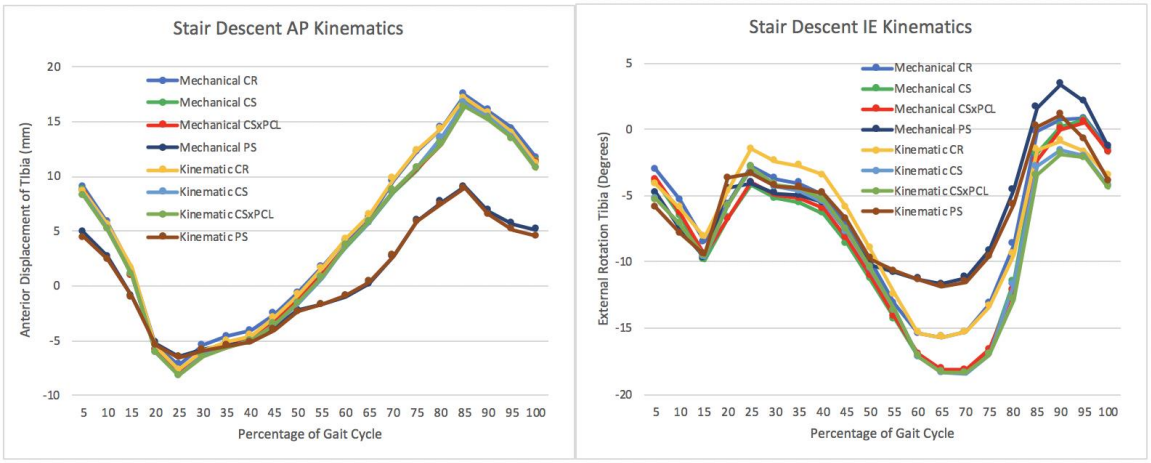

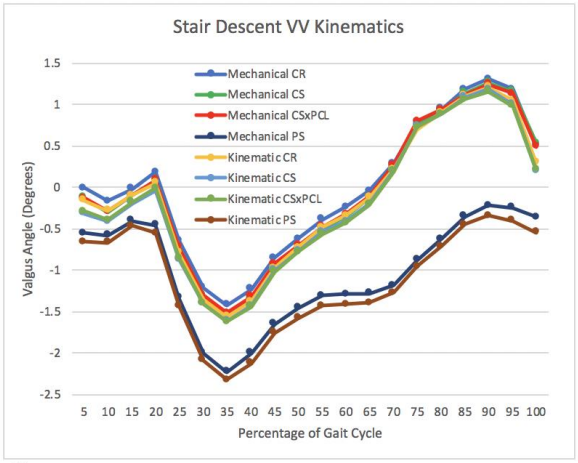

As was seen during stair descent, the AP Kinematics during stair ascent in Figure 4-10A behave almost the exact same between the two different alignments ($p>0.01$). Again, the PS component produces less overall anterior tibial translation for both MA and KA knees when comparing it to the other polys and alignments. This occurs primarily during the swing phase of stair ascent when the knee is flexed the most. With regards to IE rotation as seen in Figure 4-10B, there is no statistically significant difference between the MA and KA ($p>0.01$). However, it is noted that the different aligned similar polys behave very closely to the same during the stance phase of gait, but there is definitely some discrepancy during the swing portion of stair ascent. There is slightly more IR observed in all the KA polys when compared to the MA polys of the same type. In Figure 4-10C, it

is clear that there is no statistically significant difference in VV kinematics between the MA and KA polys, with a p>0.01. It is noted that the PS polys in both MA and KA have more VV constraint with less variation in VV motion throughout the stair ascent cycle. The PS polys also maintain a more varus position throughout the cycle.

Figure 4-10. Kinematic testing for Mechanically and Kinematically aligned CR, CS, CSxPCL and PS components during Stair Ascent. Stair Ascent begins and ends with the middle of swing phase. (A) Stair Ascent AP kinematics, (B) Stair Ascent IE Kinematics, (C) Stair Ascent VV kinematics.

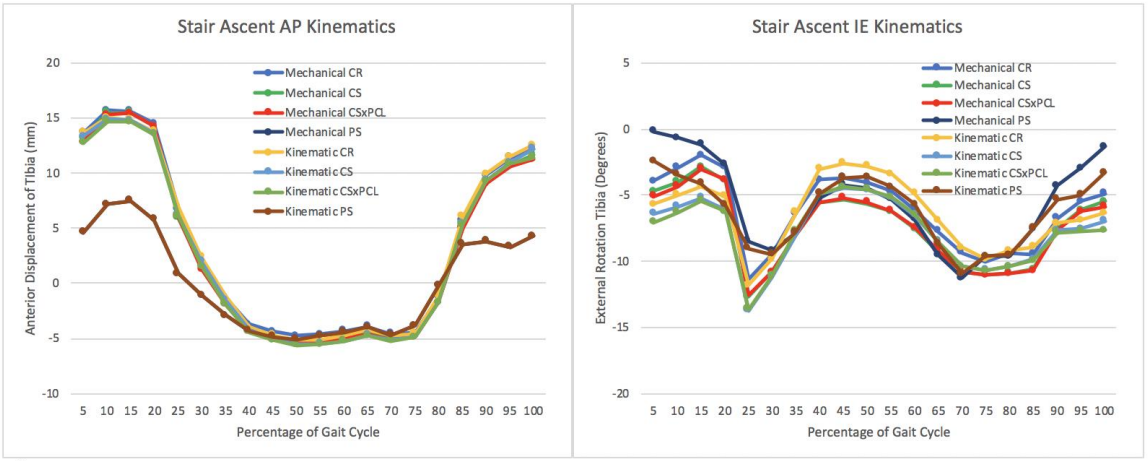

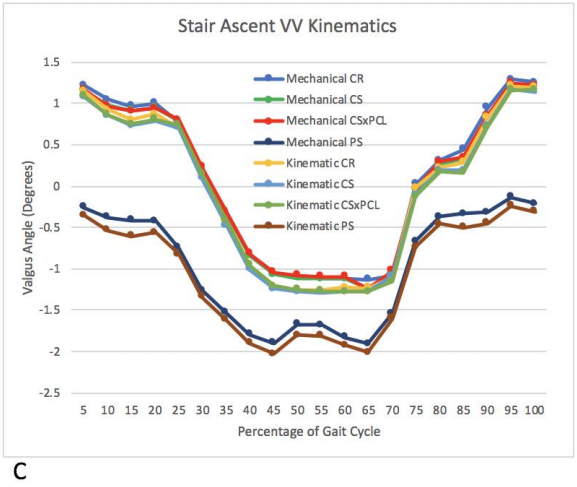

4.4.2 Joint Laxity

During AP laxity testing in neutral flexion and extension, there is no statistically significant difference ($p>0.01$) between MA and KA, as seen in Figure 4-11A. The AP laxity does show a trend in both the MA and KA polys in which the CSxPCL does not fully compensate for the lack of a PCL. The CSxPCL maintains a significantly higher posterior tibial displacement throughout the flexion cycle when compared to the CR, CS and PS polys. In Figure 4-11B, there is again no significant difference noted between the VV laxity of the MA and KA constructs, with a $p>0.01$ for all. There is a trend observed in which the KA knees are in a persistently slightly more varus position throughout the flexion cycle; however, on average this is less than 1°.

Figure 4-11. Joint laxity during neutral motion testing for mechanically and kinematically aligned CR, CS, CSxPCL and PS components through 0-90° of flexion. (A) AP laxity when 100N of posterior force applied. (B)VV laxity when 10Nm moment applied to tibial actuator.

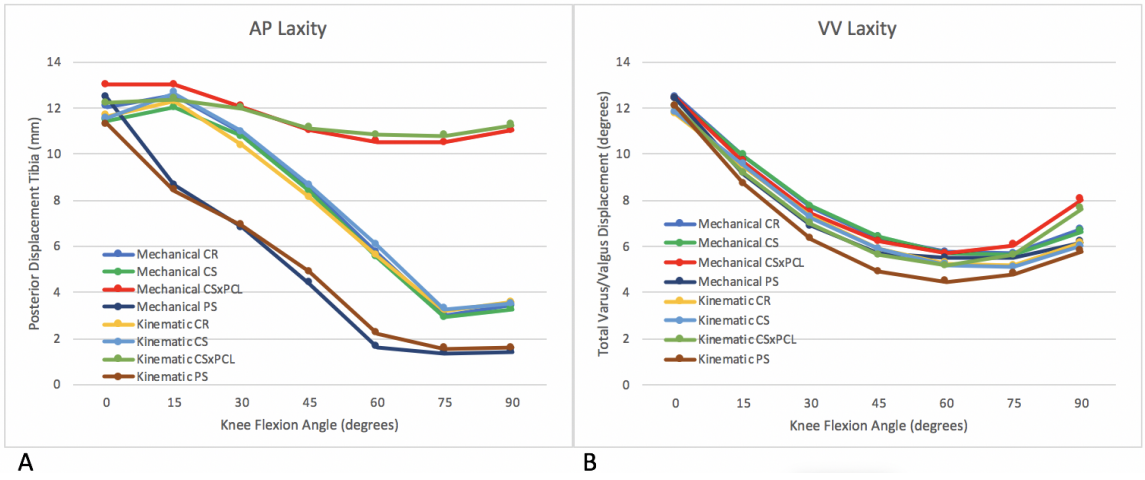

The tension across the individual ligaments was also analyzed. In Figure 4-12 the forces across each individual ligament are portrayed during the AP laxity testing. Overall, there is no statistically significant difference between MA and KA in all settings, with a $p>0.01$ for each. There are, however, a few interesting trends observed. In Figure 4-12A, during

the first 30° of flexion, there is on average 30N more force on the PCL in the KA aligned CR/CS knees compared to the MA knees. After 30°, the KA knees also maintain a slightly higher tension across the PCL through the rest of the flexion cycle. Also in Figure 4-12B, after the first 15° of flexion, there is a persistently higher tension across the sMCL in the KA polys compared to their MA counterparts. Interestingly, but not as substantial, in Figure 4-12C, the LCL forces are higher after the first 15° of flexion, but this time the MA knees produce higher forces on the LCL than the KA knees.

Figure 4-12. Individual ligament (PCL, sMCL, LCL) forces during AP laxity testing for mechanically and kinematically aligned CR, CS, CSxPCL and PS components. AP laxity testing was applied through 0-90° of neutral flexion, having 100N of posterior force applied at 15° increments.

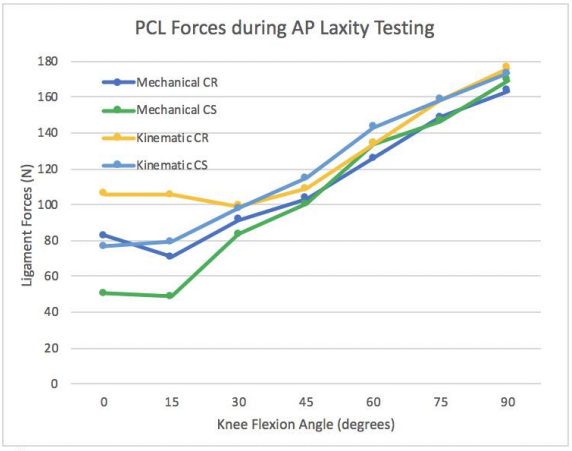

A

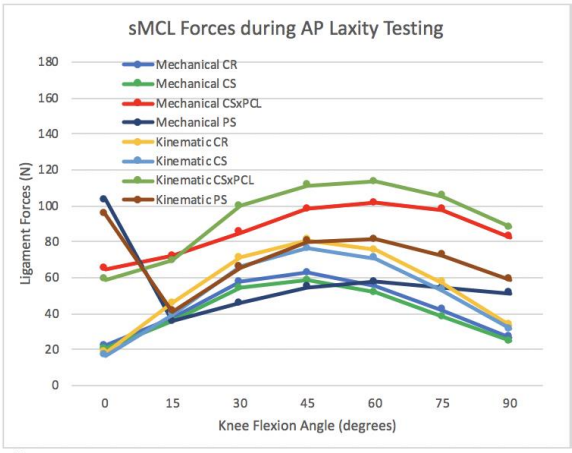

B

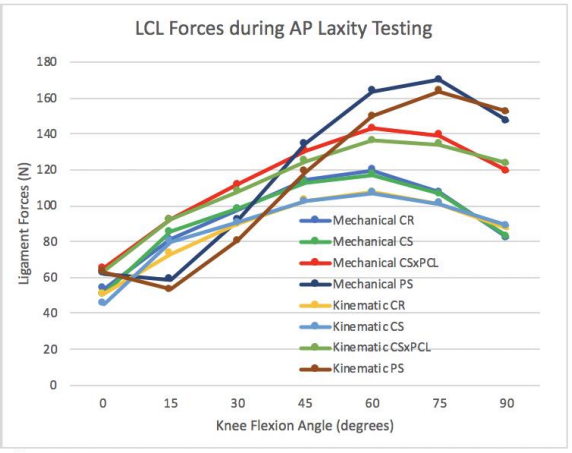

C

As would be expected, during the valgus laxity testing, there is an increase in forces across the sMCL and the PCL. However, in Figure 4-13 it is clear that the increase in forces are uniform between the MA and KA knees. Statistically, there is no difference between MA and KA knees during valgus laxity testing, with a p>0.01 for all instances.

Figure 4-13. Individual ligament (PCL, sMCL, LCL) forces during Valgus laxity testing for mechanically and kinematically aligned CR, CS, CSxPCL and PS components. Valgus laxity testing was applied through 0-90° of neutral flexion, having a 10Nm valgus torque applied at 15° increments.

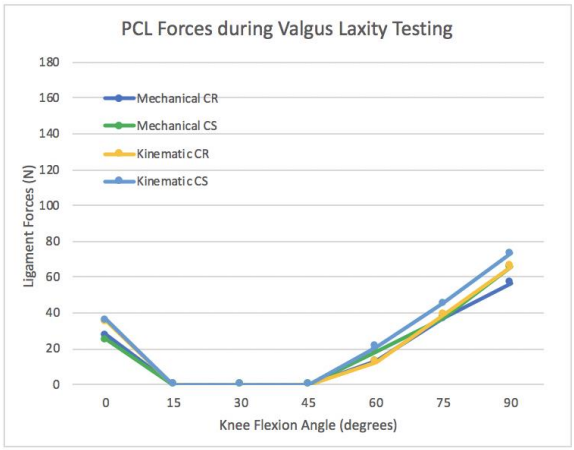

A

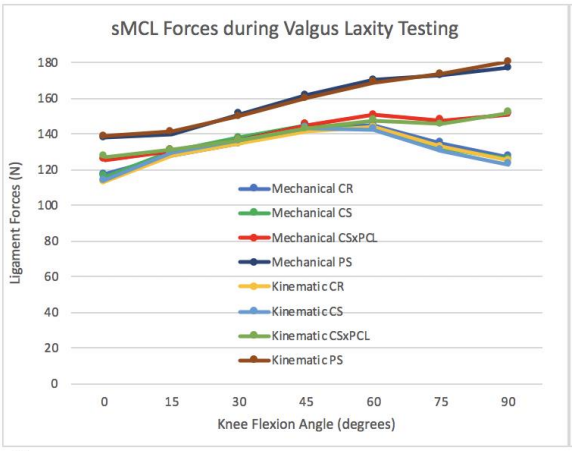

B

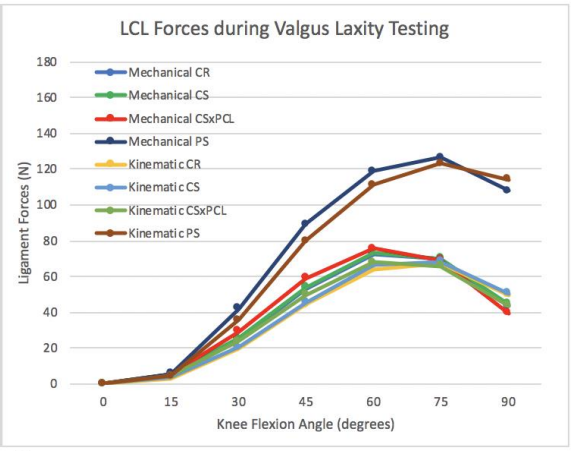

C

When performing a varus force on the knee construct as seen in Figure 4-14 there is an expected increase in forces across the LCL. According to the statistical analysis, there is no statistically significant difference between the MA and KA polys, with a p>0.01 for all

comparisons. The varus force does, however, produce an increased variation between the MA and KA PS components. With there being less force across the sMCL, it becomes apparent that the KA PS component produces more force in the sMCL than does the MA PS component. This is best demonstrated by a difference in mid-flexion of 22N. The opposite is true for the forces on the LCL. There is more force in the MA PS component on the LCL when compared to the KA PS component. This is seen at 65° of flexion, where the difference is 13N of force.

Figure 4-14. Individual ligament (PCL, sMCL, LCL) forces during Varus laxity testing for mechanically and kinematically aligned CR, CS, CSxPCL and PS components. Varus laxity testing was applied through 0-90° of neutral flexion, having a 10Nm varus torque applied at 15° increments.

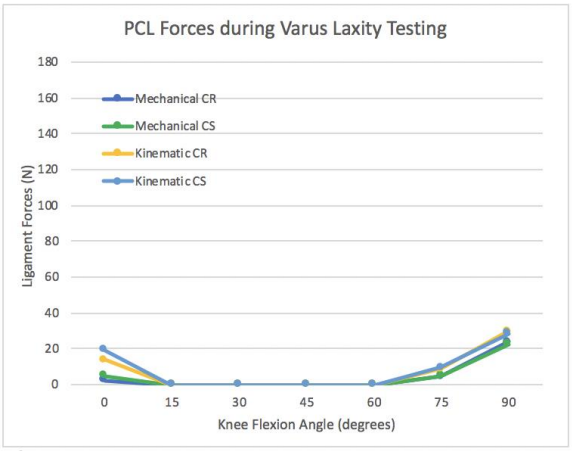

A

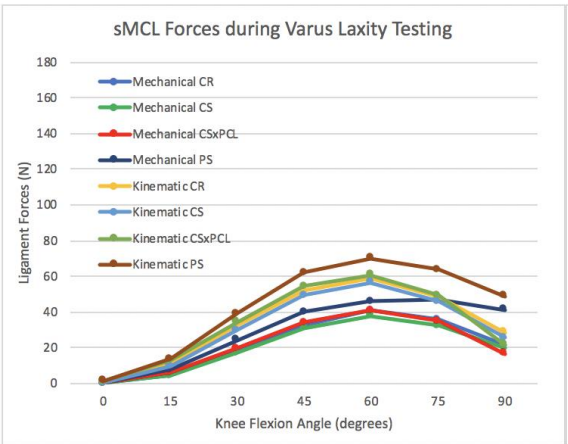

B

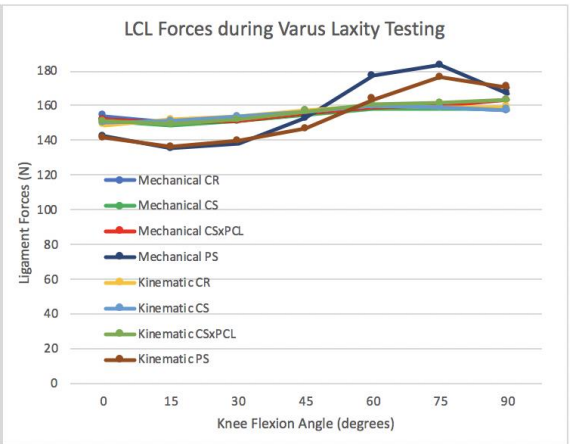

C

4.5 Discussion

Our primary goal was to compare the mechanical and the kinematic alignments of the individual polyethylene pairs. It was clear throughout all neutral flexion testing, ADL kinematic testing and all laxity tests, that there was no statistically significant difference between the MA knee constructs and the KA knee constructs. Our secondary goal was to look at the different polys within the kinematic alignment to see if the same major differences and conclusions were present in the KA knees as were found in the MA knees. The statistical breakdown of comparison between each separate poly can be seen in appendix B. Although this wasn't the main focus of this work, it was evident that the KA knees behave nearly identically to the MA knees. This equates to having the same major differences found in the MA polys of Chapter 3 to be present in the differences among the KA polys.

Among the subtle differences between MA and KA knees, we find some interesting discussion points. Firstly, as stated by Vandekerckhove et al., KA may compromise the loading vectors across a prosthetic joint, increase the risk of aseptic loosening, and has shown FEA modelling of abnormal bone strain[29]. Our work doesn't prove these claims, but it is evident that there is increased joint compression forces and ligament tensions in the KA knees. This can be seen in Figure 4-5A, which shows KA CR and CS having more femoral roll back. This is likely due to a tighter PCL, which can be seen from the slightly higher joint compressive forces in Figure 4-6 as well as the increased early engagement and higher tension across the PCL in Figure 4-12A during AP laxity tests. Also, in all the different poly configurations, there was higher total joint compressive forces as seen in Figure 4-6 as well as a persistently higher tension in the sMCL with the KA knees as seen in Figure 4-7B, Figure 4-12B, and Figure 4-14B. Albeit the opposite was true for the LCL in MA knees: there was a persistently higher tension across the LCL. Despite this difference between MA and KA soft tissue tension, joint forces were proportionately greater in the KA knees with the sMCL and PCL. These higher joint forces and soft tissue tensions could potentially lead to compromised loading vectors,

increased aseptic loosening, or abnormal bone strain, but this is not proven by what our analysis shows.

Proportionately, there is more IR with the KA CSxPCL vs CR/CS compared to the MA CSxPCL vs CR/CS, as seen in Figure 4-5B. This indicates that there will be more stress on the PCL and soft tissues, limiting IR in deeper flexion. Also, in Figure 4-5B, the KA PS components have more IR in the second half of flexion than the MA PS components. As seen in the IE kinematics during the simulated ADLs in Figure 4-8B, Figure 4-9B, and Figure 4-10B, there is persistently more IR in the KA knees in portions of the joint motion cycle where the knee is more flexed. This is another indication that the Kinematic alignment relies more heavily on the soft tissues to balance and stabilize the knee. This is evident, as previously mentioned, with the increased joint compressive forces and soft tissue tension proportionately in the KA knees compared to the MA knees. Despite these differences not showing a statistical significance, the common trend shows that the KA knees rely more on the soft tissues to maintain balance and alignment than the MA knees. It is still unclear if this is an advantage or disadvantage to knee function and longevity. It is our opinion that, if using KA for TKA, one should stick to components that preserve soft tissues to help maintain balance and stability. If the soft tissues are partially or fully compromised, maintaining MA may be more beneficial, as this seems to rely less on the soft tissues for balance and stability. For example, if persistently using a PS knee construct for KA knee, the lack of soft tissue support may transfer more of the balancing and stability forces to the remaining soft tissues or produce greater bone/implant interface stress.

There are multiple studies that show similar functional results and patient reported outcomes when comparing MA and KA TKAs[11,30,31]. From what we have shown, it is likely that KA knees will perform very similarly to MA knees. There are no major differences in the joint kinematics during neutral flexion and extension testing, nearly identical kinematics during simulated ADLs, as well as very similar responses in joint laxity testing. There are some studies, however, making large claims that KA is superior to MA and will produce better functional scores, patient reported outcomes and lead to greater longevity of the joint[32–34]. These significant claims are not backed up by what our

joint analysis shows. In this study, the joint motion simulator performed controlled, precise pre-loaded joint motions. In this accurately measured setting, the only variable that differed between MA polys and the corresponding KA polys was the overall alignment of the simulated TKA. In looking at the MA and KA difference, there is no major or significant difference between the alignments that would produce profound claims that KA knees are superior to MA knees. It is possible that the subtle differences we found between the MA and KA knees will produce functional or patient reported differences, but that remains unsupported at this time.

One of the limitations in this study is using point-to-point ligaments rather than bundles of ligaments. This does not completely represent the native ligament properties and origin/insertion footprints. Blankevoort et al. was foundational in cataloging ligament properties and most studies that address ligament properties have referenced his early paper[22]. Unfortunately, each human knee is unique in its ligament properties, including zero-load lengths, reference strains, stiffness and insertion points, making it difficult to properly capture the properties of each ligament. Many authors have attempted to establish accurate ligament properties, such as the ones we used to help guide our ligament properties[20,21]. Despite all the work that has been done to identify accurate ligament properties, there is still a significant variation in the literature. Peters et al.[24] produce a systematic review outlining what the ligament properties should be, but there is still significant variation in the literature. The knee is a complex joint; the necessary assumptions or approximations that are required to make a computational knee model produces inherent limitations in and of itself. Therefore, assuming ligaments to be point-to-point springs with origins and insertions simply within the anatomic footprint, using ligament properties that aren't exact, and only including the three main ligaments addressed in TKA balancing for our soft tissue model limit the overall accuracy of the physical/virtual construct. Another limitation is the loading parameters for the ADLs. These are based off of TKA parameters using PS polys[27], possibly altering the reaction of our CR and CS knee constructs. However, there have been other computational studies that show the applicability of the same ADL simulation loading patterns in CR components[38]. Regardless, the primary focus of this study was to compare the difference between alignments of the same poly. We used polydimethylsiloxane (silicone)-based

lubricant (HAS0001-OS, Horizon Fitness, Cottage Grove, WI) as a joint lubricant. This has been shown to be an inferior joint lubricant. A mixture of bovine serum and hyaluronic acid (HA) to lubricate the articulating surface is superior[39]; however, this was shown in high repetition wear studies. Using an alternate joint lubricant may change our results. In this study with low velocity and low volume, it is unlikely that a joint lubricant superior for wear studies would improve our precision.

In summary, there was no statistically significant difference in all joint motion simulations between the MA and KA polys. The subtle differences may elude to evidence of higher joint reaction forces and increased tension on the soft tissues around the knee in the KA compared to the MA TKA. Whether these subtle differences will result in advantageous or disadvantageous outcomes in patients with TKAs is still unknown. We prefer to use TKA constructs that preserve the most soft tissue structures if KA is to be utilized. According to the similarities reported in the MA and KA joint kinematics, it is likely that patients will have similar results with regard to functional outcome and longevity of implants. There is a possibility that the subtle differences we see here will lead to significant differences in patients with TKA; however, it is not clear if that will be the case. With regard to the differences seen between CR, CS, CSxPCL and PS TKA constructs, the same differences that were observed with MA knees are observed with KA knees.

4.6 References

1. Bellemans J, Colyn W, Vandenneucker H, Victor J. The chitranjan ranawat award. Is Neutral Mechanical Alignment Normal for All Patients? The Concept of Constitutional Varus. Clin Orthop Relat Res. 2012;470(1):45–53.
2. Papas PV, Cushner FD, Scuderi GR. The History of Total Knee Arthroplasty. Tech Orthop. 2018;33(1):2–6.
3. Bourne RB, Chesworth BM, Davis AM, Mahomed NN, Charron KDJ. Patient satisfaction after total knee arthroplasty: Who is satisfied and who is not? Clin Orthop Relat Res. 2010;468(1):57–63.
4. Williams DH, Garbuz DS, Masri BA. Total knee arthroplasty: Techniques and results. B C Med J. 2010;52(9):447–54.
5. Marsh J, Somerville L, Howard JL, Lanting BA. Significant cost savings and similar patient outcomes associated with early discharge following total knee arthroplasty. Can J Surg. 2019;62(1):20–4.
6. Bhandari M, Smith J, Miller LE, Block JE. Clinical and economic burden of revision knee arthroplasty. Clin Med Insights Arthritis Musculoskelet Disord. 2012;5:89–94.
7. Sharkey PF, Lichstein PM, Shen C, Tokarski AT, Parvizi J. Why are total knee arthroplasties failing today-has anything changed after 10 years? J Arthroplasty [Internet]. 2013;29(9):1774–8. Available from: http://dx.doi.org/10.1016/j.arth.2013.07.024
8. Lombardi A V., Berend KR, Adams JB. Why knee replacements fail in 2013: Patient, surgeon, or implant? Bone Jt J. 2014;96B(11):101–4.
9. Fehring TK, Odum S, Griffin WL, Mason JB, Nadaud M. Early failures in total knee arthroplasty. In: Clinical Orthopaedics and Related Research. 2001.
10. Smith T, Elson L, Anderson C, Leone W. How are we addressing ligament balance in TKA? A literature review of revision etiology and technological advancement. J Clin Orthop Trauma [Internet]. 2016;7(4):248–55. Available from: http://dx.doi.org/10.1016/j.jcot.2016.04.001
11. Luo Z, Zhou K, Peng L, Shang Q, Pei F, Zhou Z. Similar results with kinematic and mechanical alignment applied in total knee arthroplasty. Knee Surgery, Sport Traumatol Arthrosc [Internet]. 2019;(0123456789). Available from: https://doi.org/10.1007/s00167-019-05584-2
12. Grood ES, Suntay WJ. A joint coordinate system for the clinical description of three-dimensional motions: Application to the knee. J Biomech Eng. 1983;105(2):136–44.
13. Laprade CM, Civitarese DM, Rasmussen MT, Laprade RF. Emerging updates on the posterior cruciate ligament. Am J Sports Med. 2015;43(12):3077–92.
14. Edwards A, Bull AMJ, Amis AA. The Attachments of the Fiber Bundles of the

Posterior Cruciate Ligament: An Anatomic Study. Arthrosc - J Arthrosc Relat Surg. 2007;

15. Hosseini A, Qi W, Tsai TY, Liu Y, Rubash H, Li G. In vivo length change patterns of the medial and lateral collateral ligaments along the flexion path of the knee. Knee Surgery, Sport Traumatol Arthrosc. 2015;23(10):3055–61.
16. Nasab SHH, List R, Oberhofer K, Fucentese SF, Snedeker JG, Taylor WR. Loading patterns of the posterior cruciate ligament in the healthy knee: A systematic review. PLoS One. 2016;11(11):1–28.
17. Serra Cruz R, Olivetto J, Dean CS, Chahla J, LaPrade RF. Superficial Medial Collateral Ligament of the Knee: Anatomic Augmentation With Semitendinosus and Gracilis Tendon Autografts. Arthrosc Tech [Internet]. 2016;5(2):e347–52. Available from: http://dx.doi.org/10.1016/j.eats.2016.01.011
18. LaPrade RF, Engebretsen AH, Ly T V., Johansen S, Wentorf FA, Engebretsen L. The anatomy of the medial part of the knee. J Bone Jt Surg - Ser A. 2007;89(9):2000–10.
19. Bedi A, Laprade RF, Burrus MT. Knee Ligaments Landmarks Anatomy. 2018;1241–50.
20. Saigo T, Tajima G, Kikuchi S, Yan J, Maruyama M, Sugawara A, et al. Morphology of the Insertions of the Superficial Medial Collateral Ligament and Posterior Oblique Ligament Using 3-Dimensional Computed Tomography: A Cadaveric Study. Arthrosc - J Arthrosc Relat Surg [Internet]. 2017;33(2):400–7. Available from: http://dx.doi.org/10.1016/j.arthro.2016.07.030
21. Smith CR, Vignos MF, Lenhart RL, Kaiser J, Thelen DG. The influence of component alignment and ligament properties on tibiofemoral contact forces in total knee replacement. J Biomech Eng. 2016;138(2).
22. H. Bloemker K. Computational Knee Ligament Modeling Using Experimentally Determined Zero-Load Lengths. Open Biomed Eng J. 2012;
23. Blankevoort L, Huiskes R. Ligament-bone interaction in a three-dimensional model of the knee. J Biomech Eng. 1991;
24. Chen Z, Zhang X, Ardestani MM, Wang L, Liu Y, Lian Q, et al. Prediction of in vivo joint mechanics of an artificial knee implant using rigid multi-body dynamics with elastic contacts. Proc Inst Mech Eng Part H J Eng Med. 2014;228(6):564–75.
25. Peters AE, Akhtar R, Comerford EJ, Bates KT. Tissue material properties and computational modelling of the human tibiofemoral joint: A critical review. PeerJ. 2018.
26. Willing R, Walker PS. Measuring the sensitivity of total knee replacement kinematics and laxity to soft tissue imbalances. J Biomech [Internet]. 2018;77:62–8. Available from: https://doi.org/10.1016/j.jbiomech.2018.06.019
27. Willing R, Moslemian A, Yamomo G, Wood T, Howard J, Lanting B. Condylar-Stabilized TKR May Not Fully Compensate for PCL-Deficiency: An In Vitro Cadaver Study. J Orthop Res. 2019;

28. Bergmann G, Bender A, Graichen F, Dymke J, Rohlmann A, Trepczynski A, et al. Standardized loads acting in knee implants. PLoS One. 2014;9(1).

29. Vandekerckhove PJ, Lanting B, Bellemans J, Victor J, MacDonald S. The current role of coronal plane alignment in Total Knee Arthroplasty in a preoperative varus aligned population: An evidence based review. Acta Orthopaedica Belgica. 2016. p. 129–42.

30. Lanting BA, Williams HA, Matlovich NF, Vandekerckhove PJ, Teeter MG, Vasarhelyi EM, et al. The impact of residual varus alignment following total knee arthroplasty on patient outcome scores in a constitutional varus population. Knee [Internet]. 2018;25(6):1278–82. Available from: https://doi.org/10.1016/j.knee.2018.08.019

31. Lee YS, Howell SM, Won YY, Lee OS, Lee SH, Vahedi H, et al. Kinematic alignment is a possible alternative to mechanical alignment in total knee arthroplasty. Knee Surgery, Sport Traumatol Arthrosc. 2017;25(11):3467–79.

32. Blakeney W, Clément J, Desmeules F, Hagemeister N, Rivière C, Vendittoli PA. Kinematic alignment in total knee arthroplasty better reproduces normal gait than mechanical alignment. Knee Surgery, Sport Traumatol Arthrosc [Internet]. 2019;27(5):1410–7. Available from: http://dx.doi.org/10.1007/s00167-018-5174-1

33. Howell SM, Roth JD, Hull ML. Kinematic Alignment in Total Knee Arthroplasty Definition, History, Principle, Surgical Technique, and Results of an Alignment Option for TKA What is Kinematic Alignment in TKA? Arthropaedia. 2014;(1):44–53.

34. Rivière C, Iranpour F, Auvinet E, Howell S, Vendittoli PA, Cobb J, et al. Alignment options for total knee arthroplasty: A systematic review. Orthop Traumatol Surg Res [Internet]. 2017;103(7):1047–56. Available from: http://dx.doi.org/10.1016/j.otsr.2017.07.010

35. Freed RD, Simon JC, Knowlton CB, Orozco Villaseñor DA, Wimmer MA, Lundberg HJ. Are Instrumented Knee Forces Representative of a Larger Population of Cruciate-Retaining Total Knee Arthroplasties? J Arthroplasty. 2017;

36. Scholes SC, Joyce TJ. In vitro tests of substitute lubricants for wear testing orthopaedic biomaterials. Proc Inst Mech Eng Part H J Eng Med. 2013;227(6):693–703.

Chapter 5

5 Future Direction

In this work so far, we have performed joint kinematic and joint laxity testing using an amalgamation between a sophisticated 6 degree of freedom joint motion simulator and a virtual ligament model. Our previous studies were performed on normally aligned models, one being mechanically aligned and the other being kinematically aligned. This study has provided a baseline computational model that reproduces appropriate TKA joint kinematics and laxities, which can then be used for future studies, providing a better understanding of total knee arthroplasty. Our primary goal was to first understand the biomechanics of various joint configurations and alignments. We looked specifically at the effects of CR, CS and PS polys in mechanically aligned and kinematically aligned TKAs. Now that we have a baseline model to work with, future works can examine the effects of common errors in TKA. Some potential avenues to examine in consideration with the aforementioned computational model could include but are not limited to: malpositioned components, misalignment, soft tissue imbalance, improperly sized polyethylene inserts and error in tibial slope.

5.1 Malpositioned components

Successful TKAs rely on the component being placed within appropriate alignment and position specifications[1]. Malpositioning of components can lead to unbalanced ligaments, asymmetric tightness, catastrophic failure, pain, stiffness, limited range of motion, instability, and overall reduced patient satisfaction[2]. With current technology and instrumentation, the risk for catastrophic malpositioning of a component is low; however, malpositioning remains a potential problem that could lead to aseptic loosening and instability, which are two of the most common reasons for revision TKA[1–3]. If an implant fails due to malalignment or malpositioning primarily, it often fails early, within the first two years[1].

Component malposition can occur in any or all of the 6 degrees of freedom around the knee. Either the femur or the tibial components can be in excessive varus or valgus

alignment, internal or external rotation, or they can be flexed or extended (referred to in the tibia as reversed or excessive tibial slope). Excessive varus or valgus of the components affects the overall coronal alignment of the limb and can affect the collateral ligament balance. Malalignment of the collateral ligaments can cause asymmetrical tightness and resultant stiffness or decreased range of motion[4]. Also, it can asymmetrically load the prosthetic joint, leading to early loosening[5,6].

Since malpostioned components can occur in all 6 degrees of freedom, we can use that to examine common errors and the effects they have on the joint kinematics or laxity. Our computational model allows us to place the components in any position desired. We are then able to use the same joint motion simulations and laxity test to examine how these malpositions alter the joint kinematics and laxity. With an appropriate baseline produced through this work, we can make a direct comparison and observe the overall change.

5.2 Undersized or Oversized Poly

Knee alignment and poly thickness can both affect the stability and soft tissue balance of a TKA. One of the goals of TKA is to have a stable and balanced knee. However, instability is currently one of the top three most common reasons for TKA revision[1,3]. Approximately one third of early TKA failures are due to soft tissue imbalance and many can lead to early failures[7,8]. It is agreed that correct ligament balancing and stability are prerequisites for achieving good functional outcomes and long-term survival of TKA. Soft tissue balancing is subjective to the surgeon's feel in most cases, and it is currently unclear what the optimum soft tissue balance, tension or alignment is for TKA success[9]. Such optimal conditions may even differ with various implant designs. Future research in this area could explore how the thickness of the poly insert can affect the biomechanics of the TKA. This could then be compared between both mechanically and kinematically aligned Cruciate Retaining, Cruciate Sacrificing and Posterior Stabilized TKA constructs.

5.3 Error in Tibial slope

Changes in tibial slope can cause decreased range of motion in the knee, alter the forces in the PCL, lead to abnormal forces on the components affecting implant longevity, or

lead to instability[10,11]. Despite the significant influence the posterior tibial slope can have on biomechanics of the knee and, subsequently, on clinical outcomes, the ideal posterior slope is still debated[12,13]. There have been some studies that present appropriate amounts of tibial slope to gain the best functional and clinical outcomes[10,14]. However, our computational model allows for easily and accurately assessing various degrees of slope (eg. 0°,3°,5°,7° and 10°) in the same knee, and then comparing that effect across different poly configurations or different alignments. Through this comparison, a better understanding of the ideal tibial slope can be determined, and it may become clear which tibial slope is best for each different TKA configuration or alignment.

5.4 Summary

The supreme benefit of a computational model is that it allows for many more possibilities and scenarios to be tested in an efficient manner. With a baseline computational model that recreates TKA joint kinematics and laxities for normally aligned and balanced knees, the potential for assessing common TKA errors becomes simplified. Considering some of the limitations within our computational model, adjustments and specifications can be altered to hone the accuracy of the computational model. This will more anatomically recreate the TKA simulation. From there, we will have the ability to produce many simulations of both normal and abnormal TKA, providing a better understanding of the TKA biomechanics. In so doing, we hope that future works will allow us to better understand how to recreate stable, well-balanced and fully functional TKAs that all patients will be satisfied with.

5.5 References

1. Lombardi A V., Berend KR, Adams JB. Why knee replacements fail in 2013: Patient, surgeon, or implant? Bone Jt J. 2014;96B(11):101–4.
2. Siston RA, Maack TL, Hutter EE, Beal MD, Chaudhari AMW. Design and cadaveric validation of a novel device to quantify knee stability during total knee arthroplasty. J Biomech Eng. 2012;134(11):1–7.
3. Sharkey PF, Lichstein PM, Shen C, Tokarski AT, Parvizi J. Why are total knee arthroplasties failing today-has anything changed after 10 years? J Arthroplasty [Internet]. 2013;29(9):1774–8. Available from: http://dx.doi.org/10.1016/j.arth.2013.07.024
4. Keeney JA, Clohisy JC, Curry M, Maloney WJ. Revision total knee arthroplasty for restricted motion. Clin Orthop Relat Res. 2005;(440):135–40.
5. Fehring TK, Valadie AL. Knee instability after total knee arthroplasty. In: Clinical Orthopaedics and Related Research. 1994.
6. Insall JN, Binazzi R, Soudry M, Mestriner LA. Total knee arthroplasty. Clin Orthop Relat Res. 1985;
7. Fehring TK, Odum S, Griffin WL, Mason JB, Nadaud M. Early failures in total knee arthroplasty. In: Clinical Orthopaedics and Related Research. 2001.
8. Smith T, Elson L, Anderson C, Leone W. How are we addressing ligament balance in TKA? A literature review of revision etiology and technological advancement. J Clin Orthop Trauma [Internet]. 2016;7(4):248–55. Available from: http://dx.doi.org/10.1016/j.jcot.2016.04.001
9. Luo Z, Zhou K, Peng L, Shang Q, Pei F, Zhou Z. Similar results with kinematic and mechanical alignment applied in total knee arthroplasty. Knee Surgery, Sport Traumatol Arthrosc [Internet]. 2019;(0123456789). Available from: https://doi.org/10.1007/s00167-019-05584-2
10. Seo SS, Kim CW, Kim JH, Min YK. Clinical Results Associated with Changes of Posterior Tibial Slope in Total Knee Arthroplasty. Knee Surg Relat Res. 2013;25(1):25–9.
11. Kang KT, Koh YG, Son J, Kwon OR, Lee JS, Kwon SK. Influence of Increased Posterior Tibial Slope in Total Knee Arthroplasty on Knee Joint Biomechanics: A Computational Simulation Study. J Arthroplasty. 2018;
12. Bellemans J, Robijns F, Duerinckx J, Banks S, Vandenneucker H. The influence of tibial slope on maximal flexion after total knee arthroplasty. Knee Surgery, Sport Traumatol Arthrosc. 2005;
13. Okazaki K, Tashiro Y, Mizu-uchi H, Hamai S, Doi T, Iwamoto Y. Influence of the posterior tibial slope on the flexion gap in total knee arthroplasty. Knee. 2014;
14. Howard JL, Morcos MW, Lanting BA, Somerville LE, McAuley JP. Reproducing the Native Posterior Tibial Slope in Cruciate-Retaining Total Knee Arthroplasty: Technique and Clinical Implications. Orthopedics. 2020;

Appendices

Appendix A: An in-depth description of the virtual model creation as explained in the following excerpt from the methods section of a previous work by Montgomery et al.

Methods

Virtual Model Development

Creating a virtual knee model started with the segmentation of CT scans taken for a previous cadaveric study using the program Slicer Version 4.11.0. A threshold segmentation technique was used to extract individual bone segments as separate files. Three separates segmentations were extracted: proximal femur including the femoral head, distal femur, and proximal tibia. The proximal tibia and the distal femur – the two parts of the leg tested in the previous cadaveric study – were then assigned unique individual coordinate systems based on the coordinate system developed by Grood and Suntay. The femoral coordinate system originated at the middle of the line connecting the centre of the two spheres made by the condyles (epicondylar axis). The z-axis was defined as a line that passed from this origin to the center of a sphere-fit of the femoral head and was positive proximally[21]. The y-axis was the anteriorly positive cross-product of the epicondylar axis and z-axis. The x-axis was parallel to the sagittal plane of the femur and was the result of cross-multiplying the z and y axes. It was positive to the right. The tibial coordinate system originated at the center of the intercondylar notch. Its z-axis extended proximally from the center of the ankle joint – calculated as the midpoint of the lateral and medial malleoli – to the center of the intercondylar eminences and is positive in the proximal direction. The y-axis was calculated by cross multiplying the z-axis with a line connecting the centers of the two tibial plateaus and was positive in the anterior direction. Finally, the x-axis was the right-facing cross product of y and z axes. Note that the z-axes for both bones are coincident with the respective bone's mechanical axis. The finalized models were then saved as stereolithographic files so that they could be used in CAD software. The stereolithographic files for the TKR prosthesis were obtained directly from the manufacturer: Stryker Corporation. Both the femoral component and tibial components were given coordinate systems as well. The x-axis of the femoral component was taken as the line connecting the centre of the sphere-fits made to each of the condyles. The z-axis was the result of a cross multiplication between the x-axis and a horizontal line taken from the bottom surface of the component. The anterior facing y-axis was the cross product of the z and x axes. This coordinate system was situated at the midpoint between the two condylar sphere-fit centres. The tibial component's coordinate system was centered at the front lip of the central hole. The z-axis was defined as a line parallel to the back edge of

the component. The cross product of this and a line connecting the two posterior protuberances gave the y-axis, and the x-axis was a cross product of the z and y axis. In all cases, the z-axis was positive superiorly, the x-axis was positive to the right and the y-axis was positive anteriorly.

Resecting Models

Using SOLIDWORKS 2018, the stereolithographic (stl) files of both the bones and the prosthetic components were converted to solidpart files so that they could be resected. The stl files for the prosthetic components were obtained from the prosthetic manufacturer *Stryker*. The stl files for the bones were adapted from CT scans performed on cadaveric knees from this lab's previous experiments. References were created for all axes and corresponding planes for both bones. Three alignments were done for three different implant types: mechanical alignment, kinematic alignment, and malalignment for CR, and CS implants. Mechanical alignment involved a distal femoral resection perpendicular to the z axis and 8mm proximally into the femur. After this resection, the other four resections – which would have to be meticulously measured in an OR – were made by fitting the femoral component to the plane of the first resection and simply cutting along the outline of the femoral component. The mechanically aligned tibial resection has a 5° posterior slope with respect to the perpendicular of the z-axis. The anterior side removes 8mm of the proximal tibia. The same model will be used for CR and CS subjects as the only difference is an increased lip on the poly of the CS which does not affect any of the relevant ligament measurements. The kinematic alignment was performed similarly except the distal femoral resection was made 3° valgus compared to the mechanical alignment and the proximal tibial resection was made 3° varus compared to the mechanical alignment.

Ligament model

The insertion points of our ligament model were based on a combination of previous work in this lab as well as various previous studies[18,20,22–24,25]. Our ligament model included the sMCL, the LCL, and the PCL, (superficial medial collateral ligament, lateral collateral ligament, and posterior cruciate ligament respectively). The insertion points were added to the model in its initial orientation, co-registered to the joint motion simulator's coordinates from previous testing done in this lab. The points were then recorded once the model had been transformed, resected, and centered at the femoral component's coordinate system. This gave us new ligament insertion points in terms of the femoral component and factored in any relative change in distance change due to resections or addition of prostheses. We chose to center the model at the femoral component's center since the femoral component is placed at the joint motion simulator's origin during testing (see proceeding section). Ligament stiffnesses were obtained from literature about various computational TKR knee models[4,26,27]. Reference strains were adapted from previous studies[15,20] based on strains and lengths calculated from

models. Reference lengths were adapted from the literature for the kinematically aligned model. This is because this literature on reference strains is based off of intact knees and the kinematic alignment more closely resembles the intact knee than the mechanically aligned knee[10]. Zero-load lengths of the ligament were calculated using equation (1), where l_0 is the zero load length, l_r is the reference length calculated from our model, and ε_r is the reference strain adapted from the literature. Equation (1) was then rearranged to solve for l_r so that reference length could be calculated for the mechanical alignment from the values obtained from the kinematically aligned model.

$$l_0 = \left(\frac{l_r}{\varepsilon_r + 1}\right)$$

Appendix B: The statistical breakdown between MA and KA knee constructs. Comparison between each poly configuration can be observed. Number values represent p-values from a two tailed, two-sample equal variance T-test.

Mechanical VS Kinematic AP Kinematics				
	M - CR	M - CS	M - CSxPCL	M - PS
K - CR	0.877	0.709	0.118	0.000
K - CS	0.842	0.671	0.091	0.000
K - CSxPCL	0.216	0.320	0.847	0.001
K - PS	0.000	0.000	0.000	0.956

Mechanical VS Kinematic IE Kinematics				
	M - CR	M - CS	M - CSxPCL	M - PS
K - CR	0.818	0.893	0.047	0.738
K - CS	0.963	0.905	0.037	0.903
K - CSxPCL	0.029	0.050	0.405	0.075
K - PS	0.816	0.874	0.191	0.741

Mech vs Kin Total Joint compression forces				
	M - CR	M - CS	M - CSxPCL	M - PS
K - CR	0.801	0.791	0.811	0.380
K - CS	0.809	0.798	0.819	0.369
K - CSxPCL	0.792	0.782	0.802	0.383
K - PS	0.223	0.220	0.226	0.871

Mechanical VS Kinematic VV Kinematics				
	M - CR	M - CS	M - CSxPCL	M - PS
K - CR	0.829	0.938	0.766	0.329

K - CS	0.613	0.711	0.557	0.564
K - CSxPCL	0.887	0.999	0.822	0.260
K - PS	0.107	0.146	0.084	0.349

Mech vs Kin PCL Forces - Kinematics		
	M - CR	M - CS
K - CR	0.807	0.917
K - CS	0.824	0.934

Mech vs Kin sMCL Forces during Kinematics				
	M - CR	M - CS	M - CSxPCL	M - PS
K - CR	0.225	0.164	0.245	0.452
K - CS	0.323	0.239	0.349	0.613
K - CSxPCL	0.206	0.150	0.224	0.417
K - PS	0.103	0.073	0.114	0.232

Mech vs Kin LCL Forces during Kinematics				
	M - CR	M - CS	M - CSxPCL	M - PS
K - CR	0.691	0.645	0.596	0.105
K - CS	0.796	0.746	0.692	0.122
K - CSxPCL	0.817	0.769	0.716	0.132
K - PS	0.269	0.286	0.313	0.815

Mechanical VS Kinematic AP Laxity				
	M - CR	M - CS	M - CSxPCL	M - PS
K - CR	0.921	0.975	0.026	0.255
K - CS	0.980	0.875	0.040	0.216
K - CSxPCL	0.043	0.026	0.874	0.002
K - PS	0.208	0.245	0.001	0.995

Mechanical VS Kinematic VV Laxity				
	M - CR	M - CS	M - CSxPCL	M - PS
K - CR	0.696	0.716	0.620	0.970
K - CS	0.686	0.706	0.612	0.955
K - CSxPCL	0.802	0.823	0.724	0.920
K - PS	0.455	0.470	0.395	0.676

Mech vs Kin AP Laxity PCL

	M - CR	M - CS
K - CR	0.422	0.321
K - CS	0.680	0.506

Mech vs Kin AP Laxity sMCL				
	M - CR	M - CS	M - CSxPCL	M - PS
K - CR	0.315	0.202	0.010	0.817
K - CS	0.505	0.340	0.004	0.566
K - CSxPCL	0.000	0.000	0.519	0.010
K - PS	0.010	0.005	0.099	0.229

Mech vs Kin AP Laxity LCL				
	M - CR	M - CS	M - CSxPCL	M - PS
K - CR	0.598	0.614	0.059	0.136
K - CS	0.631	0.648	0.067	0.145
K - CSxPCL	0.198	0.190	0.857	0.754
K - PS	0.375	0.367	0.891	0.792

Mech vs Kin Valgus Laxity PCL		
	M - CR	M - CS
K - CR	0.835	0.941
K - CS	0.668	0.768

Mech vs Kin Valgus Laxity sMCL				
	M - CR	M - CS	M - CSxPCL	M - PS
K - CR	0.749	0.754	0.103	0.002
K - CS	0.755	0.760	0.105	0.002
K - CSxPCL	0.164	0.170	0.922	0.021
K - PS	0.003	0.004	0.029	0.988

Mech vs Kin Valgus Laxity LCL				
	M - CR	M - CS	M - CSxPCL	M - PS
K - CR	0.862	0.821	0.786	0.155
K - CS	0.915	0.874	0.838	0.168
K - CSxPCL	0.915	0.873	0.837	0.167
K - PS	0.234	0.247	0.261	0.915

Mech vs Kin Varus Laxity PCL		
	M - CR	M - CS

K - CR	0.587	0.607
K - CS	0.508	0.525

Mech vs Kin Varus Laxity sMCL				
	M - CR	M - CS	M - CSxPCL	M - PS
K - CR	0.289	0.220	0.282	0.738
K - CS	0.373	0.288	0.365	0.879
K - CSxPCL	0.289	0.222	0.283	0.726
K - PS	0.099	0.074	0.096	0.302

Mech vs Kin Varus Laxity LCL				
	M - CR	M - CS	M - CSxPCL	M - PS
K - CR	0.828	0.565	0.955	0.919
K - CS	0.975	0.669	0.821	0.877
K - CSxPCL	0.687	0.484	0.883	0.978
K - PS	0.781	0.884	0.716	0.757

Curriculum Vitae

Name:	Jance McGale
Post-secondary Education and Degrees:	University of Lethbridge Lethbridge, Alberta, Canada 2006-2010 BSc. University of Alberta Edmonton, Alberta, Canada 2010-2014 MD University of Alberta Edmonton, Alberta, Canada 2014-2019 FRCSC The University of Western Ontario London, Ontario, Canada 2019-2020 MSc in Surgery Candidate
Honours and Awards:	2014-2019 **Dr. Hastings Mewburn Post-Graduate Scholarship in Orthopedic Medicine,** Outstanding Merit in field of Orthopedic Surgery, Department of Surgery, University of Alberta 2017-2018 **Resident Research and Presentation Award,** Orthopedic Surgery Residency Program, University of Alberta 2010-2014 **Rural Medical School Award,** Rural Physician Action Plan, Edmonton Alberta 2011-2012 **Dr. R.F. Shaner Human Anatomy Award,** Faculty of Medicine and Dentistry, University of Alberta 2010-2011 **Harold and Opal Hess Bursaries in Medicine,** Faculty of Medicine and Dentistry, University of Alberta 2006-2010 **Dean's Honour List**, Faculty of Arts and Science, University of Lethbridge 2006-2009 **Jason Lang Scholarship** in recognition of exceptional academic achievement
Related Work	**Research Assistant,** Marcia L Clark Professional Corporation

Role: Literature review on current standards for diagnosis and treatment of prosthetic joint infections; comprehensive chart review.
2011

Experience

2019-Present **Masters of Science in Surgery Program.** Thesis: Biomechanical analysis of Mechanically versus Kinematically aligned total knee arthroplasty (TKA) using TKA implants linked to a virtual ligament model.
Supervisors: Dr. Brent Lanting, Dr. Ryan Willing

2017 **COA interesting case session.** Presentation of Pediatric aggressive MRSA osteomyelitis case.
Won interesting case presentation for the session.

2014-2019 **The effect of door opening on infection rates in lower extremity total joint arthroplasty**. Quality improvement project to assess the rate of door opening and traffic in the OR to determine what our local rates and volumes are and whether any change in practice is needed. Supervisors: Dr. Catherine Hui
Presented during Edmonton Orthopedic Research day 2015

2015-2019 **In Vitro Matrix-forming Characteristics of Human Meniscus Cells Post-expansion Culture on Adherent and Non-adherent Substrates.** In vitro growth of meniscus to maintain phenotypic characteristics for possible meniscal implantation. Supervisors: Dr. Nadr Johma, Dr. Adetola Adesida
Presented during Edmonton Orthopedic Research day 2016

2011-2012 **Prosthetic Joint Infection Quality Assurance Project.** To see how the Royal Alexandra Hospital compares to the current standards for diagnosis and treatment of prosthetic joint infections. Supervisors: Dr. Marcia Clark, Dr. Stuart Rosser
Presented to Royal Alexandra Hospital, Prosthetic Joint Infection Research committee.

Publications:
Wilson, M; **McGale, J.** 2013. Reviewing acute low back pain with emphasis on indications for imaging. University of Alberta Health Sciences Journal